Estimation and Analysis of Physical Activity Load Based on Heart Rates

Sungjoon Yoon

The Graduate School
School of Electrical and Electronic Engineering
Yonsei University

Estimation and Analysis of Physical Activity Load Based on Heart Rates

A Master's Thesis
Submitted to the Department of Electrical and Electronic Engineering
and the Graduate School of Yonsei University
in partial fulfillment of the
requirements for the degree of
Master of engineering

Sungjoon Yoon

December 2024

This certifies that the master's thesis
of Sungjoon Yoon is approved.

Thesis Supervisor: DaeEun Kim

Donghyun Kim

Dosik Hwang

The Graduate School

School of Electrical and Electronic Engineering

Yonsei University

December 2024

Acknowledgements

First and foremost, I would like to express my deepest gratitude to my advisor, Professor DaeEun Kim, for their invaluable guidance, insightful feedback, and unwavering support throughout this journey. Encouragement and expertise have been instrumental in shaping this thesis. I am also immensely thankful to the members of my thesis committee, Professor Donghyun Kim and Professor Dosik Hwang, for their constructive comments, suggestions, and for dedicating their time to review my work. Their feedback has greatly enriched the quality of this research. Special thanks go to my colleagues and friends, who provided encouragement and shared in both the challenges and successes of this journey. Your companionship has been a constant source of motivation. Finally, I am deeply indebted to my family for their unconditional love, patience, and support. Their belief in me has been my greatest source of strength. This thesis is dedicated to all those who have contributed to its completion.

Declaration

I declare that this thesis was composed by myself, that the work contained herein is my own except where explicitly stated otherwise in the text, and that this work has not been submitted for any other degree or professional qualification except as specified.

(*Sungjoon Yoon*)

Table of Contents

List of Figures

List of Tables

Abstract

This study investigates the interaction between heart rate (HR) and exercise difficulty, with a focus on combined upper and lower body movements commonly used in high-intensity interval training (HIIT) and aerobic workouts. Using a novel vector-based analysis, the research demonstrates that HR responses to combined movements are proportional to the difficulty of each component, rather than being additive, enabling precise classification of exercise intensity. These findings provide a systematic framework for designing tailored exercise programs based on specific HR responses. Building on this, the study highlights the significant influence of blood glucose (BG) dynamics on HR measurements, showing that postprandial states lead to greater HR variability compared to fasting conditions. To address this, a novel HR-based BG estimation method was introduced, utilizing decision tree models to predict BG levels non-invasively, offering a practical solution for metabolic monitoring without the need for direct BG measurements. This integration of BG variability into HR analysis emphasizes the importance of considering both metabolic and cardiovascular dynamics to optimize exercise assessments. Furthermore, the dominant role of lower body movements in driving HR levels was reinforced, while upper body exercises were found to significantly influence HR when paired with lower-intensity lower body movements. Together, these findings offer valuable insights for developing personalized exercise protocols that account for metabolic and cardiovascular interactions, contributing to advancements in fitness and health management for diverse populations.

Key words : HR analysis, Blood Glucose Analysis, Exercise Segmentation, Vector-Based movement analysis, Activity Load , HR-BG Interaction

Chapter 1

Introduction

Interest in health and medical care is increasing rapidly around the world. As a result, the growth of the digital healthcare industry is accelerating, and to support this, diagnostic tools and technologies capable of monitoring various information on health conditions are essential. As various smart wearable devices are released on the market due to the development of IT technology, personalized customized treatment and health care suggestions are possible by measuring the user's biometric signal through various sensors. Smart wearable devices are implemented with the latest technologies such as artificial intelligence, big data, and IOT, and using this, it is possible to provide customized data. However, in order for these services to be provided more valuable, it is necessary to collect accurate and reliable data by applying different processing methods according to the user's physical condition. If research and technology development continue for this, personalized health care services provided through smart wearable devices will continue to develop and grow(Topol, 2015; Lu et al., 2020).

Smart wearable devices that consumers can easily use on a daily basis generally provide biometric signal data collection functions such as heart rate, exercise amount, and sleep state (Patel et al., 2012). Through this, various application services are provided in the digital healthcare industry, and these smart wearable devices have recently been able to grasp the type and condition of exercise performed by users using various sensors such as inertial navigation devices and GPS in addition to biometric signals. It even provides various services to increase safety and efficiency by detecting a user's sudden impact and providing feedback to the user (Haghi et al., 2017).

1.1 Role of Heart Rate and Blood Glucose in Physiological and Health Conditions

The Role of Heart Rate and Blood Glucose in Physiological and Health Conditions Heart rate (HR) and blood glucose (BG) are two fundamental biomarkers that reflect the body's physiological state and are closely linked to overall health. HR, which measures the number of heartbeats per minute, serves as a primary indicator of cardiovascular function. It is influenced by various factors such as physical activity, stress, and overall fitness. Monitoring HR provides valuable insights into an individual's cardiovascular response to different stimuli, including exercise and psychological stress.

On the other hand, blood glucose is a key marker of metabolic health, indicating the concentration of glucose in the bloodstream. BG levels fluctuate in response to food intake, physical activity, and stress, with proper regulation being essential for maintaining energy balance and preventing metabolic disorders. For individuals with conditions such as diabetes, monitoring BG is particularly critical for managing health.

The interaction between HR and BG is complex but important. Physical activity, for example, increases the body's energy demand, prompting the release of glucose into the bloodstream, which in turn affects both HR and BG levels. Additionally, stress—whether physical or mental—can elevate both HR and BG, highlighting the integrated nature of the cardiovascular and metabolic systems.

Technological advances in wearable devices have made it possible to monitor HR and BG continuously. Devices such as heart rate monitors and continuous glucose monitors (CGMs) allow real-time tracking of these biomarkers, offering deeper insights into how daily activities, stressors, and lifestyle choices affect overall health. This continuous data can be used to analyze patterns and predict trends, which is especially valuable in preventing chronic conditions such as diabetes and cardiovascular disease.

Research exploring the relationship between HR and BG has shown that these biomarkers react sensitively to various events such as exercise, eating, and resting(Frampton et al., 2021). By studying how these factors influence HR and BG, it is possible to gain a better understanding of how the body responds to everyday activities and to develop personalized health interventions. Predictive models based on HR and BG data may also provide early warnings of potential health issues, allowing for more proactive health management.

1.2 Motivation and Objective

Advances in health monitoring technologies have opened new avenues for understanding physiological responses during exercise. However, the nuanced interplay between upper and lower body movements and their combined effects on HR remains underexplored. Additionally, while HR is widely used to assess exercise intensity, its potential to predict exercise difficulty and support tailored exercise protocols requires further investigation. This dissertation aims to address these gaps by examining the distinct contributions of upper and lower body movements to HR dynamics and developing a framework for integrating these insights into real-world applications, such as high-intensity interval training (HIIT) and aerobic exercises.

The objective of this research is to create a comprehensive HR analytical framework that leverages the proportional relationship between HR responses and the difficulty of individual exercise components. By classifying and quantifying exercise intensity based on the interplay of upper and lower body contributions, this study aims to enable precise customization of exercise programs. The findings have the potential to inform the design of personalized fitness regimens, including programs for individuals with physical limitations or specific fitness goals.

In addition to exercise classification, this research highlights the impact of physiological states, such as BG variability, on HR responses. By addressing how postprandial and fasting states influence HR stability, the study seeks to optimize the timing and selection of exercises for improved cardiovascular and metabolic outcomes. This dual focus on exercise dynamics and health monitoring offers a unified approach to advancing personalized fitness and health management systems.

1.3 Organization of Dissertation

The organization of this dissertation is as follows. Chapter 2 provides background information on HR and BG monitoring, as well as an overview of wearable devices and their role in health management. Chapter 3 examines the cardiovascular response of upper and lower body exercises to focus on how lower and upper body exercises interact to induce HR responses. In Chapter 4, the dynamic relationship between HR and BG levels is examined by continuously monitoring participants in different conditions, such as exercise and rest, to identify correlations. Chapter 5 focuses on predicting exercise difficulty in dynamic movements, like aerobics, using HR data. It assesses whether

HR metrics from static exercises can accurately predict real-time responses in more complex activities. Finally, Chapter 6 offers a detailed summary of the dissertation, highlighting the main conclusions from the findings. It also discusses future research directions and potential improvements to further develop the proposed approach.

Chapter 2

Background

In the near past, the growing interest in health and wellness has led to significant advancements in digital healthcare technologies. Among these innovations, wearable devices have emerged as essential tools for continuously monitoring various physiological signals, such as heart rate (HR) and blood glucose (BG). These devices are increasingly integrated into everyday life, offering personalized insights into fitness, metabolic health, and overall well-being.

The ability to track HR and BG in real time has opened new possibilities for health management, particularly in exercise optimization and chronic disease prevention. By providing users with immediate feedback on their physiological responses to physical activity and other lifestyle factors, wearable technologies contribute to more informed health decisions and proactive care. As the role of continuous monitoring grows, it is critical to understand the physiological underpinnings of HR and BG, their interaction during different activities, and how the data they generate can be leveraged for personalized health interventions.

This chapter provides an overview of the physiological significance of HR and BG, their role in health monitoring, and the existing research on their combined use in personal fitness and healthcare applications. It sets the foundation for the study's investigation into the relationship between HR and BG during exercise and the potential to predict health outcomes using real-time data from wearable devices.

2.1 Role of Heart Rate (HR) in Health and Exercise

HR is one of the most widely used physiological markers for assessing overall health and fitness. It provides not only an immediate measure of cardiovascular activity but

also a window into how the body responds to various stimuli, including physical exertion, emotional stress, and recovery. More than just a count of heartbeats per minute, HR is a reflection of the autonomic nervous system's regulation of bodily functions, encompassing both sympathetic and parasympathetic activities. This makes HR an invaluable tool in various fields of health management—from optimizing athletic performance to monitoring and preventing cardiovascular diseases. A deeper understanding of how HR behaves in different contexts allows for more tailored and effective interventions that promote long-term well-being and fitness.

2.1.1 Heart Rate as a Key Health Indicator

Heart rate serves as a critical measure of cardiovascular efficiency, with the ability to reflect an individual's overall health status. In its resting state, HR typically falls within a range of 60-100 beats per minute (bpm) for most adults, with lower resting heart rates often associated with better cardiovascular fitness. However, persistent elevations in resting HR can signal an increased risk for cardiovascular diseases and even mortality, underscoring its significance as a vital health indicator (Cooney et al., 2010).

In addition to static measures like resting heart rate, heart rate variability (HRV) plays a pivotal role in evaluating health. HRV, which refers to the variations in time between successive heartbeats, provides insight into the balance between the sympathetic (fight-or-flight) and parasympathetic (rest-and-digest) branches of the autonomic nervous system. A higher HRV generally reflects better adaptability and recovery, while reduced HRV has been linked to increased stress levels and a heightened risk for cardiovascular events. Monitoring HRV offers a more nuanced view of an individual's cardiovascular and autonomic health, making it an important component in both clinical and personal health assessments (Tsuji et al., 1996).

2.1.2 Heart Rate in Exercise and Fitness

Heart rate is a dynamic marker that responds directly to the intensity of physical exertion, making it an invaluable tool in exercise monitoring. During physical activity, HR increases to supply muscles with the oxygen they need for sustained performance. Monitoring HR allows individuals to adjust the intensity of their workouts based on their fitness goals, ensuring they stay within optimal target heart rate zones. These zones are typically calculated as a percentage of maximum heart rate (MHR), which varies by age and individual fitness level. For moderate-intensity exercise, HR gen-

erally hovers around 50-70% of MHR, while vigorous activities push HR into the 70-85% range (Tanaka et al., 2001).

As exercise continues, the heart rate reaches a steady state in aerobic activities, reflecting the body's balance between oxygen consumption and energy output. This steady state is crucial for endurance training, as it indicates that the body can maintain prolonged activity without overly taxing cardiovascular reserves. In contrast, anaerobic activities like high-intensity interval training (HIIT) create rapid fluctuations in heart rate, often pushing it closer to maximum capacity. These fluctuations stimulate cardiovascular adaptations that can improve both heart efficiency and metabolic health over time (Weston et al., 2014).

The ability to monitor heart rate in real-time during workouts enables athletes and fitness enthusiasts to fine-tune their exercise regimens. By ensuring they stay within their target zones, individuals can optimize fat-burning, improve aerobic capacity, or enhance cardiovascular strength depending on their specific goals.

2.1.3 Clinical and Everyday Applications of Heart Rate Monitoring

While heart rate monitoring is integral to fitness, its applications extend far beyond athletic performance. In clinical settings, HR plays a crucial role in managing patients with cardiovascular diseases, particularly during rehabilitation following events such as heart attacks or surgeries. Continuous HR monitoring helps clinicians ensure that patients are engaging in safe levels of physical activity while reducing the risk of adverse cardiac events during recovery. By keeping patients within a controlled heart rate range, healthcare providers can facilitate a safer, more effective rehabilitation process that promotes long-term heart health.

In everyday life, wearable devices like smartwatches and fitness trackers have revolutionized how people monitor their heart rate. These devices provide real-time data on HR, allowing individuals to track their heart's response to daily activities, stress, and recovery. For many, this continuous monitoring fosters a proactive approach to managing both physical fitness and emotional well-being. Wearable technologies have demonstrated impressive accuracy in HR tracking, making them accessible tools for personal health management (Shcherbina et al., 2017). Users can now receive immediate feedback on their physical and emotional states, enabling more informed decisions about exercise intensity, sleep patterns, and stress reduction.

Ultimately, heart rate monitoring—whether in clinical settings or through everyday

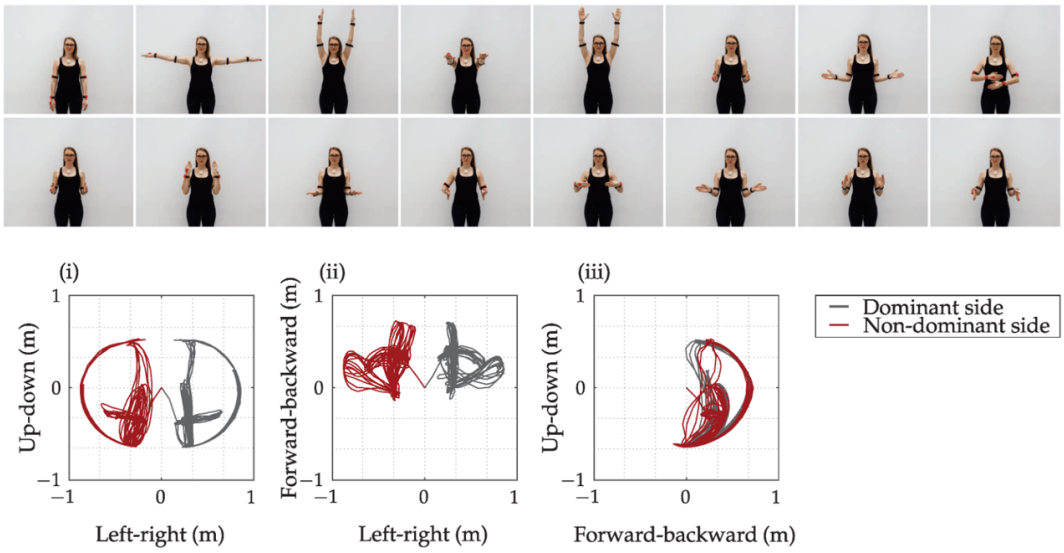

Figure 2.1: Symmetrical upper limb movement demonstration of a healthy subject with the corresponding trajectories of the arm in the frontal (i), transversal (ii) and sagittal (iii) plane (Šlajpah et al., 2023). Black line represents the position of the dominant hand and red line represents the position of the non-dominant hand.

wearable devices—provides a wealth of information that can be used to enhance both individual and population health outcomes. As technology continues to evolve, the integration of HR data with other biometric signals promises even greater opportunities for personalized health interventions, disease prevention, and the promotion of overall well-being.

2.2 Upper and Lower Body Exercise Segmentation and Gesture Analysis

Understanding how upper and lower body movements differ during exercise is essential for accurately analyzing HR and BG responses. Recent studies have focused on segmenting these movements to better comprehend their distinct physiological impacts, which provides valuable insights for optimizing exercise routines and health interventions.

2.2.1 Analysis of Upper Body Movements

Upper body exercises often involve complex, multi-joint movements, requiring an understanding of muscle coordination and activation patterns. Šlajpah et al. (2023) analyzed upper-limb movements using both time-based and path-based segmentation, demonstrating how wearable sensors, particularly inertial measurement units (IMUs), can capture the dynamic nature of these movements (Šlajpah et al., 2023). This study highlighted the difference between unimanual (single-hand) and bimanual (two-hand) tasks, showing that upper body movements require advanced segmentation techniques to capture variations in intensity, direction, and coordination accurately.

In another study, Hug et al. (2021) demonstrated that muscles from the same upper limb group (e.g., triceps surae) do not always share common activation patterns during exercise, which suggests that different upper-body exercises may require distinct analytical approaches (Hug et al., 2021). This finding underlines the importance of detailed gesture analysis when examining upper body movements, as even seemingly similar exercises may engage muscles differently, resulting in unique HR responses.

2.2.2 Analysis of Lower Body Movements

The lower body is often involved in exercises that generate significant cardiovascular responses due to the involvement of larger muscle groups. Ema et al. (2016) investigated the unique activation of the quadriceps femoris during both single- and multi-joint exercises, emphasizing that the type of exercise (e.g., squats vs. leg presses) leads to different patterns of muscle engagement and metabolic demand (Ema et al., 2016). Understanding these differences is crucial for analyzing how lower body exercises influence HR, especially when comparing exercises of varying intensities.

Kinoshita et al. (2023) further explored lower body exercise segmentation by comparing the hypertrophic effects of standing versus seated calf-raise training (Kinoshita et al., 2023). Their findings demonstrated that exercise position significantly affects muscle activation patterns and metabolic responses, suggesting that exercise posture should be considered when analyzing HR and BG responses.

2.2.3 Comparative Studies of Upper vs. Lower Body Exercise

When comparing upper and lower body exercises, distinct physiological and metabolic responses emerge. MacInnis et al. (2017) conducted a study using unilateral exercise

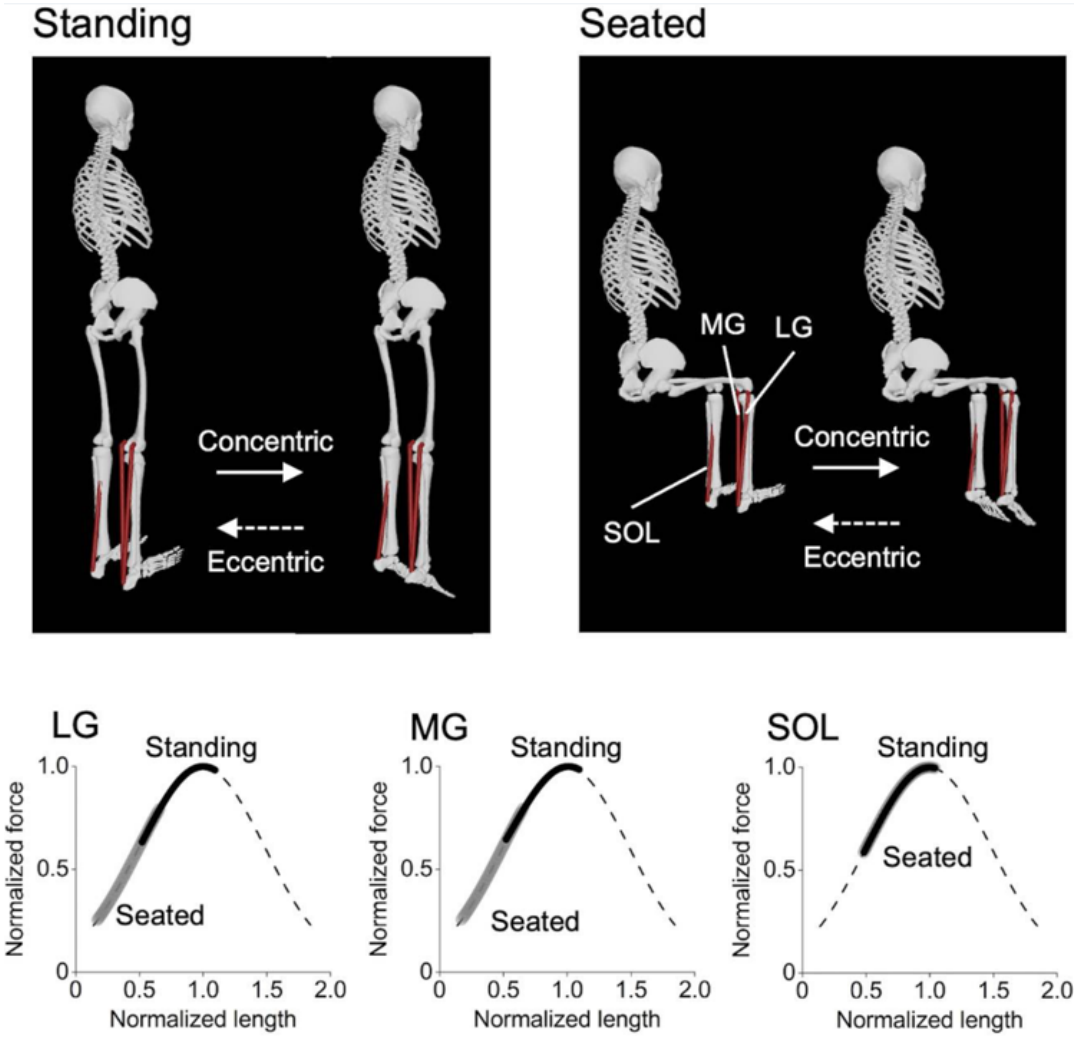

Figure 2.2: Postures of the standing and seated calf-raise exercises and operating ranges of each triceps surae muscle on the normalized force–length curve during the exercises (Kinoshita et al., 2023). These were obtained using the OpenSim Gait 2392 model (Delp et al., 2007), with the knee joint 0° and 90° for the standing and seated conditions, respectively, and the ankle joint angle ranging from 20° dorsiflexed to 30° plantarflexed positions for both conditions. It can be clearly seen that the lateral and medial gastrocnemius (LG and MG) operate at longer muscle lengths in the standing than seated condition, while there is no difference between the conditions in the soleus (SOL).

models and found that upper and lower limb exercises induced different patterns of skeletal muscle activation, which resulted in varied HR responses (MacInnis et al., 2017). This finding aligns with the concept that upper and lower body movements elicit different cardiovascular and metabolic demands, making it important to differentiate

these exercises when analyzing their impact on HR and BG.

Additionally, a systematic review by Kassiano et al. (2023) analyzed how different exercise types, including straight-leg versus bent-leg calf raises, influence muscle swelling in the triceps surae. They found that bent-leg exercises elicited greater muscle swelling and metabolic activity than straight-leg exercises, providing further evidence that subtle variations in exercise type and technique can lead to different physiological responses (Kassiano et al., 2023).

2.3 Blood Glucose and Its Importance in Metabolic Health

Blood glucose is a vital marker of metabolic health and plays a central role in maintaining the body's energy balance. Glucose serves as the primary source of fuel for cells, particularly in the brain and muscles, making its regulation crucial for overall health. The body's ability to maintain stable blood glucose levels, a process known as glucose homeostasis, is fundamental to preventing metabolic disorders. Any disruption in this balance whether through dietary changes, physical activity, or stress can significantly affect an individual's metabolic health, making blood glucose monitoring essential for both healthy individuals and those with conditions like diabetes.

2.3.1 Blood Glucose Regulation

The body maintains glucose homeostasis through a complex system involving the pancreas, liver, and various hormones. When BG levels rise after a meal, the pancreas secretes insulin, which facilitates the uptake of glucose into cells for energy use or storage. Conversely, during fasting or periods of low glucose availability, the hormone glucagon prompts the liver to release stored glucose, ensuring a continuous supply of energy (Jiang and Zhang, 2003). This regulatory system keeps blood glucose levels within a narrow range, which is crucial for normal cellular function.

Fluctuations in BG levels occur in response to food intake, stress, and physical activity. While transient increases after eating are normal, chronic elevations in BG levels, as seen in conditions like type 2 diabetes, can lead to long-term damage to the body's tissues and organs. The consequences of poor glucose regulation include increased risks for cardiovascular disease, nerve damage, and kidney dysfunction (Fujimoto, 2000). Therefore, maintaining stable BG levels is a key factor in long-term health, and disruptions in this balance can have serious implications.

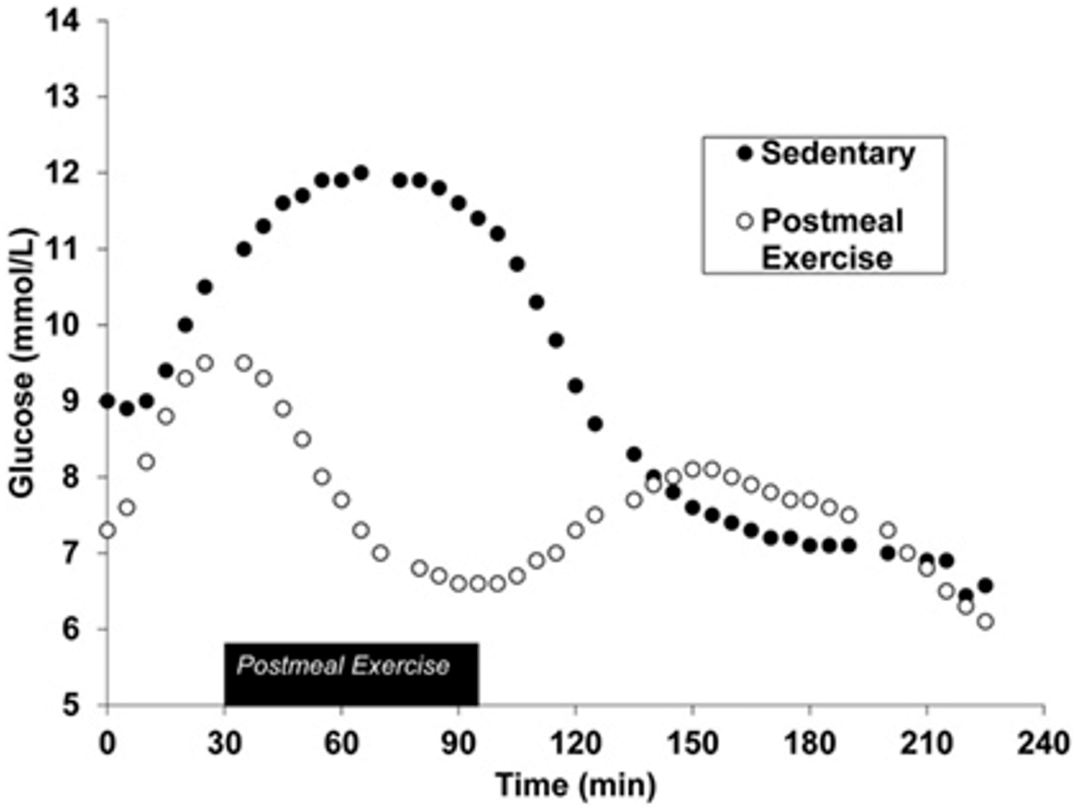

Figure 2.3: Continuous glucose monitoring data during the postprandial phase of both sedentary and postmeal exercise conditions after a standardized meal in the same individual. Figure has been adapted from (Erickson et al., 2017b).

2.3.2 Impact of Physical Activity on Blood Glucose Levels

Physical activity plays a significant role in regulating blood glucose levels by improving insulin sensitivity and facilitating glucose uptake by muscles. During exercise, muscle contractions increase the demand for energy, prompting cells to take up glucose more efficiently, independent of insulin. This not only helps lower blood glucose levels during and after exercise but also improves overall glucose metabolism (Hawley and Lessard, 2008).

For individuals with metabolic disorders like diabetes, physical activity becomes even more critical in managing blood glucose. Exercise can prevent or mitigate dangerous fluctuations in blood glucose levels—hyperglycemia (high blood glucose) and hypoglycemia (low blood glucose)—that can occur due to insulin resistance or impaired insulin production. Aerobic exercises, such as walking and swimming, are particularly effective in lowering blood glucose levels over time, while resistance training can enhance insulin sensitivity and promote muscle glucose uptake (Colberg et al.,

2010). Studies also show that post-meal exercise can significantly reduce postprandial BG levels, especially when initiated 15-30 minutes after eating (Erickson et al., 2017a; Pahra et al., 2017).

However, individuals with diabetes must carefully monitor their blood glucose levels before, during, and after exercise to prevent adverse events like hypoglycemia, which can occur if glucose is rapidly depleted without proper adjustments to medication or diet. Regular blood glucose monitoring is, therefore, an integral part of exercise management for both diabetic and non-diabetic populations (Engeroff et al., 2023).

This approach highlights the importance of personalized exercise timing, especially in preventing postprandial glucose spikes through strategic exercise initiation soon after meals (Hawley and Lessard, 2008; Colberg et al., 2010; Erickson et al., 2017a).

2.3.3 Blood Glucose Monitoring for Health Management

For both healthy individuals and those managing diabetes, continuous blood glucose monitoring (CGM) offers a more comprehensive understanding of the body's metabolic responses to lifestyle choices. Traditional BG monitoring methods, such as finger-prick tests, provide only snapshots of glucose levels at specific times. In contrast, CGM systems track glucose levels in real-time, offering continuous data that can reveal trends and fluctuations throughout the day (Friedman et al., 2023).

CGM devices use sensors placed under the skin to measure glucose in interstitial fluid. These systems allow users to monitor their glucose levels via connected devices, enabling more immediate adjustments to diet, physical activity, and medication. The availability of real-time data is particularly beneficial for individuals with diabetes, as it helps prevent extreme glucose fluctuations and promotes tighter glucose control. Studies have shown that CGM systems can improve glycemic control, reduce hypoglycemic events, and enhance overall quality of life for people with diabetes (Battelino et al., 2019).

For non-diabetic individuals, BG monitoring can still provide valuable insights into how different foods, activities, and stressors affect their metabolic health. Some wearables now integrate CGM technology, allowing users to track their glucose levels alongside other physiological data such as HR and physical activity, offering a more holistic view of health.

2.4 Interaction Between Heart Rate and Blood Glucose

The relationship between HR and BG is a complex but essential aspect of understanding the body's response to physical activity, stress, and metabolic health. These two biomarkers, often considered separately, are intricately linked through physiological processes, particularly during exercise and recovery. Monitoring both HR and BG simultaneously offers a more comprehensive picture of an individual's overall health, enabling better personalization of fitness and health management strategies.

2.4.1 Physiological Link Between HR and BG

During physical activity, the body's demand for energy increases, leading to a cascade of physiological responses. As the muscles require more energy to sustain exercise, the body begins to draw on glucose as a primary fuel source. This increased glucose utilization is accompanied by a corresponding rise in heart rate, which accelerates to supply oxygen and nutrients, including glucose, to the working muscles (Holloszy and Booth, 1976). The interaction between HR and BG is particularly evident during prolonged or high-intensity exercise, where glucose demand surges and the heart works harder to meet the metabolic needs of the body.

Glucose uptake by muscles during exercise can occur both through insulin-dependent and insulin-independent pathways. The latter is particularly important during exercise, as it enables glucose to enter muscle cells without the need for insulin, ensuring a rapid supply of energy even in insulin-resistant states (Goodyear and Kahn, 1998). This mechanism helps explain why BG levels tend to decrease during moderate-to-vigorous physical activity, as glucose is shuttled into muscle cells to fuel continued exertion.

Beyond exercise, the physiological connection between HR and BG is also influenced by other factors such as stress and rest. During stress, the body releases hormones like adrenaline and cortisol, which can cause an increase in HR while simultaneously raising BG levels to provide the energy needed for the fight-or-flight response. Conversely, during rest or recovery periods, both HR and BG typically decrease as the body shifts into a state of restoration and energy conservation (Sharma et al., 2022). This dynamic interplay highlights how HR and BG can offer complementary insights into an individual's physiological state, whether during activity or periods of rest.

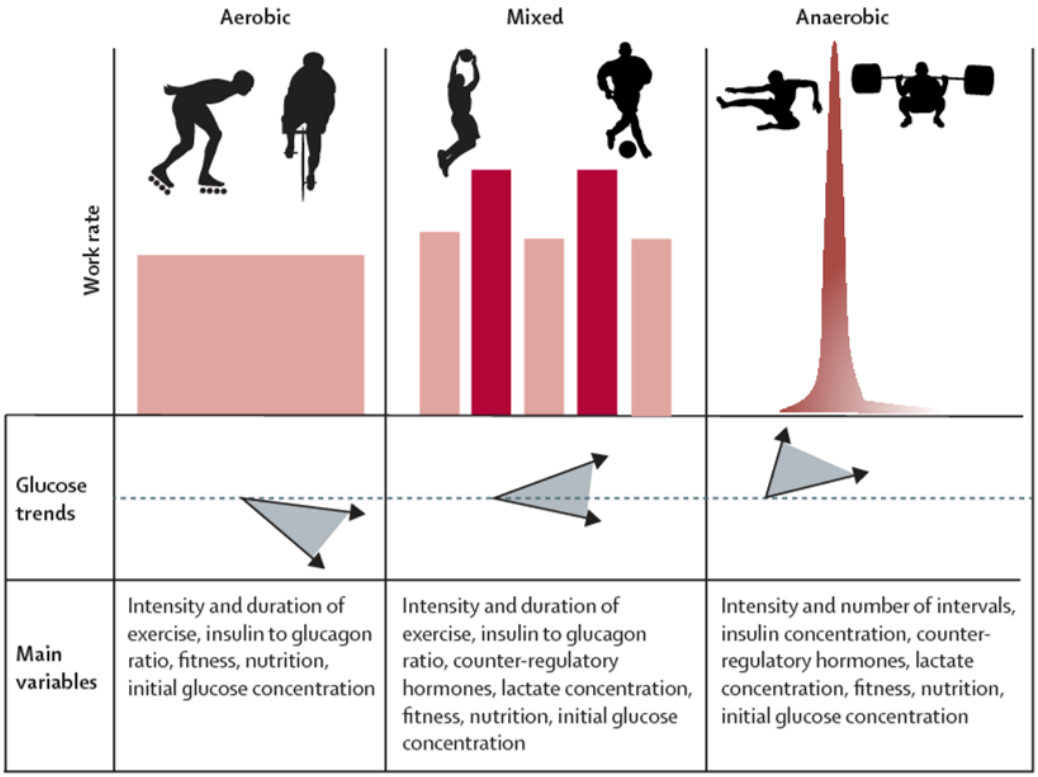

Figure 2.4: Variablility in BG responses to different forms of exercise in people (Riddell et al., 2017). BG responses to different types of exercise in individuals with type 1 diabetes show substantial variation. The arrows and shaded areas illustrate this variability. Typically, aerobic exercise leads to a drop in blood glucose levels, while anaerobic exercise causes an increase. Mixed activities tend to result in stable glucose levels. However, individual responses vary based on several factors, such as exercise duration and intensity, baseline BG levels, fitness, insulin and glucagon concentrations, other counter-regulatory hormones in the bloodstream, and the individual's nutritional state.

2.4.2 Research on HR and BG Monitoring

Recent studies have begun to explore the benefits of monitoring HR and BG together, particularly in the context of exercise and recovery. Research suggests that analyzing both biomarkers can provide a more holistic view of an individual's metabolic and cardiovascular responses, allowing for the development of tailored interventions. For example, a study by Yardley et al. (2013) examined how physical activity affects blood glucose levels in individuals with type 1 diabetes. The researchers found that HR and BG were closely linked during exercise, with moderate-intensity activity leading to significant reductions in BG alongside increased HR (Colberg et al., 2015). Monitoring

both HR and BG allowed for more precise adjustments in insulin dosing and activity levels to prevent hypoglycemia during and after exercise.

Furthermore, studies in people with type 2 diabetes have shown that simultaneous monitoring of HR and BG can improve exercise interventions by optimizing the timing and intensity of workouts. Riddell and Perkins (2009) highlighted that understanding the interaction between these two biomarkers can help individuals with diabetes manage their condition more effectively, particularly in preventing BG fluctuations that could lead to either hyperglycemia or hypoglycemia during physical activity (Riddell and Perkins, 2009).

Wearable technologies have made it easier to continuously monitor HR and BG in real-time. CGM systems, often paired with HR tracking devices, allow users to see how their bodies respond to different types of exercise or stress. This real-time feedback enables individuals to make more informed decisions about their health, whether adjusting their exercise intensity or making nutritional changes to support stable blood glucose levels. Studies using wearable CGMs have shown that combining HR and BG data can significantly enhance personalized health management, particularly for those with metabolic disorders like diabetes (Battelino et al., 2019; Dehghani Zahedani et al., 2021).

By leveraging both HR and BG data, healthcare professionals and individuals can develop more comprehensive health interventions that take into account the dynamic relationship between cardiovascular and metabolic health. This dual-monitoring approach can also help predict physiological responses to future stressors or activities, making it possible to intervene before adverse health outcomes occur.

2.5 Technological Advances and Their Role in Health Monitoring

The rapid progress in wearable technology has transformed the field of health monitoring by offering continuous, real-time data collection for key physiological metrics such as HR and BG. These wearable devices, which have gained widespread popularity, are not only tools for fitness tracking but have become integral to personalized health management. With advanced data analysis and machine learning, these technologies are paving the way for more accurate, individualized health insights.

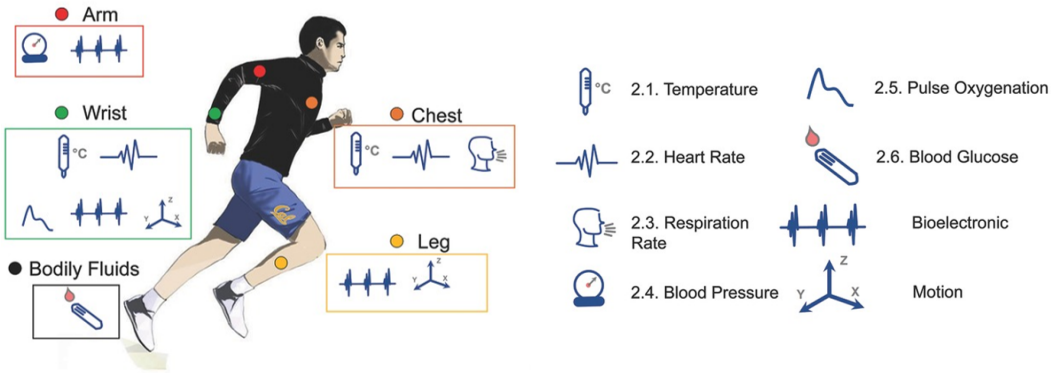

(a) (b)

Figure 2.5: Biosignals and sensing locations (Khan et al., 2016). (a) Wearable medical devices use various body locations to measure biosignals. For example, blood pressure and surface electromyography (sEMG) are typically measured on the arm (red dot). The wrist (green dot) is a versatile spot, capturing signals like temperature, heart rate, pulse oxygenation, bioelectrical, and motion data. The chest (orange dot) can also detect temperature, heart rate, and respiration. The leg (yellow dot) primarily captures bioelectrical and motion signals. Electrochemical sensing, such as from sweat or tears (black dot), can be conducted at various body parts. Other sites, like the finger, earlobe, or forehead, are suitable for pulse oxygenation. The focus here is on non-intrusive measurement sites. (b) Biosignals and their related categories.

2.5.1 Wearables as Tools for Health Data

Wearable devices like smartwatches and fitness trackers are now widely used to monitor health data, including HR and BG. Devices such as the Apple Watch, Fitbit, and Garmin have incorporated sensors that enable the real-time monitoring of vital signs, allowing users to track their health around the clock. In particular, CGM systems like Abbott's Freestyle Libre 2 or Dexcom G7 have revolutionized diabetes management by providing a comprehensive view of glucose fluctuations throughout the day (Moser et al., 2010; Zheng et al., 2020). These CGM systems, often integrated with HR monitors, allow individuals to see how their blood sugar responds to activities like exercise, eating, and sleep, making them valuable tools for maintaining metabolic control.

Wearable technology goes beyond fitness, now providing critical insights into everyday health. For example, users can monitor HR to assess cardiovascular performance and receive notifications of irregular heartbeats or elevated heart rates, offering early detection of potential issues like arrhythmias (Cheung et al., 2018). Simultane-

(a) (b) (c)

Figure 2.6: Various types of HR monitoring tools (Hahnen et al., 2020). (a) BodiMetrics Performance Monitor tricoder. Vital signs are measured by placing the right index finger on the plethysmography sensor located in the upper right corner beneath the flap. (b) Everlast smartwatch. Vital signs are measured by the electrodes and a photoplethysmography sensor located at the back plate. (c) Polar verity sense. Vital signs are measured by the electrodes and a photoplethysmography sensor located at the back plate.

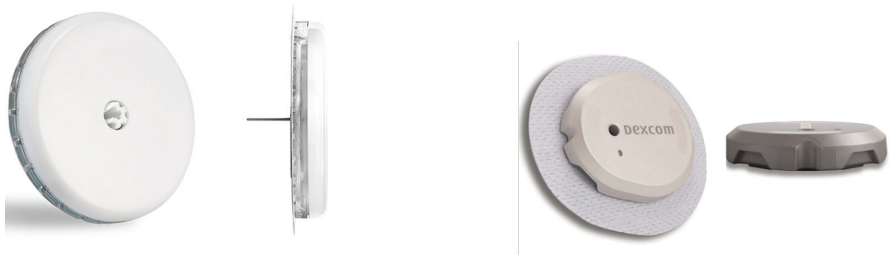

(a) (b)

Figure 2.7: Various types of CGM sensors (Blum, 2018). (a) Freestyle Libre 2. The sensor measures interstitial glucose levels by inserting a small filament just beneath the skin, providing real-time glucose readings for up to 14 days without the need for fingerstick calibrations. (b) Decom G7. This device offers continuous glucose monitoring with a discreet sensor applied on the skin, transmitting glucose data every 5 minutes to a connected device.

ously, continuous BG monitoring offers users a comprehensive understanding of how their lifestyle choices—such as diet and activity—affect their glucose levels, providing actionable insights to manage conditions like diabetes more effectively. As these devices become more sophisticated, their potential for enhancing personalized healthcare continues to expand(Schwartz et al., 2018).

2.5.2 Data Interpretation and Personalized Health

The vast amounts of data collected from wearables offer a new frontier in personalized health management. The integration of HR and BG data, for example, allows healthcare providers and users to gain a clearer understanding of their health trends. HR data reveals insights into cardiovascular health and exercise intensity, while BG data sheds light on metabolic responses to food, stress, and physical activity (Riddell et al., 2017). When analyzed together, these metrics offer a more complete picture of an individual's health, helping tailor fitness programs, optimize diets, and prevent the onset of chronic conditions.

Data from wearable devices can also help predict potential health risks. For instance, abnormal HR patterns combined with fluctuating BG levels may signal poor cardiovascular fitness or the early stages of insulin resistance. Wearable technology equipped with AI-driven analytics can assess this data and generate personalized health insights, improving decision-making for both individuals and healthcare providers. By continuously monitoring these markers, wearables can alert users to potential risks, enabling them to take proactive steps to maintain their health. Recent studies have shown that using both HR and BG data can significantly improve outcomes for patients with type 1 and type 2 diabetes, as well as those aiming to enhance their fitness levels (Barbara and Grobelna, 2022; DeBoer et al., 2017).

Furthermore, advancements in machine learning allow for predictive health models, which help forecast how users' behaviors, such as their exercise or eating habits, will affect their health. These models can help individuals avoid hyperglycemic or hypoglycemic events during exercise or adjust their workout intensity based on their cardiovascular response (Yang and Gao, 2019; Adams and Nsugbe, 2021). For example, by analyzing how BG levels fluctuate in response to certain types of physical activity, users can develop more effective exercise routines that are safe and aligned with their metabolic needs.

In summary, the rise of wearable technology has given users and healthcare professionals unprecedented access to continuous HR and BG data. The ability to track and interpret these metrics in real-time allows for more personalized, data-driven health interventions, ultimately enhancing fitness management, chronic disease prevention, and overall health outcomes.

2.6 Current Gaps and Research Directions

2.6.1 Research Gaps

While advancements in wearable technology and continuous monitoring have significantly enhanced personalized health management, there remain several gaps in research, particularly in the integration of HR and BG data during exercise. Many studies focus on these metrics separately, but few investigate how HR and BG interact during varying exercise types, such as upper and lower body workouts, or dynamic activities like aerobics. This lack of understanding leaves a gap in optimizing fitness programs that consider both cardiovascular and metabolic responses.

Furthermore, although CGM has been transformative for diabetes management, it remains underutilized in non-diabetic populations to explore the interplay of BG and HR in general fitness contexts. Existing wearable devices primarily provide real-time data but lack sophisticated pattern recognition algorithms capable of predicting physiological responses during different types of physical exertion. This is particularly critical for individuals managing chronic conditions or those participating in HIIT, where fluctuations in BG and HR can significantly impact performance and health outcomes (de Oliveira Teles et al., 2022; Hong et al., 2018).

Additionally, most research into predictive models of BG primarily addresses type 1 or type 2 diabetes but does not focus on how these models can be applied to healthy populations or in scenarios involving complex physical activities. The challenge lies in designing models that can integrate HR and BG data to provide early warnings for metabolic or cardiovascular risks, especially during unpredictable exercises or high-stress environments (Nahiduzzaman et al., 2020; Lee and Lee, 2020).

2.6.2 Future Directions in Personalized Health Monitoring

Future developments in personalized health monitoring will likely involve the deeper integration of HR and BG data, enhanced by machine learning and artificial intelligence. As data collection from wearables becomes more sophisticated, predictive models can be refined to offer real-time insights tailored to the individual. For example, wearable devices that monitor multiple parameters—such as heart rate, BG, oxygen saturation, and physical activity—could provide highly specific feedback to users, predicting how their bodies will respond to different types of physical exertion. This would be particularly beneficial for users engaging in high-intensity exercise or

those with metabolic conditions (Haghi et al., 2017; Kusmakar et al., 2018).

In addition to personalized fitness programs, the future of health monitoring could include early detection systems that flag potential health issues before symptoms manifest. Continuous monitoring of HR and BG could identify subtle trends that indicate the early onset of conditions like insulin resistance or cardiovascular strain. This would allow users to make lifestyle adjustments proactively, reducing the likelihood of more serious complications. With the use of advanced data analytics, wearable devices may also provide healthcare providers with comprehensive datasets to inform more personalized treatment plans, moving beyond reactive care to preventive health management (Khan et al., 2016; Hong et al., 2018).

As more research delves into the relationship between HR, BG, and exercise difficulty, the development of comprehensive predictive models will enable a broader range of users to benefit from wearable technologies—not only those managing chronic diseases but also athletes and fitness enthusiasts seeking to optimize performance and health outcomes. Ultimately, wearable technology will become an even more powerful tool for personalized health, bridging the gap between real-time monitoring and long-term disease prevention.

2.7 Summary of Chapter 2

This chapter provides a comprehensive overview of the background and context necessary to understand the integration of HR and BG monitoring in the field of personalized health care and exercise management. It starts by outlining the significance of HR and BG as essential biomarkers for assessing cardiovascular and metabolic health, respectively. Wearable devices are highlighted as key tools in collecting real-time data, particularly through technologies like CGM and heart rate monitors (HRMs).

The chapter discusses how HR and BG interact physiologically during physical activities, as both biomarkers respond dynamically to exercise, stress, and rest. This interaction is critical for understanding the body's metabolic demands and optimizing health outcomes. It also covers how the data collected by wearables can be interpreted to develop personalized health programs, prevent chronic conditions, and improve fitness routines.

However, despite the advances in wearable technologies, current research gaps remain, especially regarding the integration of HR and BG data in predicting exercise outcomes and understanding how different types of exercise affect these biomarkers.

Chapter 2 closes by identifying potential future directions in personalized health monitoring, emphasizing the role of machine learning and predictive models in offering real-time insights and early warnings for metabolic or cardiovascular issues. This lays the foundation for exploring new methodologies that leverage HR and BG data to enhance both fitness and health management strategies.

Chapter 3

HR Modeling Using HR Analysis of Multiple Exercise

Understanding heart rate (HR) responses to physical activity is essential for advancing exercise physiology, health monitoring, and personalized training. This study investigates HR dynamics during combined upper and lower body exercises, exploring the interactions between cardiovascular and muscular systems to better evaluate activity load and individual variability.

Traditional metrics, such as peak HR or resting HR differences, often fall short of capturing the complex and dynamic nature of exercise-induced changes. To address this, we propose a vector-based approach that leverages HR data to analyze intensity through vector magnitudes, dot product calculations, and partial order analysis. This method reveals the consistency and variability of HR responses across exercise combinations and participants, offering novel insights into exercise physiology.

Key findings include the identification of the 40-second rule, where HR patterns stabilize, and the consistent influence of lower body movements in amplifying HR responses, even when paired with static upper body exercises. Partial order analysis further highlighted predictable transition patterns between exercise combinations, demonstrating that the relative intensity of upper and lower body movements is preserved. Similarity assessments supported these findings by validating the robustness of partial orders across participants while identifying unique physiological responses.

By integrating advanced vectorization techniques and partial order analysis, this study provides a comprehensive framework for evaluating activity load. These findings contribute to a deeper understanding of exercise-induced cardiovascular responses, paving the way for more efficient and personalized training protocols that adapt to

individual response patterns and exercise characteristics. This chapter's contents are being prepared for submission to a journal (Yoon and Kim, 2025b).

3.1 Methods

3.1.1 Subjects

All participants were provided with detailed information regarding the study's objectives and gave their informed consent by signing a consent form prior to participating in any experimental procedures. Additionally, all researchers involved in this study completed online research ethics education before the study commenced. The study was conducted according to the protocol approved by the Institutional Review Board (IRB) of Yonsei University, the affiliated institution (Registration number: 7001988-202410-HR-2376-04).

Participants were selected based on specific inclusion and exclusion criteria. The inclusion criteria were as follows: 1) Participants needed to be able to wear a sensor on the left side of their chest; 2) They had to be free of mobility issues, not reliant on walking aids, and capable of visiting the research facility; 3) Participants had to be aged between 20 and 35 years; 4) They needed to be willing to participate voluntarily.

The exclusion criteria were: 1) Individuals with severe communication impairments, such as those resulting from cognitive disabilities or aphasia; 2) Those with serious cardiovascular, cardiopulmonary, or other significant internal medical conditions; 3) Individuals with a history of musculoskeletal or neurological surgeries or diseases; 4) Anyone deemed unsuitable for participation by the researcher.

The demographic and physical characteristics of the participants, including sex, age, height, weight, and BMI, are summarized in Table 3.1 below.

3.1.2 Experiment

3.1.2.1 Experimentation Platform

In the study, ECG data was collected using the Solmitech RE:FIT patch SHC-U8, a mobile holter electrocardiograph. This ECG experimental tool consists of six channels with 250 SPS and a filter range of 0.5Hz to 40Hz. It is a simplified ECG module compared to the traditional 12-lead method commonly used in clinical settings. This module is clinically approved and capable of recording electrocardiograms by attach-

Table 3.1: Characteristics of the subjects. (SD, standard Deviation)

Characteristic	***Values***
Sex (male/female)	4/1
Age (mean± SD)	25.4 ± 1.14 [years]
Height (mean± SD)	175.46 ± 8.01 [cm]
Weight (mean± SD)	71.6 ± 16.28 [kg]
BMI (mean± SD)	23.12 ± 4.15 [kg/m^2]

Note: BMI denotes body mass index.

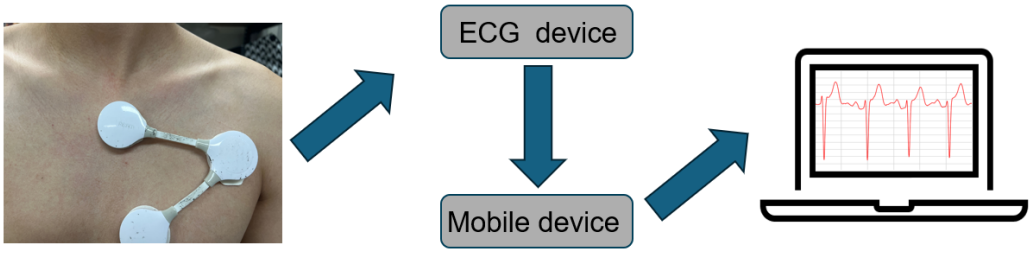

Figure 3.1: ECG sensing system. Monitoring and analysis system of ECG sensor used in this research.

ing electrodes to specific areas on the body surface. It detects the action potentials generated when the myocardium is activated and wirelessly transmits the measured data to a mobile device (figure 3.1). The module is typically worn on the chest in a patch form to measure the ECG.

For the measurements in this study, electrodes were attached to pre-determined positions on the body surface, as identified by the researcher. The placement locations are shown in Figure 3.2 (b). The data measured using the equipment shown in Figure 3.2 (a) was transmitted to a mobile device. The study was conducted based on the data stored on the mobile device.

The utilization of these advanced tools and technologies ensured accurate and reliable data collection, enhancing the credibility and applicability of the study's findings (Salman et al., 2012). The integration of state-of-the-art equipment and software reflects the commitment to producing high-quality research with practical implications for personalized rehabilitation and exercise interventions (Gupta and Saxena, 2012).

(a)

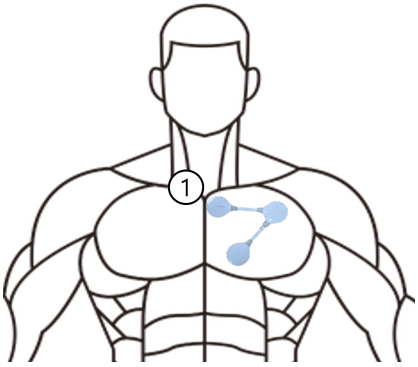

(b)

Figure 3.2: Sensor & sensor attachment drawing. (a) Sensor and patch used in the research. (b) Sensor attachment location.

3.1.2.2 Heart rate difference before and after eating

During the study, control of resting HR was very important. When the resting heart rate was not stable, the maximum heart rate showed a completely different random tendency from the existing criterion. Due to the increase in HR caused by blood transfer to the digestive system after meals, a comparison experiment between before and after meals has proceeded.

3.1.3 Experimental Protocol

The experimental protocol for Chapter 3 was designed based on insights gained from several pilot studies that aimed to establish optimal exercise combinations, intensities, and measurement techniques for HR analysis. The primary goal was to investigate HR

Table 3.2: Exercises Used in Research

Number	Abbreviation	Original Exercise Name
	No-op	No Operation (exclusion of either upper or lower body movement)
ex1(upper)	RF	Reversefly
ex3(upper)	CC	Cross Crunch
ex4(upper)	A180	Arm Full Extend with 180-degree Low Spread
ex5(upper)	FE	Full Lateral Extend
ex1(lower)	SS	Sidestep
ex2(lower)	KU	Kneeup

responses across different exercise types, ensuring precise and consistent measurements by incorporating strict control over exercise execution and resting conditions.

3.1.3.1 Exercise Selection and Combinations

The pilot studies guided the selection of exercise combinations that would provide a comprehensive spectrum of HR responses. Initially, a variety of upper and lower body exercises were considered, but through repeated testing, the final selection was narrowed down to five upper body exercises (No-op, Reverse Fly (RF), Cross Crunch (CC), Arm Full Extend 180 Angle Low Spread (A180), and Full Lateral Extend (FE)) and three lower body exercises (No-op, Sidestep (SS), and Kneeup (KU)). These exercises were chosen based on their ability to elicit distinct HR responses and to represent a range of exercise intensities.

The main experiment involved conducting exercise sessions for all combinations of the selected upper and lower body exercises, resulting in 14 unique exercise combinations, excluding the combination of exclusion of both upper and lower body movement. These combinations, detailed in Table 3.2, provided a comprehensive analysis of HR responses during upper and lower body exercise interactions. Every exercise was performed at a uniform pace of 60 BPM to maintain consistency across sessions, ensuring that variations in HR were due solely to activity load and not speed.

3.1.3.2 Experimental Structure and Data Collection

Each exercise session was divided into two distinct phases: a 1-minute resting phase followed by a 1-minute exercise phase. The resting phase was crucial for establishing a baseline HR, allowing for accurate comparisons between exercises. During this phase,

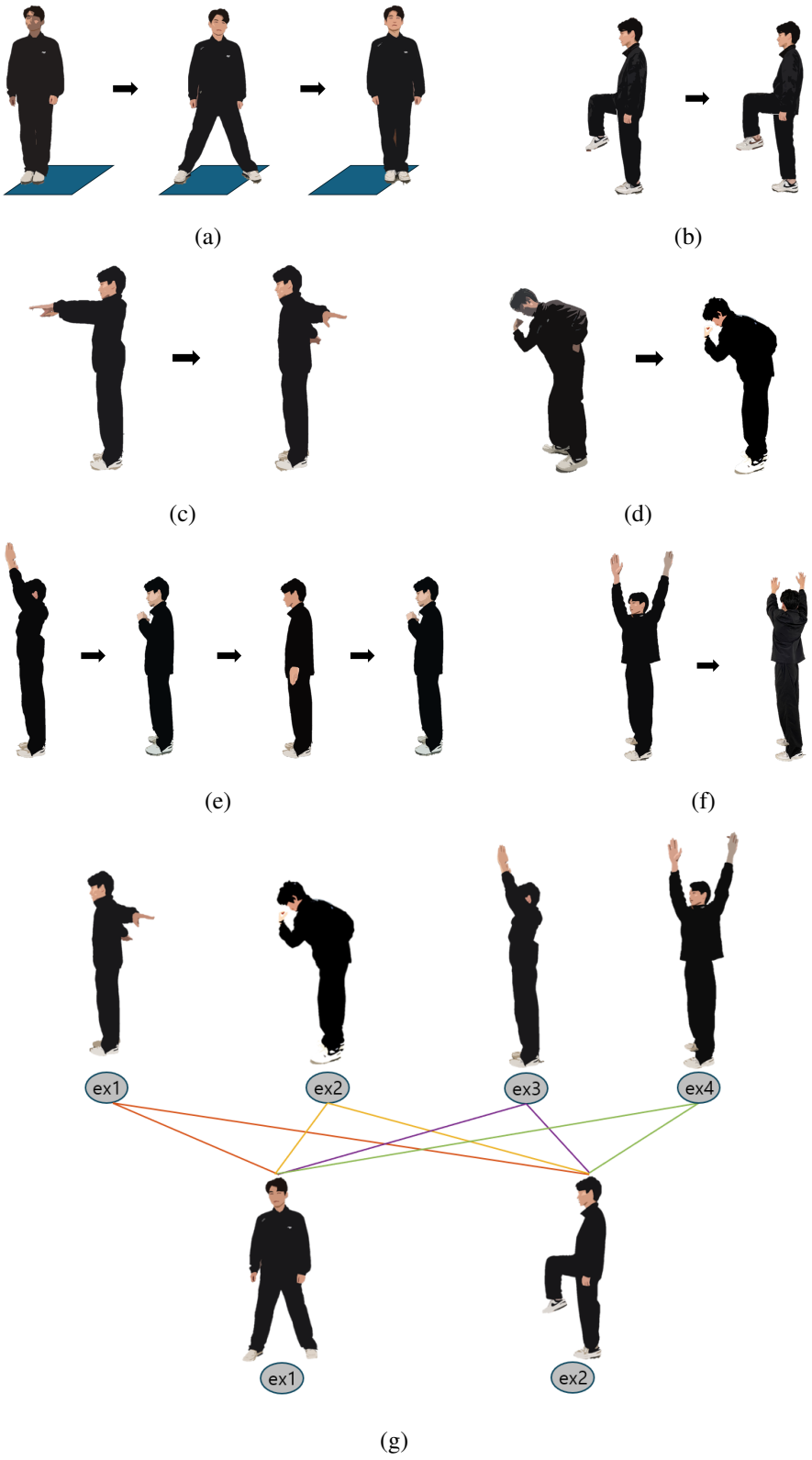

Figure 3.3: Sequence and combination of upper body exercises and lower body exercises. Each lower body exercise proceeded with a combination of 4 upper body exercises(shown in (g)). (a) to (f) shows a sequence in the following order: SS, KU, RF, CC, A180, FE

participants maintained a stationary position to capture an accurate resting HR, which served as the reference point for subsequent HR analysis.

The exercise phase involved performing the designated upper and lower body movements simultaneously for 1 minute. The 60 BPM rhythm was used to synchronize movements across all participants, ensuring consistency in activity load and cadence. This rhythmic control was critical, as any deviation could influence the HR response, thus affecting the reliability of the data.

The HR sensor was carefully positioned to minimize motion-related noise and ensure precise HR monitoring throughout the study. As detailed in the experimental setup, the sensor was strategically placed at locations that optimized data accuracy, capturing clean and consistent HR signals across all exercise combinations.

3.1.3.3 Considerations for Resting Heart Rate and Exercise Control

One of the key findings from the pilot studies was the significant role of controlling the resting HR before starting the exercise phase. Any instability in the resting HR led to unpredictable fluctuations in the maximum HR observed during the exercise, which complicated the accurate assessment of activity load. Therefore, careful measures were implemented to ensure that each participant commenced every exercise session with a stabilized resting HR.

Additionally, the pilot study explored an extended exercise phase lasting up to 3 minutes, with a 1-minute resting phase preceding it. This was conducted to determine the optimal duration needed to capture meaningful HR changes. Through this analysis, it was found that participants were unable to sustain a consistent HR pattern or maintain a steady dot product trend beyond the first minute of exercise. As illustrated in Figure 3.4, which depicts dot product trends from 10 seconds to 180 seconds, HR fluctuations became more pronounced over time. This inconsistency in maintaining a steady dot product trend reflects challenges participants faced in sustaining consistent exercise loads, likely due to factors such as increased fatigue or difficulty maintaining the exercise movement.

Ultimately, these fluctuations highlighted the importance of choosing a 60-second exercise duration for the main study. This duration allowed the capture of the most representative and consistent HR response patterns, ensuring that the observed data truly reflected the activity load without being influenced by the participant's fatigue or difficulties in maintaining the exercise load over extended periods.

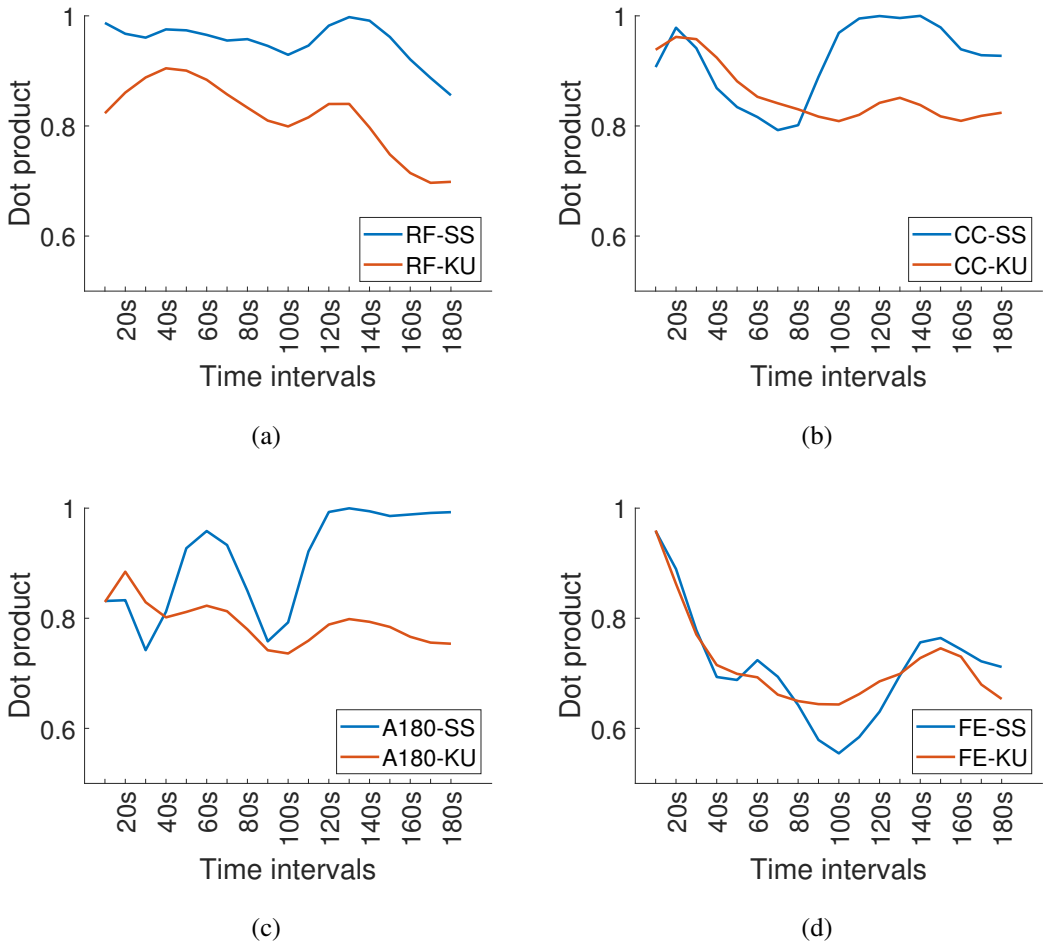

Figure 3.4: Trend graphs showing dot product levels over 3 minutes for both upper-body-based exercise combinations.

3.1.3.4 Managing Physical Fatigue and Data Quality

To ensure data quality and manage physical fatigue, mandatory 10-minute rest intervals were enforced between each exercise combination. This allowed participants' HR to return to baseline levels, ensuring that each exercise session began under comparable conditions. This rest period was essential for maintaining consistency and reducing the risk of accumulated fatigue affecting HR responses.

Additionally, the experiment protocol accounted for potential influences from factors such as food intake. It was observed that postprandial (after eating) increases in HR could interfere with baseline measurements. Therefore, comparisons of HR before and after meals were conducted to account for these variations, ensuring that the data collected accurately reflected the physiological impact of the exercises themselves.

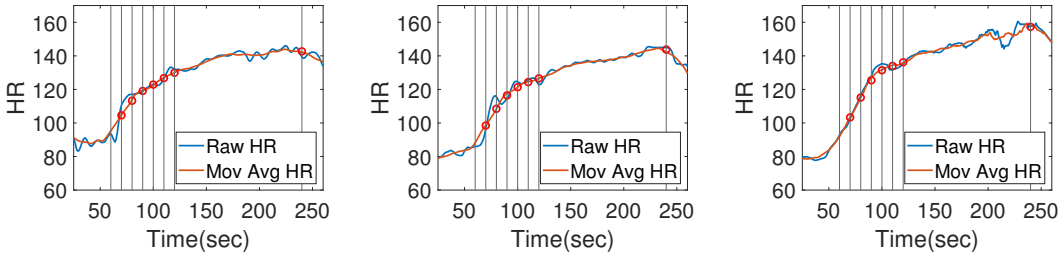

(a) (b) (c)

Figure 3.5: An example of HR data acquisition process used for the analysis. The blue line represents the raw HR data, while the red line is the smoothed HR data, obtained by applying a moving average to reduce fluctuations in the raw signal. Each vertical black line marks specific time intervals at 10 sec, 20 sec, 30 sec, 40 sec, 50 sec, 60 sec, and 3 min. At each marked interval, HR data was calculated by averaging the moving average HR over a 10-second window before and after the respective time point.

3.1.3.5 Refining the Analysis: Insights from Pilot Studies

The pilot studies played a crucial role in highlighting the need for precise exercise control to ensure consistent and reliable HR patterns. It became evident that HR responses were significantly more stable and predictable when exercises were performed under controlled and consistent loads, emphasizing the importance of maintaining movement cadence and resting HR stabilization. This insight was pivotal in shaping the main experimental design, ensuring that each exercise was executed with the necessary precision to yield accurate HR data.

Furthermore, establishing the integrity of the collected HR data was essential for the vector-based analysis. As demonstrated in Figure 3.5, the HR readings consistently exhibited a monotonic increase throughout the exercise duration, confirming the authenticity and reliability of the data. This continuous upward trend aligns with the physiological understanding that HR naturally rises with sustained physical exertion. Such confirmation provides more than just technical assurance; it serves as a foundation of trust in the data, allowing for a deeper exploration of intricate patterns and interactions in subsequent analyses. This stable and representative dataset sets the stage for the vector-based approach, ensuring that any deviations observed are genuinely reflective of exercise characteristics rather than anomalies.

3.1.4 Data Analysis

3.1.4.1 Data Preprocessing

Robust data preprocessing was imperative for the ECG signals due to their susceptibility to biological and mechanical noise (Gupta et al., 2021). To ensure the reliability of subsequent analyses, a meticulous preprocessing pipeline was implemented (Tejedor et al., 2019). The raw ECG signal underwent a 60Hz Notch filter to eliminate power noise, a common interference arising from electrical systems. Subsequently, both high-pass and lowpass filters were applied to analyze signals, focusing on the bandpass frequencies of 10Hz to 30Hz. These steps ensured the extraction of accurate HR data, devoid of undesirable noise artifacts (Flandrin et al., 2003). The implementation of these preprocessing steps fortified the quality and reliability of the data, establishing a robust foundation for the subsequent analysis of the HR signals during the experimental exercises.

3.1.4.2 Analysis in HR from ECG data

In ECG, the R-peak represents the apex of the QRS complex (Manikandan and Dandapat, 2012; Shaik and Ramakrishna, 2015), signifying the ventricular depolarization of the heart(Kligfield and Lauer, 2006). The RR interval, the temporal span between two consecutive R-peaks, serves as a pivotal parameter for HR calculation(Park and Lee, 2017). After preprocessing, R-peak points were identified, and the HR(Achten and Jeukendrup, 2003; Shaik and Ramakrishna, 2015) was computed using the equation:

$$\mathrm{HR}_{subject} = \frac{60}{\mathrm{RR}_{interval}}\mathrm{sec} \tag{3.1}$$

3.1.4.3 activity load Calculation

To assess activity load in this study, the difference between the heart rate during exercise ($HR_{exercise}$) and the resting heart rate (HR_{rest}) was utilized. This simplified approach builds upon the widely recognized Karvonen formula, which is commonly used for activity load estimation through heart rate measurements (She et al., 2015). The Karvonen formula is expressed as:

$$\mathrm{Intensity}\% = \frac{HR_{exercise} - HR_{rest}}{HR_{max} - HR_{rest}} \tag{3.2}$$

While the Karvonen formula incorporates both the maximum heart rate (HR_{max}) and the resting heart rate (HR_{rest}) to normalize intensity levels, this study adopts a

modified version that simplifies the calculation by omitting the denominator. The activity load is therefore calculated as:

$$\text{Intensity} = HR_{exercise} - HR_{rest} \tag{3.3}$$

This adaptation was made to focus on intra-individual comparisons of activity load based on heart rate variations induced by upper and lower body movements. By simplifying the calculation, the study aims to highlight relative intensity differences between exercise types within each participant, rather than across participants. This approach provides a straightforward yet effective metric for analyzing the dynamics of combined upper and lower body exercises.

3.2 Vector Representation and Plotting of Data

The data is represented as a matrix $\mathbf{D}$ with dimensions (α, β), where $\alpha \in \{1, 2, \ldots, m\}$ represents different lower exercise levels (y-axis), and $\beta \in \{1, 2, \ldots, n\}$ represents upper exercise HR data (x-axis). Each dimensions was set m = 3, n = 5. The data matrix is defined as:

$$\mathbf{D} = \{d_{\alpha,\beta} \mid \alpha \in \{1, 2, \ldots, m\}, \beta \in \{1, 2, \ldots, n\}\}. \tag{3.4}$$

When the upper body is fixed and lower body values are used as the x-axis for calculations, the matrix $\mathbf{D}$ is transposed to ensure consistency in the computation process. The dat matrix is defined as: The data matrix is defined as:

$$\mathbf{D}' = \{d_{\beta,\alpha} \mid \beta \in \{1, 2, \ldots, n\}, \alpha \in \{1, 2, \ldots, m\}\}. \tag{3.5}$$

Each column of $\mathbf{D}$ is plotted against corresponding α-values. The x-axis values for the β-th column are given by:

$$x_\beta = d_{\alpha,\beta}, \quad \beta \in \{1, 2, \ldots, n\}. \tag{3.6}$$

The y-axis values are extracted from the first column ($\beta = 1$) as:

$$y_\alpha = d_{\alpha,1}, \quad \alpha \in \{1, 2, \ldots, m\}. \tag{3.7}$$

Thus, each plot line is represented as:

$$\text{Line}_\beta = \{(x_\beta, y_\alpha) \mid \alpha \in \{1, 2, \ldots, m\}\}. \tag{3.8}$$

Each data point is represented as a vector $\mathbf{v}_{\alpha,\beta}$ defined by:

$$\mathbf{v}_{\alpha,\beta} = \begin{bmatrix} x_{\alpha,\beta} \\ y_{\alpha,\beta} \end{bmatrix}, \tag{3.9}$$

Where:

$$x_{\alpha,\beta} = d_{\alpha,\beta} - d_{1,\beta}, \quad y_{\alpha,\beta} = d_{\alpha,1}. \tag{3.10}$$

The magnitude $A_{\alpha,\beta}$ of each vector is computed as:

$$A_{\alpha,\beta} = \|\mathbf{v}_{\alpha,\beta}\| = \sqrt{x_{\alpha,\beta}^2 + y_{\alpha,\beta}^2}. \tag{3.11}$$

Each vector is normalized to have unit magnitude:

$$\hat{\mathbf{v}}_{\alpha,\beta} = \begin{bmatrix} \frac{x_{\alpha,\beta}}{A_{\alpha,\beta}} \\ \frac{y_{\alpha,\beta}}{A_{\alpha,\beta}} \end{bmatrix}. \tag{3.12}$$

The angle $\theta_{\alpha,\beta}$ of each vector is calculated as:

$$\theta_{\alpha,\beta} = \tan^{-1}\left(\frac{y_{\alpha,\beta}}{x_{\alpha,\beta}}\right). \tag{3.13}$$

This angle is adjusted relative to the initial vector ($\mathbf{v}_{1,1}$) to compute the refined degree:

$$\text{Refined Degree}_{\alpha,\beta} = \theta_{\alpha,\beta} - \theta_{1,1}. \tag{3.14}$$

The dot product between a vector $\mathbf{v}_{\alpha,\beta}$ and the initial vector $\mathbf{v}_{1,1}$ is computed as:

$$\text{Dot Product}_{\alpha,\beta} = A_{\alpha,\beta}^2 \cdot A_{1,1}^2 \cdot \cos(\text{Refined Degree}_{\alpha,\beta}). \tag{3.15}$$

Using normalized vectors, the dot product is simplified as:

$$\text{Normalized Dot Product}_{\alpha,\beta} = \hat{\mathbf{v}}_{\alpha,\beta} \cdot \hat{\mathbf{v}}_{1,1}. \tag{3.16}$$

The set of all vectors can be defined as:

$$\mathcal{V} = \{\mathbf{v}_{\alpha,\beta} \mid \alpha \in \{1,2,\ldots,m\}, \beta \in \{1,2,\ldots,n\}\}. \tag{3.17}$$

3.3 Results

3.3.1 Transforming HR Data into Vectors: A New Perspective on Exercise Analysis

3.3.1.1 Visualizing activity load with Vectorization

Traditionally, activity load has been quantified by looking at metrics like the maximum HR or the difference between maximum HR and resting HR (Figure 3.6). While

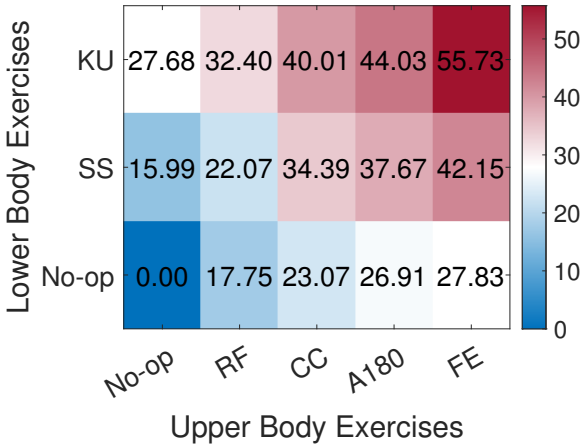

Figure 3.6: Heatmap representation of the difference between maximum HR and resting HR for various exercise combinations at the 60-second mark. The x-axis represents different upper body exercises, while the y-axis shows different lower body exercises. The color intensity indicates the magnitude of the HR difference, with warmer colors representing greater increases in HR relative to resting levels. The No-op on the x-axis represents the exclusion of upper body movement, while the No-op on the y-axis represents the exclusion of lower body movement.

effective to an extent, these conventional metrics often fail to capture the dynamic and multi-dimensional nature of physical activity. In this study, we introduced a novel approach by converting HR data into vector forms, offering a fresh perspective on understanding activity load.

To overcome the limitations of conventional HR metrics, we transformed HR data into vector forms, allowing for a multi-dimensional representation of activity load. Figure 3.6 provides an initial comparison using a traditional colormap, showing the differences between maximum HR and resting HR for various exercise combinations. Warmer colors indicate more significant HR differences, suggesting higher intensity. While this approach offers a straightforward visualization, it lacks the ability to capture the nuanced shifts in activity load over time.

Moving beyond this traditional representation, Figure 3.7 introduces the vector-based method (based on equations 3.4, 3.6 to 3.8), where each exercise combination is represented as a distinct vector path over time intervals. By plotting HR values from upper and lower body exercises, we observed that vector paths provide a clearer distinction between exercise intensities. For example, at the 40-second mark in Figure 3.7, the vectors show a more pronounced separation between exercises, indicating that

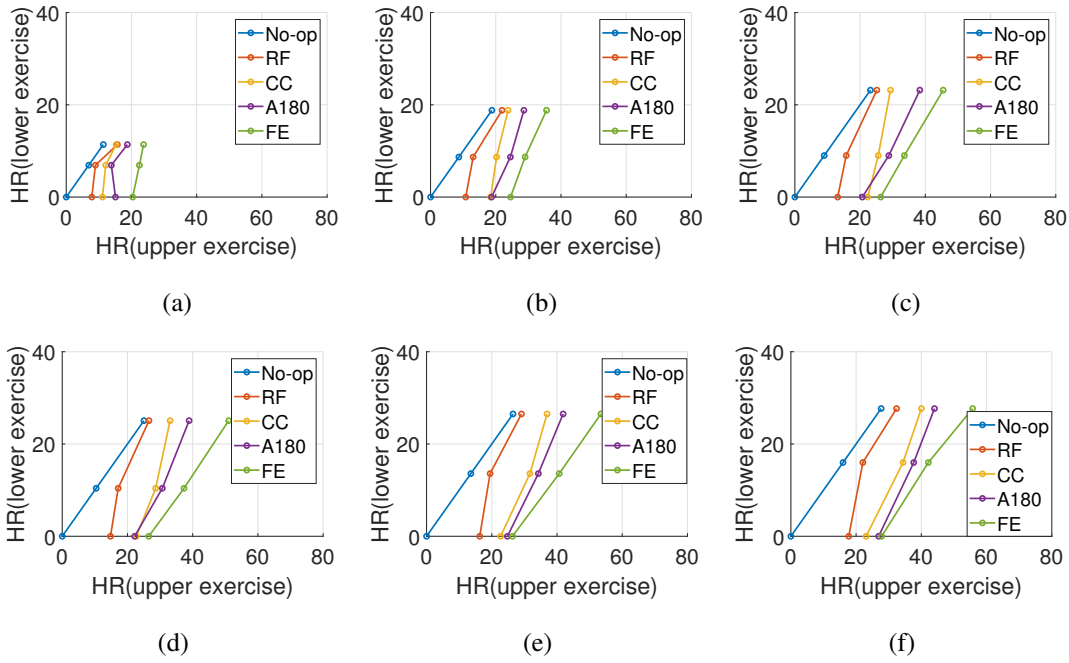

Figure 3.7: Time-series comparison of HR responses during various upper and lower body exercise combinations. The x-axis represents HR measurements for upper body exercises while the y-axis is fixed with the HR observed during the combination of a specific lower body exercise with the exclusion of an upper body exercise. No-op represents the exclusion of upper body movement. The subplots correspond to different durations of exercise: (a) 10 sec, (b) 20 sec, (c) 30 sec, (d) 40 sec, (e) 50 sec, (f) 60 sec.

this method effectively captures intensity differences that become more apparent over time. This finding aligns with our earlier assertion that exercise trends can be efficiently captured within 40 seconds, making it an optimal interval for assessing activity load.

In Figure 3.8, the HR vectors are further refined, demonstrating how each vector progresses over different time intervals (based on equations 3.9 and 3.10). This process enables the visualization of how exercises with similar intensities exhibit similar vector trajectories, thus providing an intuitive understanding of exercise similarity and difficulty. This vector representation serves as a foundation for subsequent dot product analysis, where these vectors are used to quantify the degree of similarity or difference between exercises.

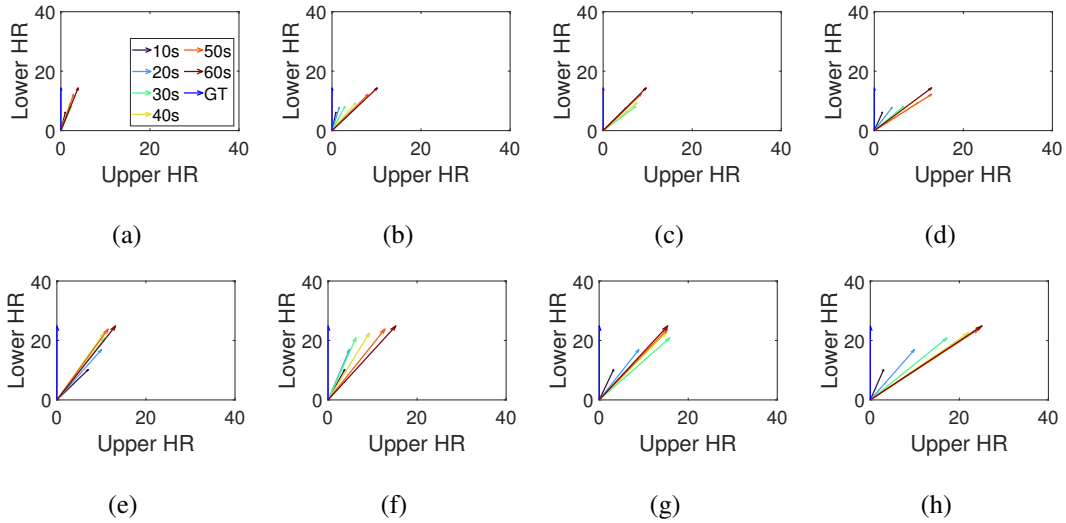

Figure 3.8: Visualization of the HR vectors derived from combinations of upper and lower body exercises over different time intervals. The HR vectors are plotted for each upper body exercise paired with two different lower body exercises. The x-axis represents the HR of the upper body exercise, and the y-axis represents the level of HR for the lower body exercise. Subplots (a) to (d) correspond to combinations of the 'SS' lower body exercise with the following upper body exercises in sequence: (a) RF, (b) CC, (c) A180, and (d) FE. Subplots (e) to (h) represent the same upper body exercises in the same order but paired with the 'KU' lower body exercise. The different colored arrows indicate the HR changes over time, with each arrow corresponding to different time points (10s, 20s, 30s, 40s, 50s, 60s). Also, the last arrow corresponds to Ground Truth which is a baseline for the dot product.

3.3.1.2 Normalizing HR Vectors and Establishing Ground Truth

Figure 3.9 showcases the normalized representation of the HR vectors from Figure 3.8 (based on equations 3.11 and 3.12). By normalizing the vectors, we ensure that activity load comparisons are not skewed by the absolute values of HR, but rather reflect the relative intensity patterns across different exercises. This normalization process makes it possible to observe how different exercise combinations converge or diverge in terms of their intensity profiles, providing a more accurate comparison.

In Figure 3.10, the comparison between vector magnitudes and actual HR data reveals a similarity in the trends (based on equation 3.11). This similarity underscores the validity of the vector-based method in capturing activity load patterns. The magnitude of a vector directly correlates with the overall HR response, confirming that

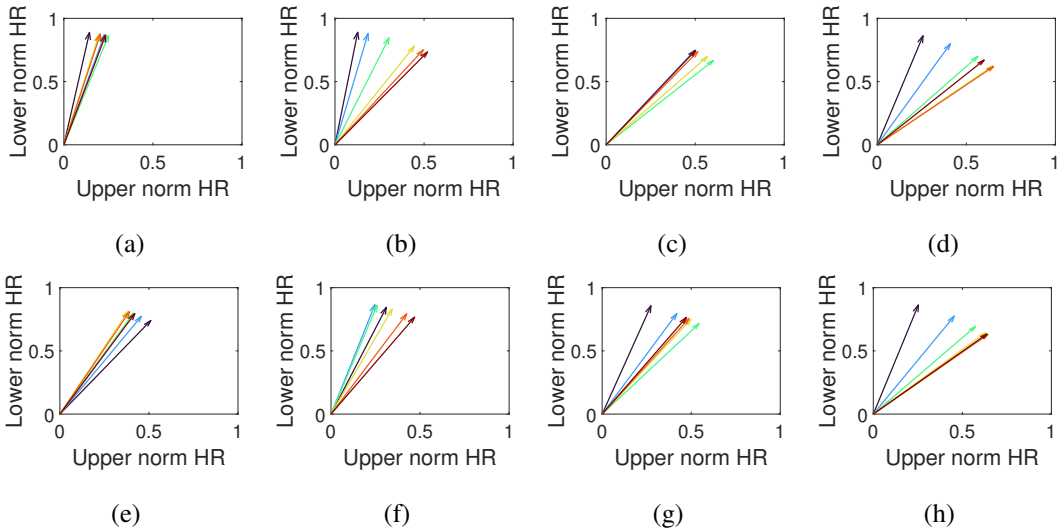

Figure 3.9: Normalized representation of HR vectors from Figure 3.8, depicting the relationship between upper and lower body exercises. The x-axis and y-axis represent the normalized HR values for upper and lower body exercises, respectively, over time. Each vector corresponds to a specific time point, showing how HR changes relative to the maximum HR for each exercise combination. Subplots (a) to (d) correspond to the 'SS' lower body exercise paired with the following upper body exercises in sequence: (a) RF, (b) CC, (c) A180, and (d) FE. Subplots (e) to (h) represent the same upper body exercises paired with the 'KU' lower body exercise. The normalization allows a clearer comparison of HR change patterns between different exercise combinations by scaling HR values between 0 and 1.

our vectorization approach effectively represents the intensity and effort involved in each exercise combination. This insight not only reinforces the accuracy of the vector method but also demonstrates that this approach is capable of capturing the essential aspects of activity load that traditional HR metrics might overlook.

3.3.2 Exploring the 40-Second Rule: A Key Insight into Activity Load

3.3.2.1 Dot Product Analysis and Consistent Intensity Trends

One of the most significant findings in this study is the identification of the 40-second rule, which suggests that activity load patterns stabilize around the 40-second mark, regardless of exercise type or combination. Figure 3.11 provides a detailed analysis of dot product comparisons between different upper body exercises paired with a sidestep

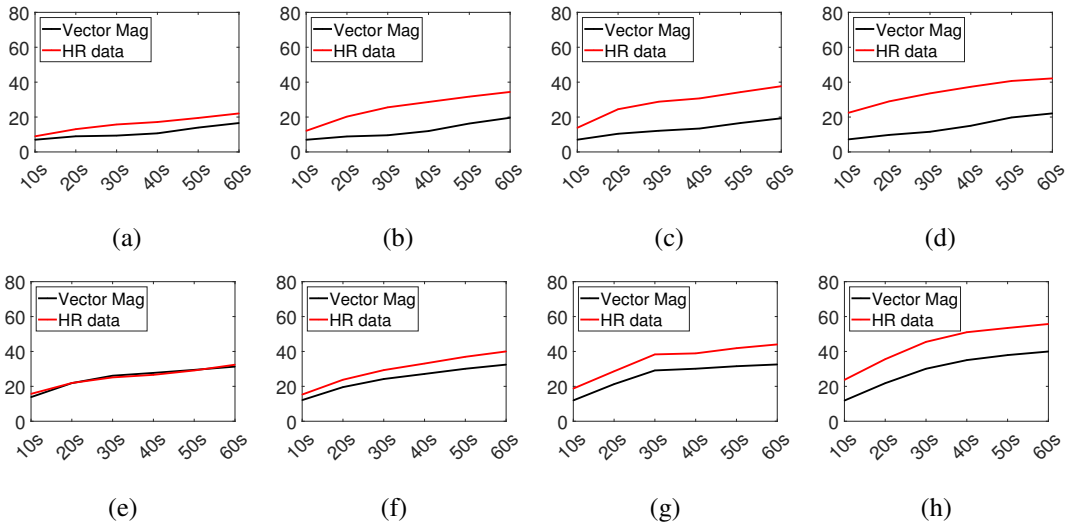

Figure 3.10: Comparison between vector magnitudes and actual HR data over time for different exercise combinations. The x-axis represents time intervals (10s, 20s, 30s, 40s, 50s, 60s), while the y-axis shows the values of vector magnitude (black line) and actual HR data (red line). Subplots (a) to (d) correspond to the 'SS' lower body exercise paired with upper body exercises in the sequence: (a) RF, (b) CC, (c) A180, and (d) FE. Subplots (e) to (h) represent the same upper body exercises paired with the 'KU' lower body exercise.

and kneeup lower body exercise over various time intervals (based on equations 3.13 to 3.16). The dot product values show a clear trend, where after 40 seconds, the intensity levels across different exercise combinations become more consistent. Same analysis is done with the transposed data sets, for where upper body values are fixed and the lower body valuse are used as the x-axis for calculations (shown in Figure 3.12) (based on equations 3.5, 3.9 and 3.10). This observation supports the idea that prolonged exercise durations may not be necessary to gauge intensity accurately, making the 40-second interval an efficient measure for exercise assessment.

Furthermore, Figure 3.14 (a) to (d) (based on equation 3.16), which focuses on upper-body-based exercise combinations, confirms this finding. By observing the dot product trends, we see that the patterns begin to stabilize around the 40-second mark, indicating that this interval is sufficient to capture the exercise's full impact. This consistency not only validates the 40-second rule but also highlights its potential for practical applications in exercise protocol design, particularly for individuals who may struggle with longer exercise durations.

To further explore the robustness of the 40-second rule, we extended the dot prod-

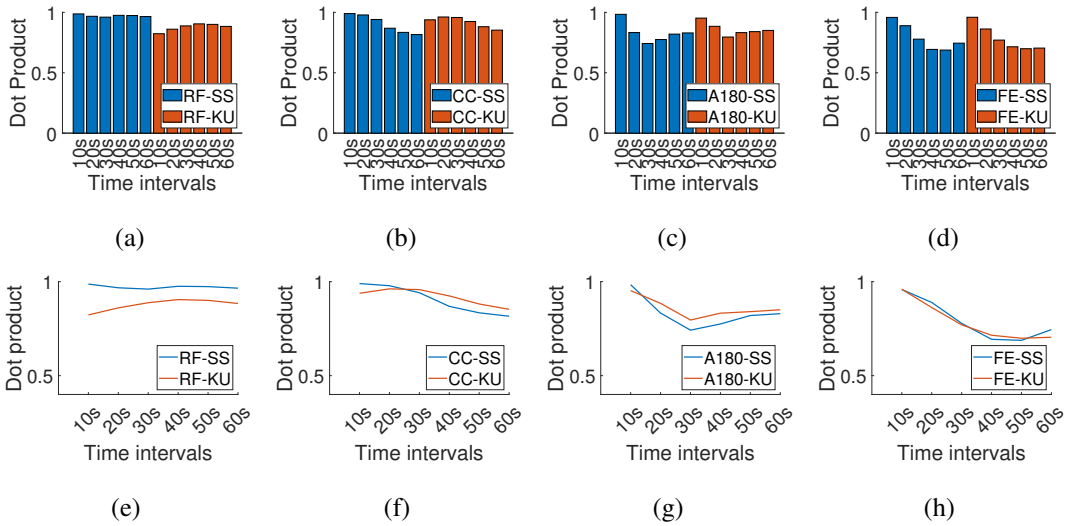

Figure 3.11: Analysis of dot product comparisons between different upper body exercises paired with a sidestep and kneeup lower body exercises over various time intervals. Subplots (a) to (d) represent the dot product values for each upper body exercise paired with SS (blue bars) and KU (orange bars), in sequence: (a) RF, (b) CC, (c) A180, and (d) FE. Subplots (e) to (h) convert the data from (a) to (d) into line graphs to illustrate the trends more clearly.

uct analysis to multiple participants, as shown in Figures 3.14 and 3.15. These figures illustrate the HR responses at the 40-second mark for different individuals, with subplots representing both upper and lower body exercise combinations. Despite variations in individual physiological responses, the dot product trends consistently align with the 40-second rule, indicating a universal pattern in how activity load is reflected in HR data.

Figure 3.15, which examines lower body fixed combinations, reveals similar findings. Across different participants, the trend graphs show that the dot product values stabilize around the 40-second mark, further reinforcing the idea that this interval is a reliable measure of activity load (based on equations 3.5, 3.15). This consistency across individuals suggests that the 40-second rule can be broadly applied, making it a valuable tool for activity load assessment in diverse populations.

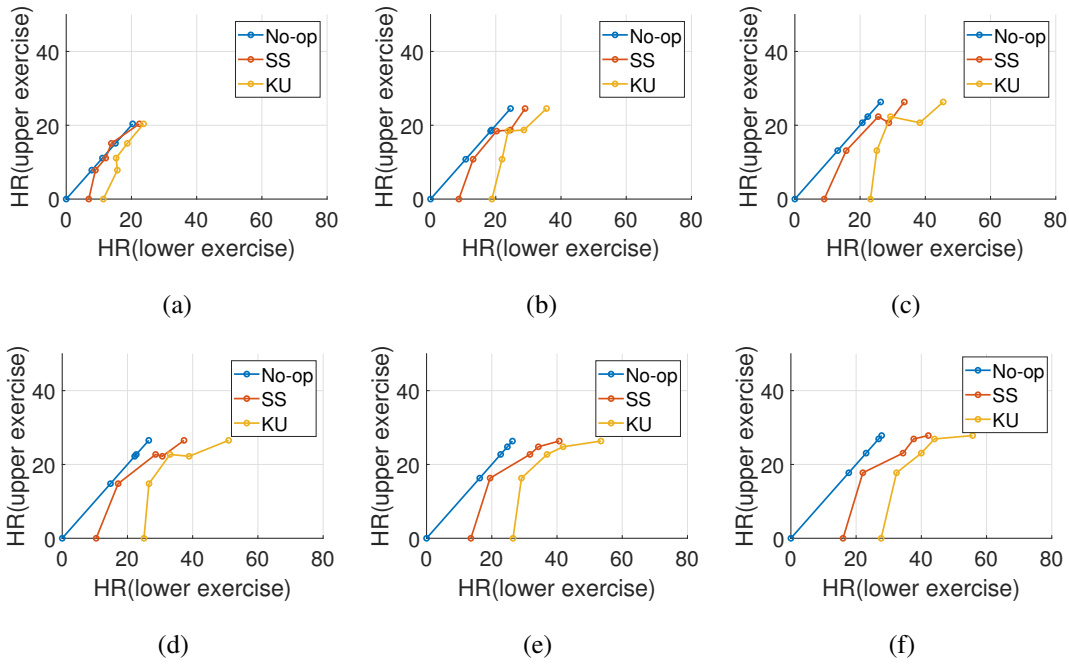

Figure 3.12: Transposed time-series comparison of HR responses during various upper and lower body exercise combinations. The x-axis represents HR measurements for lower body exercises, while the y-axis is fixed with the HR observed during the combination of a specific upper body exercise with the exclusion of a lower body exercise. No-op represents the exclusion of lower body movement. Each subplot corresponds to a different exercise duration: (a) 10 sec, (b) 20 sec, (c) 30 sec, (d) 40 sec, (e) 50 sec and (f) 60 sec.

3.3.3 Analysis of Exercise Characteristics Through Pattern Recognition

In this section, we analyze the characteristics of different exercises by examining the pattern trends from the figures, particularly focusing on the upper and lower body contributions to HR changes. Through the analysis of Figures 3.14 to 3.16, we can observe distinct patterns in how different exercises influence the HR response, allowing us to better understand the intensity and difficulty of each exercise.

3.3.3.1 Identifying activity load Patterns

One of the key observations from Figure 3.13 is the distinct shape patterns in the HR responses at the 40-second mark for different participants(based on equations 3.5 to 3.9). Specifically, an upward-bending shape, resembling an ‘Γ’, indicates that lower

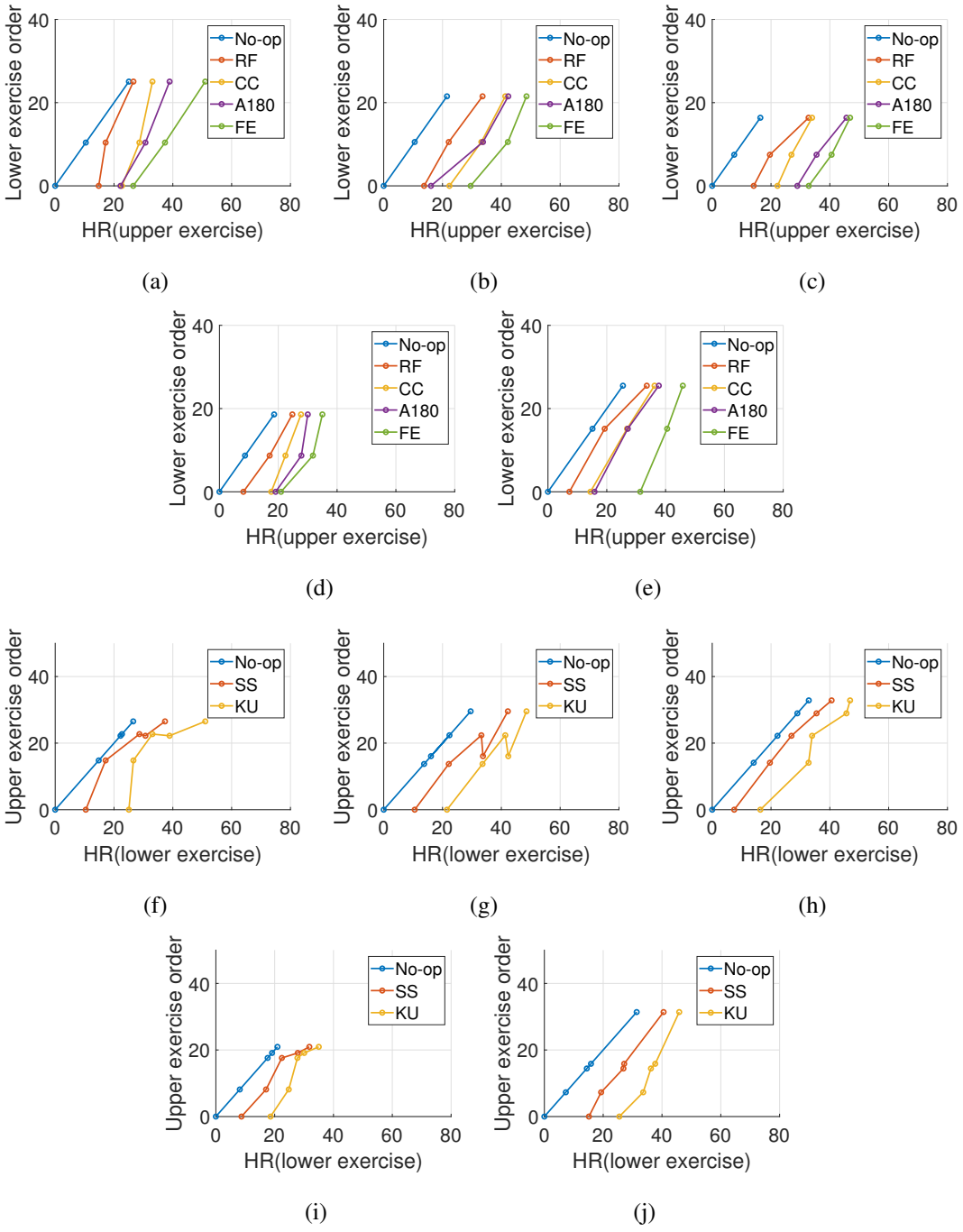

Figure 3.13: Comparison of HR responses at the 40-second mark for different participants. Subplots (a)-(e) represent the plots for all participants, based on the figure shown for a single participant in Figure 3.7(d). Subplots (f)-(j) represent the plots for all participants, based on the figure shown for a single participant in Figure 3.12(d). For (a)-(e) No-op represents the exclusion of upper body movement, and for (f)-(j) No-op represents the exclusion of lower body movement.

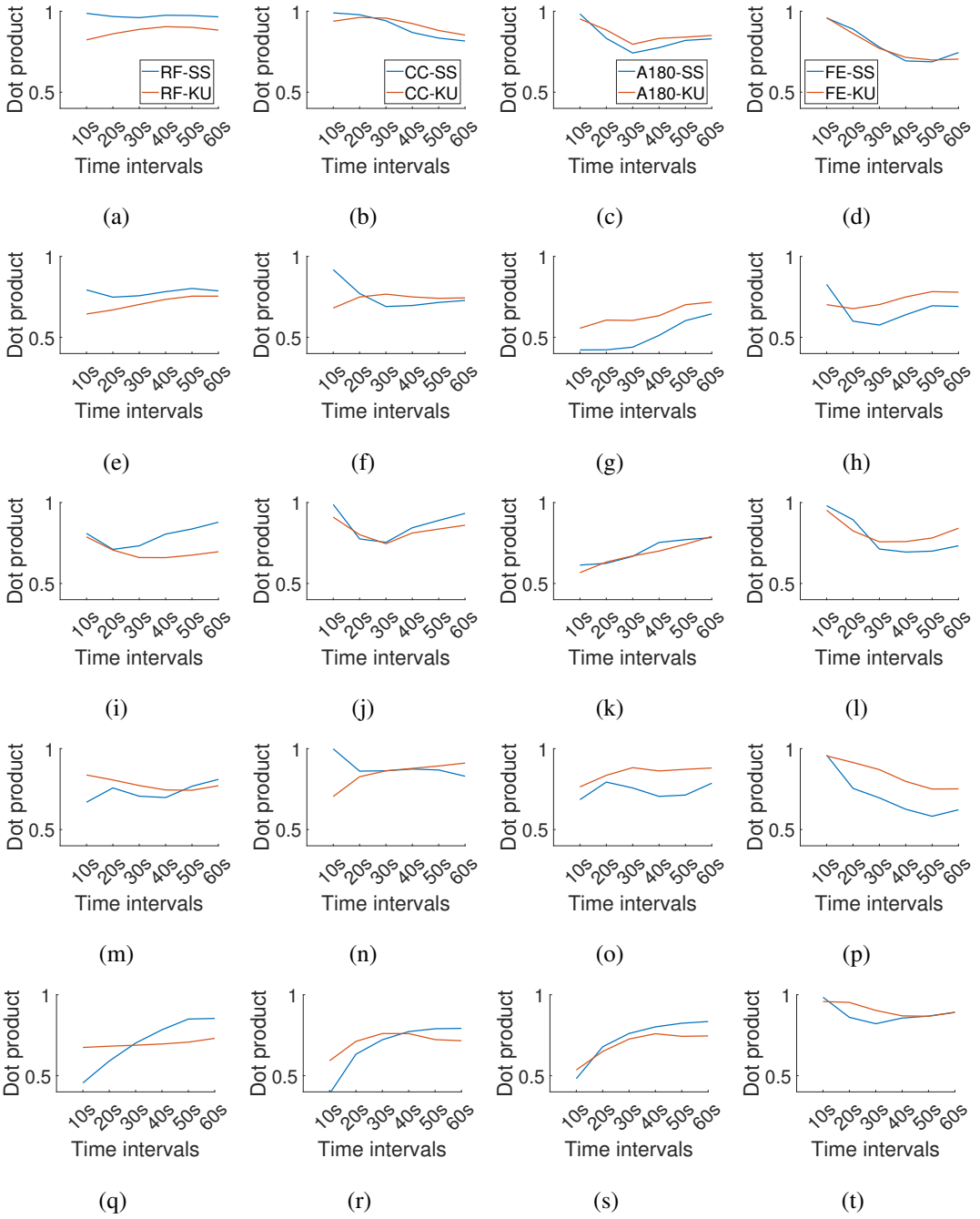

Figure 3.14: Dot product trends for different subjects at each 10-second interval for varying upper and lower body exercise combinations. Subplots of each horizontal line represent the same participants as shown in Figure 3.11.

body exercises, such as KU, have a greater influence on HR changes compared to SS. Conversely, a downward-bending shape, resembling a 'J', suggests that upper body exercises contribute more significantly to HR changes, as observed in the comparison between KU and SS.

For example, when comparing RF and FE exercises, we observe that FE exercises, which are more challenging based on HR response rates, show more downward-bending shapes, indicating stronger upper body involvement. In contrast, RF exercises exhibit more upward-bending shapes, suggesting a greater contribution from the lower body. This pattern recognition approach allows us to visualize and compare the relative difficulty of each exercise based on HR response patterns.

3.3.3.2 Dot Product Analysis for Exercise Comparison

Further analysis of the dot product values in Figure 3.14 allows us to quantify the contributions of the upper and lower body exercises to HR changes over time (based on equation 3.16). A lower dot product value indicates that the x-axis (upper body HR values) is larger, meaning that the lower body has less influence on HR. On the other hand, a higher dot product value suggests that the y-axis (lower body HR values) is larger, signifying a greater impact from the lower body. This provides a deeper understanding of how specific exercises contribute to HR changes throughout the exercise session.

By analyzing these patterns, we can identify which exercises have a dominant influence on HR at different time intervals. For example, as observed in Figure 3.14, exercises like FE show a higher dot product, indicating a stronger contribution from the upper body, while exercises like KU demonstrate a greater influence from the lower body. This analytical approach is valuable for assessing the characteristics of individual exercises, helping to design more targeted training regimens that focus on either upper or lower body engagement.

3.3.3.3 Influence of Exercise Duration on Upper and Lower Body Contributions

The same pattern recognition can be applied to the upper-body-fixed graphs in Figure 3.15, where we observe how different lower body exercises influence HR. In these graphs, a lower dot product value suggests that the x-axis (lower body HR values) is larger, meaning that the upper body has less influence. Conversely, a higher dot product value indicates that the upper body is more dominant in affecting HR changes. This provides a complementary perspective to the lower-body-fixed graphs in Figure 3.14, offering a more complete analysis of how upper and lower body exercises interact during the session.

By comparing the lower-body-fixed graphs (Figure 3.14) and the upper-body-fixed

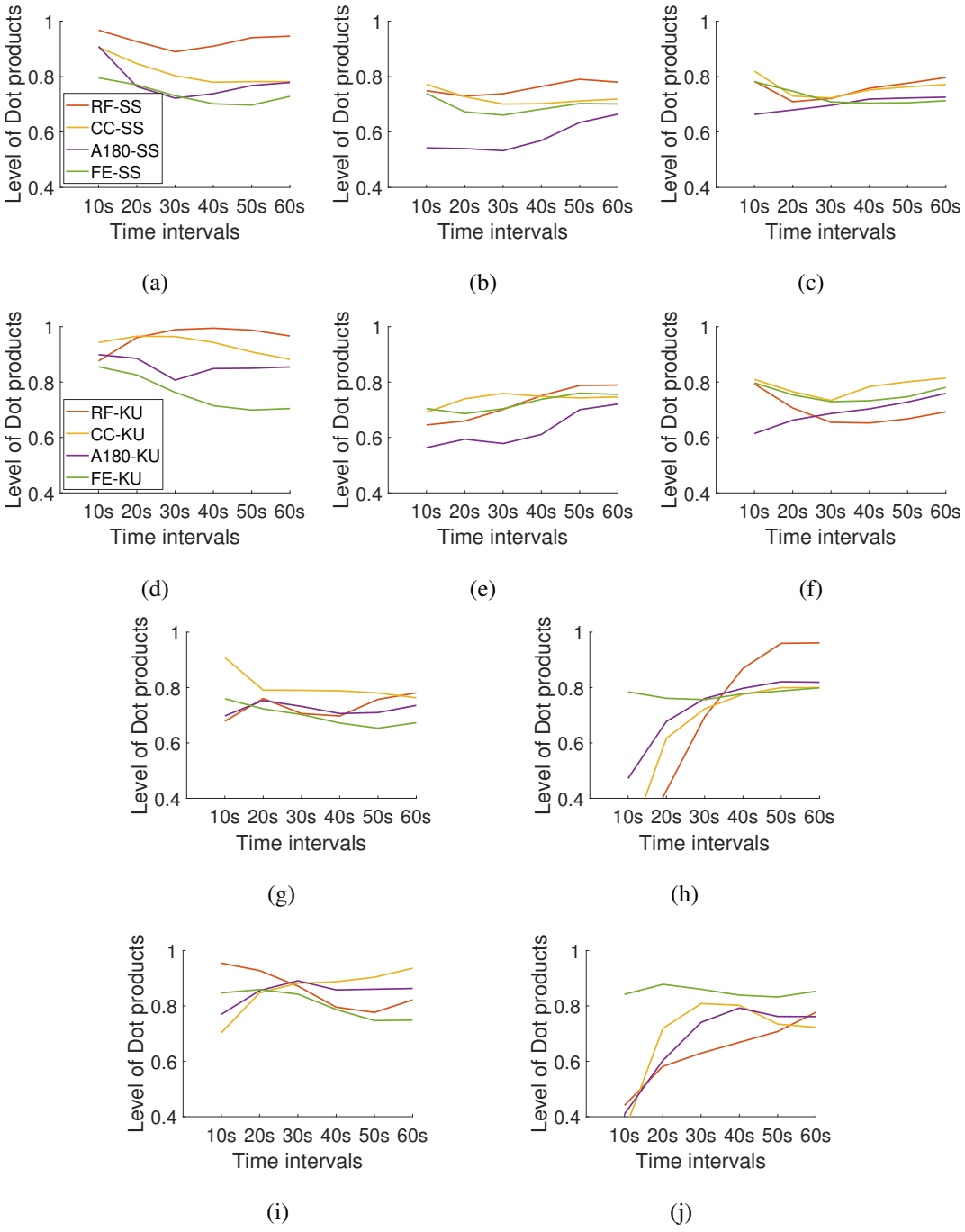

Figure 3.15: Trend graphs showing dot product values for different subjects over time intervals at each 10-second mark. Two pairs (SS and KU) of vertical subplots are in a same participant order as Figure 3.14.

graphs (Figure 3.15), we can better understand the temporal influence of each muscle group on HR responses. This comparative analysis allows us to analyze which exercises have a more significant impact on HR at different time points, providing useful insights for activity load analysis and training program development.

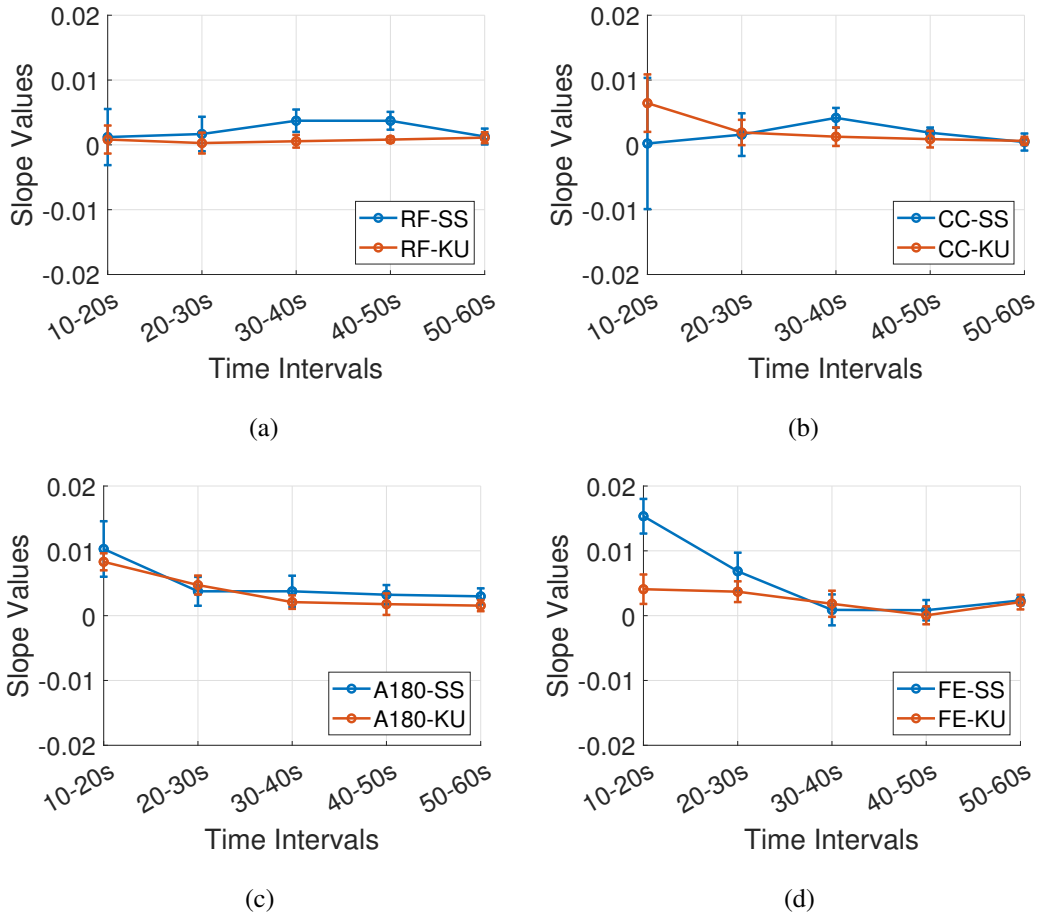

Figure 3.16: Average slope values of dot product trends for all subjects based on Figure 3.14. Subplots (a)-(d) correspond to the absolute slope values for the subject's average dot product trend graph of different exercise combinations.

3.3.3.4 Practical Applications of Pattern-Based Analysis

The ability to identify these patterns and quantify the contributions of upper and lower body exercises using vector and dot product analysis provides a powerful tool for analyzing exercise characteristics. This method can be applied to assess how different exercises influence cardiovascular effort over time, offering valuable insights for exercise program design. By recognizing which exercises induce greater HR fluctuations and which remain more stable, practitioners can tailor training regimens to suit individual needs, ensuring that participants are engaging in exercises that match their cardiovascular capacity and fitness goals.

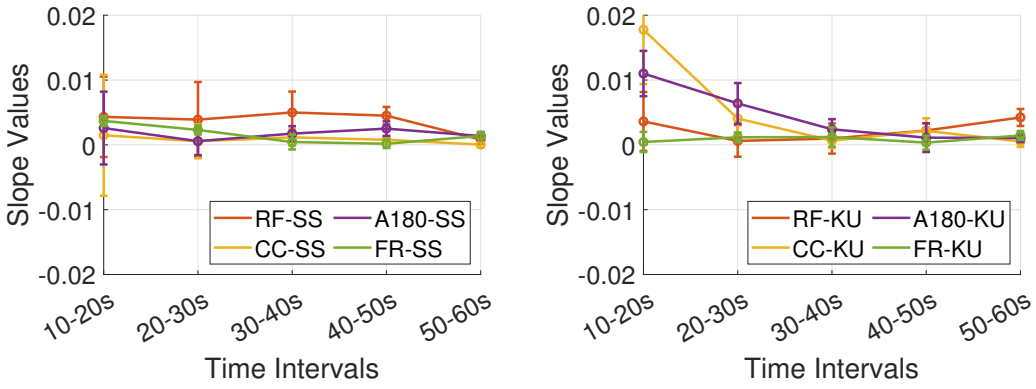

(a) (b)

Figure 3.17: Average slope values of dot product trends for all subjects based on Figure 3.15. Subplots (a), and (b) illustrate the absolute slope values for the subject's average dot product trend graph of different exercise combinations.

3.3.4 Deciphering Exercise Characteristics Through Slope Analysis

3.3.4.1 Understanding the Influence of Exercise Difficulty on HR Fluctuations

The slope analysis presented in Figures 3.16 and 3.17 provides additional insights into how exercise difficulty influences HR responses over time. In Figure 3.16, the absolute slope values of the dot product trends indicate that exercises with higher difficulty exhibit less fluctuation in HR responses (based on equation 3.16). This finding suggests that as the load of an exercise increases, the HR response becomes more stable, resulting in a smoother trend. For example, the KU exercise, known to be more challenging, displayed lower slope values compared to the simpler SS exercise, which exhibited greater fluctuations.

This observation has practical implications, as it suggests that more challenging exercises induce a more consistent cardiovascular response, making them suitable for assessing endurance and sustained effort. Conversely, exercises with higher HR fluctuation may indicate that the participant is not fully adapted to the exercise load, making them less efficient for intensity assessment.

In contrast, Figure 3.17 shows that upper body exercises do not exhibit the same clear relationship between slope values and intensity levels (based on equation 3.5 and 3.16). This suggests that upper body movements have a less significant impact on HR fluctuations compared to lower body exercises. However, this observation is still valu-

able, as it highlights the importance of selecting exercises that produce consistent HR responses when designing training programs. For example, exercises like "arm180," which exhibit inconsistent load effects, may be less suitable for intensity assessment, as they do not provide a reliable measure of cardiovascular effort.

3.3.5 Exercise Segmentation Possibility

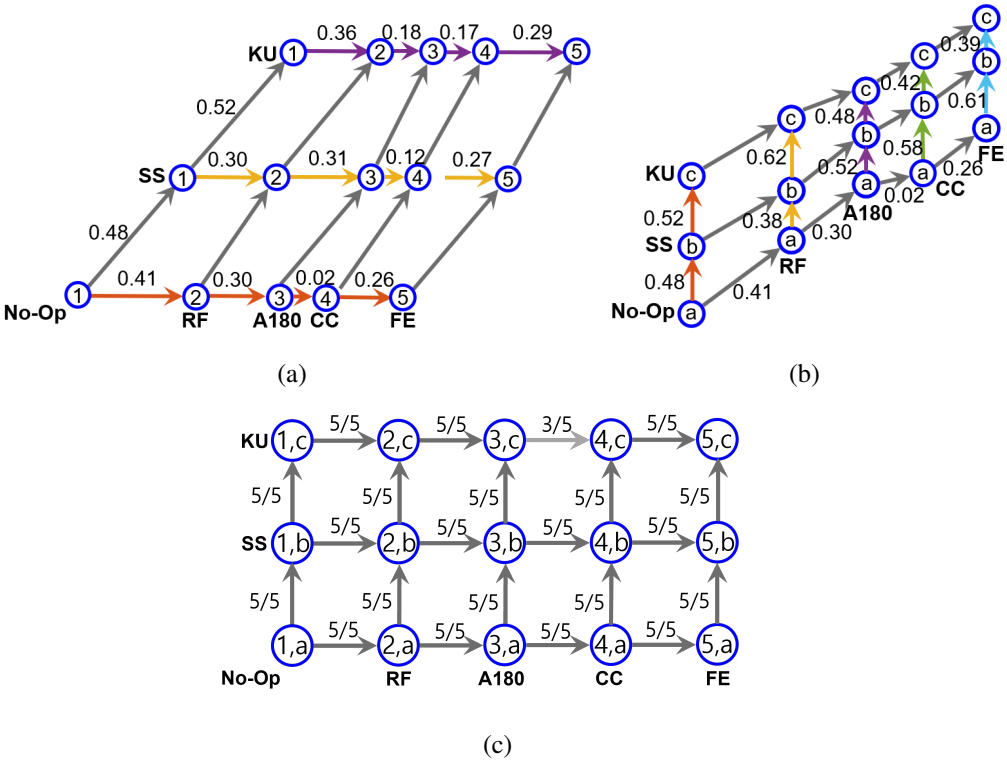

Figure 3.18: Partial order representation of all exercises shown in Figure 3.6, normalized as the mean across all participants. The diagram illustrates the relative relationships and transition probabilities between different exercise combinations, with edge weights representing the normalized average values of HR difference. No-op means movement exclusion of upper(for y-axis) or lower body(for x-axis) exercise.

The segmentation of exercise combinations was explored by analyzing the partial order of heart rate (HR) responses across different movement patterns. To validate whether consistent partial orders exist both within and across participants, two distinct analyses were conducted using Figure 3.18 and Table 3.3. Figure 3.18 provides a visual representation of the average partial order across all participants for exercise combinations. Each node represents a specific combination of upper and lower body movements, and the edges indicate the normalized mean transition probabilities de-

Table 3.3: Similarity of the subjects. Value was calculated using cosine similarity

Similarity					
Subject	1	2	3	4	5
row1 & row2	0.83	0.91	0.99	0.88	0.97
row1 & row3	0.47	0.90	0.89	0.82	0.98
col1 & col2	0.93	0.99	0.96	0.99	0.99
col1 & col3	0.96	0.99	0.99	0.99	0.98
col1 & col4	0.98	0.94	0.99	0.83	0.99
col1 & col5	1.00	0.94	0.98	0.85	0.93

rived from HR differences. This figure confirms that participants, on average, exhibit a consistent partial order when performing exercise combinations. For instance, the transitions from "No-Op(exclusion of lower body movement) x Upper Body" to combinations involving lower body movements follow predictable pathways, suggesting that lower body movements consistently modulate HR responses even when paired with static upper body exercises. The overall structure of the partial order highlights the dynamic interplay between upper and lower body movements. For example, transitions involving "KU" (knee-up) consistently rank higher in HR response compared to static or less intensive lower body movements. This reinforces the hypothesis that partial order can be preserved when combining exercises with varying upper and lower body contributions.

Table 3.3 extends the analysis to individual participants, focusing on whether the partial order is preserved in more granular scenarios. Rows and columns correspond to arrays of HR responses from specific exercise combinations as described in Figure 3.6. Row 1 represents "No-Op(exclusion of lower body movement) x Upper Body" combinations, serving as the baseline, while Rows 2 and 3 represent upper body movements combined with lower body exercises. The cosine similarity values indicate how well the partial order is maintained when upper body exercises are paired with lower body movements. Across most participants, high similarity values (e.g., 0.83 to 0.99) suggest robust maintenance of the partial order. However, Participant 1 shows a significant deviation (0.47) in the similarity between Row 1 and Row 3. This deviation is attributed to the combination of "CC" (cross-crunch) with "KU" (knee-up), where the lower body movement appears to reduce the intensity of the upper body action. This unique physiological response highlights the interplay of exercise characteristics and

individual movement strategies. Column 1 represents "No-Op(exclusion of upper body movement) x Lower Body" combinations, serving as the baseline, while Columns 2 to 5 represent lower body movements paired with different upper body exercises. High similarity values (e.g., 0.83 to 1.00) confirm that partial order is generally preserved when lower body exercises are combined with upper body movements. For Participant 3, the near-perfect similarity values across all columns underscore consistent HR response patterns, regardless of exercise combinations.

The combination of visual analysis (Figure 3.18) and quantitative assessment (Table 3.3) demonstrates the feasibility of exercise segmentation based on HR response patterns. While the average partial order is robust across participants, individual-level deviations, such as those observed in Participant 1, underscore the importance of personalized exercise profiling. The results suggest that HR-based segmentation can effectively differentiate between exercise intensities and combinations. Furthermore, the use of cosine similarity to evaluate partial order maintenance provides a nuanced approach to assessing not only the sequence but also the magnitude of HR differences between movements. This level of detail can inform personalized fitness programs and adaptive training protocols by identifying individual-specific tendencies, such as the influence of lower body movements on upper body intensity. Overall, the analyses confirm that exercise segmentation based on HR responses is not only viable but also reveals critical insights into the interaction between upper and lower body exercises. Future studies could further refine these findings by incorporating additional metrics, such as recovery time and perceived exertion, to enhance the segmentation framework.

3.4 Discussion

This study effectively demonstrated the utility of a vector-based approach in capturing heart rate (HR) responses during combined upper and lower body exercises, offering a comprehensive analysis beyond traditional HR metrics. By employing vectorization and dot product analysis, the activity load was visualized and quantified in a multi-dimensional manner. A pivotal finding, the 40-second rule, revealed that activity load patterns stabilize around this mark, challenging the conventional reliance on longer durations to gauge intensity accurately. This discovery is particularly valuable for designing efficient exercise protocols, especially for individuals with limited exercise capacity.

The study also introduced the analysis of partial orders in HR responses, as repre-

sented in Figure 3.18, revealing consistent transitions and relationships among exercise combinations across participants. The visualization of these transitions highlighted that lower body movements, such as knee-ups (KU), consistently produced higher HR responses compared to static or less intensive lower body movements, even when paired with upper body exercises. This finding underscores the dynamic interplay between upper and lower body contributions, emphasizing that their relative intensities are maintained in combined exercises.

Furthermore, Table 3.3 validated the robustness of these partial orders at an individual level using cosine similarity, demonstrating high similarity across participants while identifying unique physiological deviations, such as those seen in Participant 1. These variations provided additional insights into how individual movement strategies and physiological responses influence overall HR patterns. This layered analysis reinforces the potential of HR-based segmentation to differentiate between exercise intensities and combinations, while simultaneously paving the way for personalized exercise profiling.

Additionally, slope analyses from Figures 3.16 and 3.17 highlighted that more demanding exercises exhibit consistent HR responses over time, offering an objective method to distinguish exercise difficulty. These findings, combined with the partial order maintenance across exercises, further validate the adaptability and precision of the proposed method in capturing dynamic HR responses. Overall, the integration of vector-based metrics with partial order analysis provides a versatile framework for understanding and optimizing exercise protocols tailored to individual needs.

3.5 Conclusion

This study introduced a novel vector-based approach to analyzing HR responses during combined upper and lower body exercises, providing a dynamic and accurate method for assessing activity load. By transforming HR data into vectors and analyzing their dot products, we identified activity load trends with greater precision, with the 40-second rule emerging as a key metric for understanding stabilization patterns in HR responses.

The addition of partial order analysis further enhanced this framework, revealing consistent relationships among exercise combinations while identifying individual-specific deviations. This insight offers practical applications for personalizing exercise protocols based on unique movement strategies and physiological tendencies. The

ability to maintain partial orders across exercises, coupled with high inter-participant consistency in cosine similarity, highlights the robustness of the method in differentiating activity load and combinations.

These findings hold significant implications for designing shorter and more efficient exercise protocols, particularly for individuals unable to sustain longer durations. By uncovering the contributions of upper and lower body movements to overall intensity, the vector-based approach offers valuable applications in both training and rehabilitation settings. Future research could incorporate additional physiological metrics, such as recovery time and perceived exertion, to further deepen our understanding of exercise impacts on the human body. This framework represents a promising step toward more personalized, effective, and efficient exercise programs.

3.6 Summary of Chapter 3

Chapter 3 presented a novel vector-based approach to evaluating activity load through HR analysis during combined upper and lower body exercises. Traditional methods, such as maximum HR or simple differences, proved limited in capturing the dynamic and multidimensional nature of activity load. To address these shortcomings, vectorization and dot product analysis were employed, offering a more comprehensive understanding of exercise patterns.

A significant finding was the identification of the 40-second rule, demonstrating that activity load trends stabilize around this point, challenging the need for longer durations to assess intensity accurately. This insight provides a practical basis for designing efficient exercise assessments, particularly for individuals with limited capacity for prolonged activity.

Additionally, partial order analysis was introduced to explore HR response patterns among exercise combinations, as shown in Figure 3.18. The visualization revealed consistent transitions across exercises, particularly the influence of lower body movements like knee-ups, which modulate HR responses even when paired with static upper body exercises. Table 3.3 supported these findings, confirming the robustness of partial orders across participants while highlighting individual physiological variations.

These findings emphasize the adaptability of the vector-based approach across individuals, offering a reliable and personalized tool for assessing activity load. By integrating vectorization, dot product analysis, and partial order representation, this chapter advances our understanding of exercise-induced cardiovascular responses and pro-

vides practical applications for designing tailored and effective exercise programs.

Chapter 4

HR Modeling through Split up Analysis of Exercise Sequence

This chapter delves into the intricate relationship between upper and lower body movements in shaping heart rate (HR) responses during combined exercises. It highlights that activity load arises from dynamic interactions between these components, rather than being a simple additive sum of their individual effects. This insight is especially significant for high-intensity interval training (HIIT) and aerobic workouts, where rapid transitions between combined movements necessitate a sophisticated framework for assessing exercise difficulty.

Building upon previous findings, the study emphasizes the proportional relationships between upper and lower body contributions, offering a systematic method for predicting activity load. Using the foundational exclusion of upper or lower body exercises as a baseline, the chapter introduces a robust prediction model based on partial order preservation. This approach leverages vector-based methodologies, such as dot product calculations and normalized HR responses, to estimate and classify the difficulty of diverse exercise combinations with high accuracy.

The findings underscore the feasibility of predicting activity load through relative rankings rather than absolute HR values, with lower body movements demonstrating superior consistency in preserving partial order. This framework provides a reliable and scalable tool for designing personalized exercise routines, enabling tailored protocols for various fitness levels, rehabilitation programs, age-specific needs, and optimized HIIT sessions.

By bridging theoretical HR analysis with practical applications, this chapter establishes a foundation for understanding and predicting exercise difficulty, advancing

both research and real-world fitness program design. This chapter's contents are being prepared for submission to a journal (Yoon and Kim, 2025a).

4.1 Methods

4.1.1 Subjects

We recruited ten adult male participants for this study. Each individual was thoroughly informed about the purpose of the study and provided their consent by signing a consent form prior to engaging in any experimental activities. Furthermore, all researchers involved in this project completed online research ethics training before the experiments began. The study protocol received approval from the Institutional Review Board (IRB) of Yonsei University, the institution overseeing this research (Registration number: 7001988-202410-HR-2376-04).

Participants were selected based on specific inclusion and exclusion criteria. The inclusion criteria were: 1) The ability to wear a sensor on both upper arms; 2) No mobility impairments or reliance on assistive walking devices, and the capability to attend the research facility; 3) An age range of 20 to 35 years; 4) A voluntary willingness to participate.

Exclusion criteria were: 1) Individuals with significant communication difficulties, such as those due to cognitive impairments or aphasia; 2) Those with severe cardiovascular, cardiopulmonary, or other major internal medical conditions; 3) Individuals with a history of surgeries or conditions related to musculoskeletal or neurological issues; 4) Participants deemed unsuitable for the study by the researcher.

The participants' demographic and physical characteristics, including sex, age, height, weight, and BMI, are presented in Table 4.1 below.

4.1.2 Experiment

4.1.2.1 Experimentation Platform

In the study, ECG data was collected using the Solmitech RE:FIT patch SHC-U8, a mobile holter electrocardiograph. This ECG experimental tool consists of six channels with 250 SPS and a filter range of 0.5Hz to 40Hz. It is a simplified ECG module compared to the traditional 12-lead method commonly used in clinical settings. This module is clinically approved and capable of recording electrocardiograms by attach-

Table 4.1: Characteristics of the subjects. (SD, standard Deviation)

Characteristic	***Values***
Sex (male/female)	7/3
Age (mean± SD)	27.4 ± 3.56 [years]
Height (mean± SD)	172.46 ± 8.29 [cm]
Weight (mean± SD)	66.8 ± 15.75 [kg]
BMI (mean± SD)	22.38 ± 4.02 [kg/m^2]

Note: BMI denotes body mass index.

ing electrodes to specific areas on the body surface. It detects the action potentials generated when the myocardium is activated and wirelessly transmits the measured data to a mobile device (figure 1). The module is typically worn on the chest in a patch form to measure the ECG.

The utilization of these advanced tools and technologies ensured accurate and reliable data collection, enhancing the credibility and applicability of the study's findings (Salman et al., 2012). The integration of state-of-the-art equipment and software reflects the commitment to producing high-quality research with practical implications for personalized rehabilitation and exercise interventions (Gupta and Saxena, 2012).

4.1.2.2 Experimental Protocol

The experimental protocol for Chapter 4 builds upon the findings and methodologies established in Chapter 3, with a particular focus on analyzing the difficulty of HIIT (high-intensity interval training) and aerobic exercises. The goal was to assess the HR responses to both upper and lower body movements, separately and in combination, thereby identifying patterns in activity load across various configurations.

From a pool of commonly used HIIT exercises (19 upper-body and 16 lower-body movements), as listed in Table 4.2, ten upper-body and ten lower-body exercises were carefully selected for this study. The selection process considered three primary criteria: (1) clear differentiation in HR response between movements, (2) feasibility for participants to perform accurately, and (3) representation of various exercise intensities. These selected exercises covered a range of intensities and allowed for a comprehensive analysis of HR responses.

The final set of exercises, as outlined in Table 4.3, included both separated and combined movements to comprehensively analyze the HR responses. Due to time con-

Table 4.2: Existing representative HIIT exercises

	Upper body	Lower body		Upper body	Lower body
1	Wrist shake off	Step side	11	Alt superman punch	Shuffle
2	Walk swing	Step front	12	Hammering	Side hop
3	Fold reverse fly	Calf raise	13	Lateral swing	Quater squat
4	Sheating	Jog in place	14	Upper punch	Frontkick
5	Superman row	Lunge	15	Elbow twist	Squat
6	Rowing swing	Extended Lunge	16	Arm full extend	Skater
7	Interlock twist	Step back	17	Two hand overhead kneetouch	
8	Reversefly	Kneeup	18	Angel fly	
9	Front punch	Rotate side step	19	Full lateral extend	
10	Long pull	Small hop kick			

straints, it was not feasible to complete all possible 11x11 combinations of upper and lower body exercises. Instead, a structured approach was adopted to ensure meaningful insights. First, each upper and lower body exercise was conducted individually pairing it with a "No-operation" to establish baseline HR responses. Second, to evaluate the contributions of upper body exercises, all upper body movements were paired with the lower body exercise "Side Hop" (SH), a moderate-intensity movement, allowing a focused analysis of upper body influence. Third, the original combined movements were performed to reflect realistic exercise scenarios. Lastly, the full 5x5 grid of upper and lower body combinations was completed to ensure clear differentiation among exercises. This strategy allowed for a practical yet comprehensive evaluation of the interplay between upper and lower body movements and their respective effects on HR responses.

The experimental protocol was implemented to explore the interaction between upper and lower body movements. As shown in Figure 4.1, exercises were performed with precise timing and controlled intensity to ensure consistency across participants. For example, upper-body exercises such as "Reverse Fly" (RF) were combined with lower-body movements like "Side Hop" (SH), providing insights into how these combinations influence overall HR response.

Table 4.3: Exercises used in research

Number	Exercise Type	Seperated Exercise Name	Combined Exercise Name
1	Upper	Wrist shake off(WSO)	Arm leg shake off(ASO)
	Lower	Small hop kick(SHK)	
2	Upper	Walk swing(WS)	Jogging(JG)
	Lower	Jog in place(JIP)	
3	Upper	Fold reversefly(FRF)	Leg arm extend(LAE)
	Lower	Calf raise(CR)	
4	Upper	Rowing swing(RWS)	Rowing(RW)
	Lower	Step back(SB)	
5	Upper	Reversefly(RF)	Quater squat reversefly(SR)
	Lower	Quater squat(QS)	
6	Upper	Alt superman punch(ASP)	Superman(SM)
	Lower	Buttkick(BK)	
7	Upper	Skater arm swing(SAS)	Skater(ST)
	Lower	Skater leg swing(SLS)	
8	Upper	Upper punch(UP)	Arm reach punch(ARP)
	Lower	Rotate side step(RS)	
9	Upper	Elbow twist(ET)	Cross Crunch(CC)
	Lower	Kneeup(KU)	
10	Upper	Angel fly(AF)	Jumping Jack(JJ)
	Lower	Side hop(SH)	

4.1.3 Data Analysis

4.1.3.1 Data Preprocessing

Robust data preprocessing was imperative for the ECG signals due to their susceptibility to biological and mechanical noise (Gupta et al., 2021). To ensure the reliability of subsequent analyses, a meticulous preprocessing pipeline was implemented (Tejedor et al., 2019). The raw ECG signal underwent a 60Hz Notch filter to eliminate power noise, a common interference arising from electrical systems. Subsequently, both high-pass and lowpass filters were applied to analyze signals, focusing on the bandpass frequencies of 10Hz to 30Hz. These steps ensured the extraction of accurate HR data, devoid of undesirable noise artifacts (Flandrin et al., 2003). The implementation of

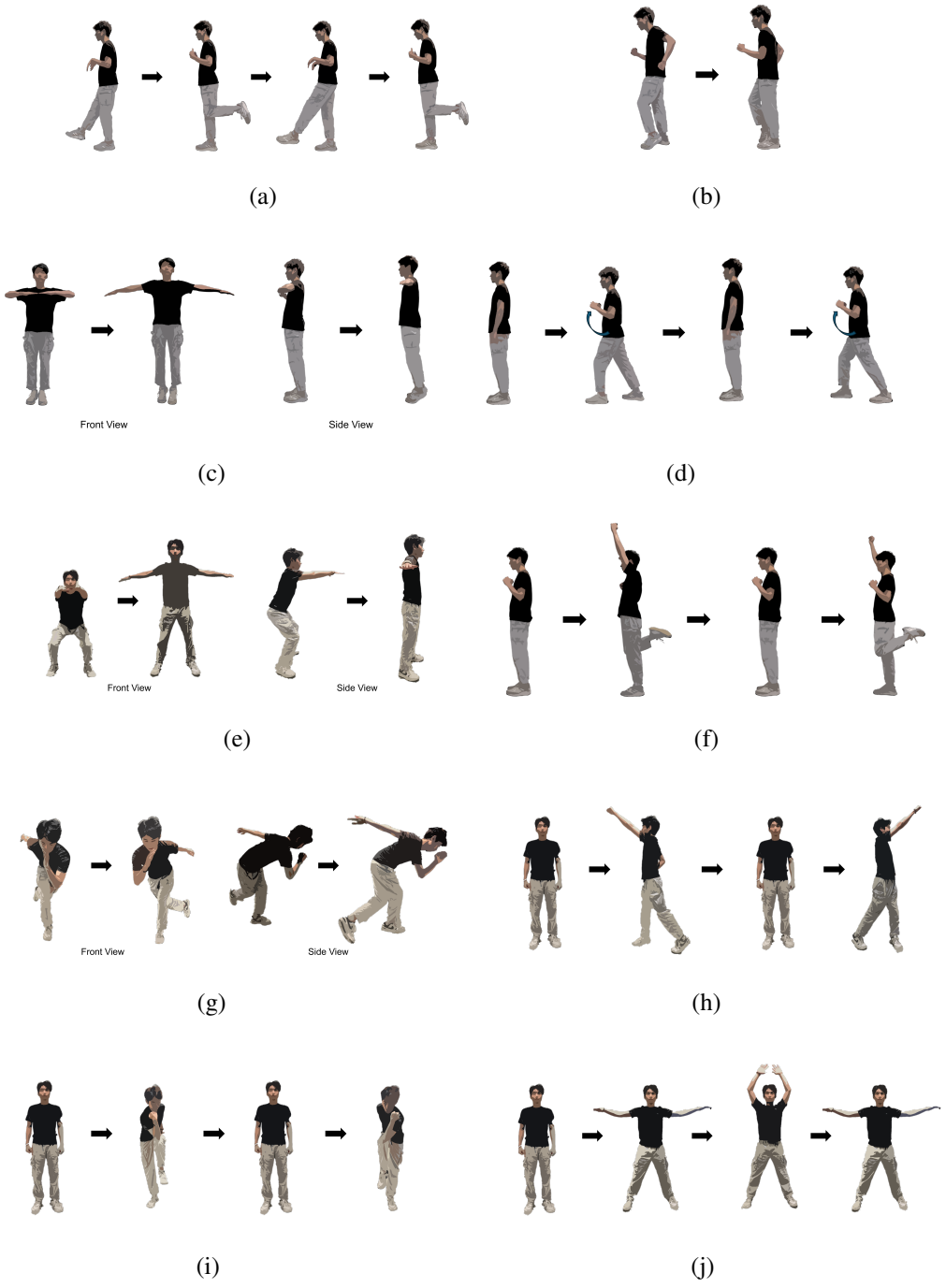

Figure 4.1: Sequence of exercises used in research. (a) Sequence of ASO. (b) Sequence of JG. (c) Sequence of LAE. (d) Sequence of RW. (e) Sequence of SR. (f) Sequence of SM. (g) Sequence of ST. (h) Sequence of ARP. (i) Sequence of CC. (j) Sequence of JJ,

these preprocessing steps fortified the quality and reliability of the data, establishing a robust foundation for the subsequent analysis of the HR signals during the experimen-

tal exercises.

4.1.3.2 Analysis in HR from ECG data

In this section, the analysis of heart rate (HR) derived from electrocardiogram (ECG) data is presented, building upon the methodology outlined in (Yoon and Kim, 2025b). The HR is calculated using the RR interval, which represents the time between two consecutive R-peaks in the ECG signal, as described in former research (Achten and Jeukendrup, 2003; Shaik and Ramakrishna, 2015). The equation for HR computation is expressed as follows:

$$\mathrm{HR}subject = \frac{60}{\mathrm{RR}interval}\mathrm{sec} \tag{4.1}$$

For activity load assessment, the simplified method introduced in chapter 3 (Yoon and Kim, 2025b) was adopted. This method calculates intensity as the difference between HR during exercise and resting HR, expressed as:

$$\text{Intensity} = HR_{exercise} - HR_{rest} \tag{4.2}$$

This adaptation, differing from the traditional Karvonen formula, focuses on intra-individual comparisons of intensity, enabling the analysis of relative differences across exercise types within each participant. By leveraging the methodological foundation established in (Yoon and Kim, 2025b), this section extends the analysis to broader applications of HR monitoring in exercise contexts.

The data is represented as a matrix $\mathbf{D}$ with dimensions (α, β), where $\alpha \in \{1, 2, \ldots, 11\}$ represents different lower exercise levels (y-axis), and $\beta \in \{1, 2, \ldots, 11\}$ represents upper exercise HR data (x-axis). The data matrix is defined as:

$$\mathbf{D} = \{d_{\alpha,\beta} \mid \alpha \in \{1, 2, \ldots, 11\}, \beta \in \{1, 2, \ldots, 11\}\}. \tag{4.3}$$

When the lower body is fixed and used as the x-axis for calculations, the matrix $\mathbf{D}$ is transposed to ensure consistency in the computation process.

Each column of $\mathbf{D}$ is plotted against corresponding α-values. The x-axis values for the β-th column are given by:

$$x_\beta = d_{\alpha,\beta}, \quad \beta \in \{1, 2, \ldots, 11\}. \tag{4.4}$$

The y-axis values are extracted from the first column ($\beta = 1$) as:

$$y_\alpha = d_{\alpha,1}, \quad \alpha \in \{1, 2, \ldots, 11\}. \tag{4.5}$$

Thus, each plot line is represented as:

$$\text{Line}_\beta = \{(x_\beta, y_\alpha) \mid \alpha \in \{1, 2, \ldots, 11\}\}. \tag{4.6}$$

$$\Delta\text{meanRR} = \text{meanRR}_{\text{exercise}} - \text{meanRR}_{\text{rest}}, \tag{4.7}$$

where meanRR is the average time interval (in milliseconds) between consecutive R-wave peaks in the ECG signal.

$$\text{Ratio}_{\text{rMSSD}} = \frac{\text{rMSSD}_{\text{exercise}}}{\text{rMSSD}_{\text{rest}}}, \tag{4.8}$$

where rMSSD is the root mean square of successive differences between adjacent RR intervals, indicating parasympathetic nervous system activity.

$$\text{Ratio}_{\text{pNN50}} = \frac{\text{pNN50}_{\text{exercise}}}{\text{pNN50}_{\text{rest}}}, \tag{4.9}$$

where pNN50 is the percentage of consecutive RR intervals differing by more than 50 ms.

The correlation between the proposed HR_{load} metric and HRV-based metrics is defined as:

$$r_{X,Y} = \frac{\sum(X_i - \bar{X})(Y_i - \bar{Y})}{\sqrt{\sum(X_i - \bar{X})^2 \sum(Y_i - \bar{Y})^2}}, \tag{4.10}$$

4.2 Results

The results of this study demonstrate that the intensity of combined upper and lower body exercises is not a simple additive function of each component's HR impact. Instead, the HR response reflects a proportional relationship to the individual intensities of upper and lower body movements. This nuanced interaction provides insights into how movement combinations in HIIT or aerobic workouts can be strategically designed to achieve specific intensities and tailored physiological outcomes.

4.2.1 Dominance of Lower Body Movements

Figure 4.4 highlights the HR difference in various exercise combinations, with combined upper and lower body movements displayed in plot Figure 4.4 (c). A noticeable trend across these plots is the strong influence of lower body exercises. Specifically, the HR difference in the combined movements closely mirrors the trends observed in

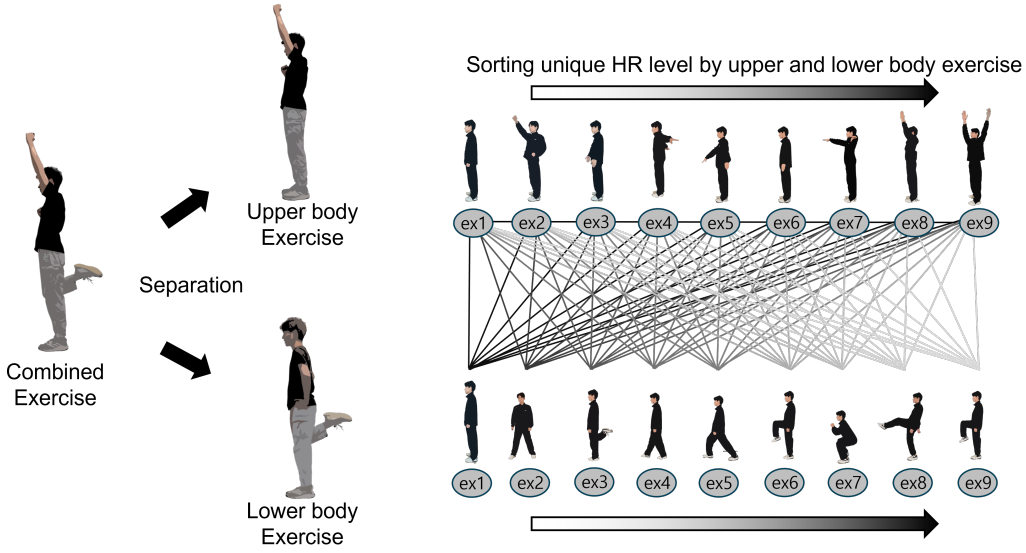

(a)

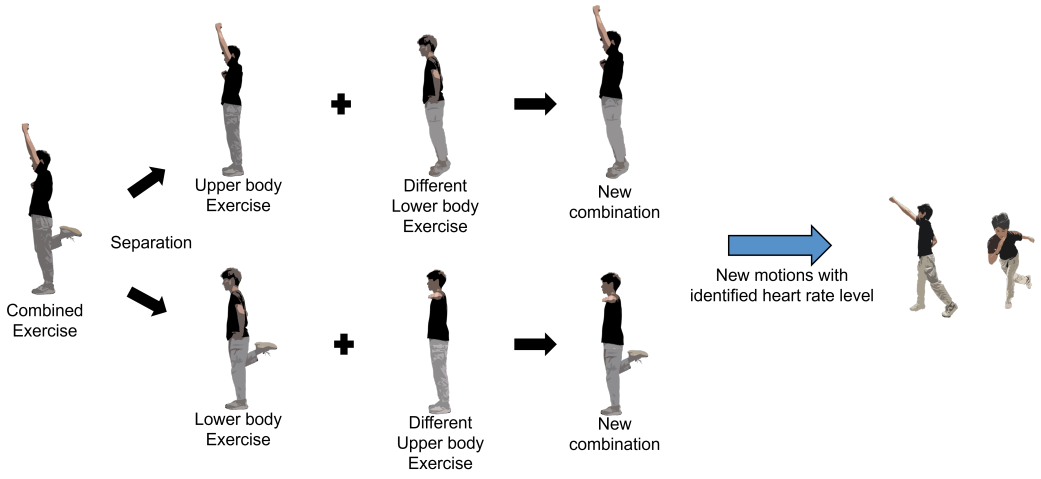

(b)

Figure 4.2: Overview of exercise analysis framework. (a) Separation of combined exercises into upper and lower body components, enabling the sorting of unique HR levels and exploring diverse movement combinations. (b) Creation of new exercise combinations by pairing different upper and lower body movements, facilitating tailored routines with identifiable HR levels.

the lower body-only exercises shown in Figure 4.4 (b). This suggests that the lower body component exerts a disproportionately strong effect on HR during aerobic or HIIT movements. For instance, movements involving more intense lower body exercises such as SH or QS consistently result in larger HR differences, regardless of the upper body exercise being performed.

This observation implies that the cardiovascular demands of the lower body exercises dominate when combined with upper body movements. In practical applications, such as designing HIIT or aerobic training programs, this suggests that the choice of lower body exercise is critical in modulating overall activity load. However, the data also raises the question: how significant is the influence of upper body movements when paired with lower-intensity lower body exercises?

4.2.2 The Influence of Upper Body Movements

To investigate the role of upper body movements, we look to Figure 4.5, where the SS, a relatively low-intensity lower body exercise, is combined with different upper body movements. The results in the plot (b) demonstrate that although the SS exercise does not induce a significant HR increase on its own, combining it with upper body movements leads to noticeable differences in HR values. However, the rank of upper body exercises remains largely consistent, reinforcing that the lower body dominates when the overall intensity is driven by leg movements.

Interestingly, in the case of the upper body movements combined with SS, we observe that the HR values increase but without dramatic reordering of the exercise ranks. This suggests that while the lower body component may set a baseline for cardiovascular demand, upper body movements still contribute to HR increases. Therefore, the influence of upper body movements becomes more evident when combined with less intense lower body exercises.

Figure 4.6 delves into the interaction between upper and lower body contributions by analyzing combinations with the moderately demanding SH exercise. The pattern observed here differs from the previously analyzed SS combinations. While SS combinations showed a subdued influence on upper body movements due to the low intensity of the lower body exercise, SH introduces a moderate cardiovascular demand, allowing upper body movements to play a more complementary role. This highlights that, under moderate-intensity conditions, the contributions of upper body exercises to HR differences become more pronounced.

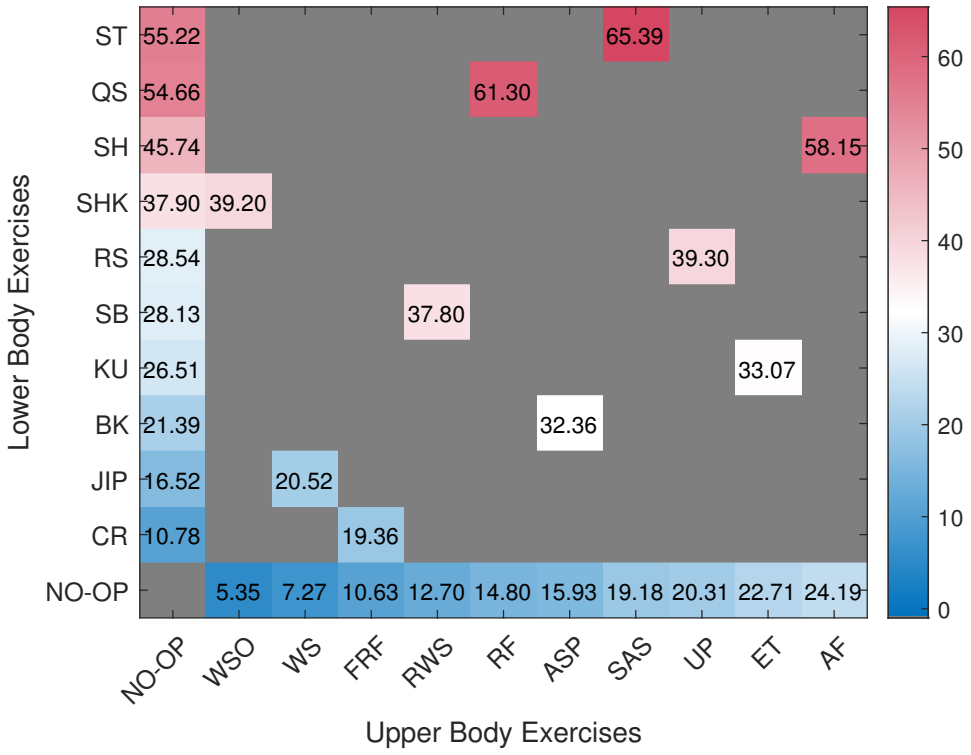

Figure 4.3: An example heart rate heatmap of 10 exercises and its correspoing upper and lower body exercise. Heatmap represents the difference between maximum HR and resting HR for various exercise combinations. The x-axis represents different upper body exercises, while the y-axis shows different lower body exercises. The color intensity indicates the magnitude of the HR difference, with warmer colors representing greater increases in HR relative to resting levels. Each shows the values of a different subject. The No-op on the x-axis represents the exclusion of upper body movement, while the No-op on the y-axis represents the exclusion of lower body movement.

In this context, upper body movements such as SAS and ET demonstrate consistently higher HR differences when paired with SH. These findings suggest that certain upper body movements, characterized by greater biomechanical complexity or muscular demands, such as bending or intricate motion patterns, can amplify HR responses when combined with moderately intense lower body exercises like SH.

Interestingly, the AF exercise displays a relatively lower HR difference when paired with SH, despite involving arm swings. This could be attributed to the biomechanical assistance provided by the jumping motion in SH, which may reduce the effort required for the upward arm movement in AF, thereby lowering the overall cardiovascular strain. This observation underscores the importance of understanding how specific

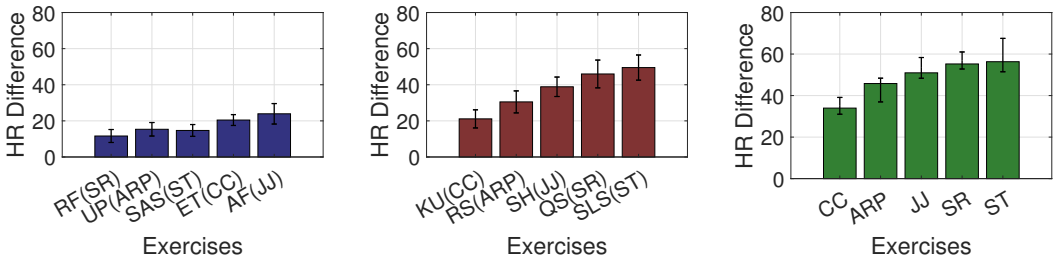

(a) (b) (c)

Figure 4.4: Average HR difference across different exercise combinations for multiple participants. (a) Upper-body exercises with no lower body movements. (b) Lower-body exercises with no upper body movements. (c) Combined upper and lower body exercises. Exercise names in parentheses indicate their paired combination during full aerobic movements.

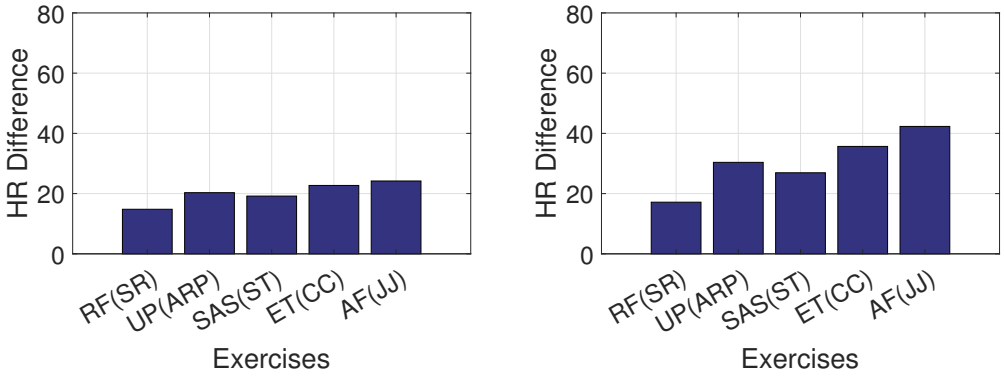

(a) (b)

Figure 4.5: Comparison of HR differences across exercises. (a) HR difference for upper-body exercises without lower body movements from Figure 4(a). (b) HR differences for combinations of the SS lower-body exercise (from Chapter 3) and all upper-body exercises.

biomechanical interactions between upper and lower body movements influence HR responses during combined exercises.

By focusing on SH, a movement with moderate cardiovascular impact, Figure 4.6 reinforces the idea that the interplay between upper and lower body movements is dynamic. Upper body exercises can significantly influence HR responses, especially when the lower body component does not overwhelmingly dominate the cardiovascular workload. This finding complements the earlier results and highlights the nuanced role of upper body intensity in shaping the overall exercise difficulty.

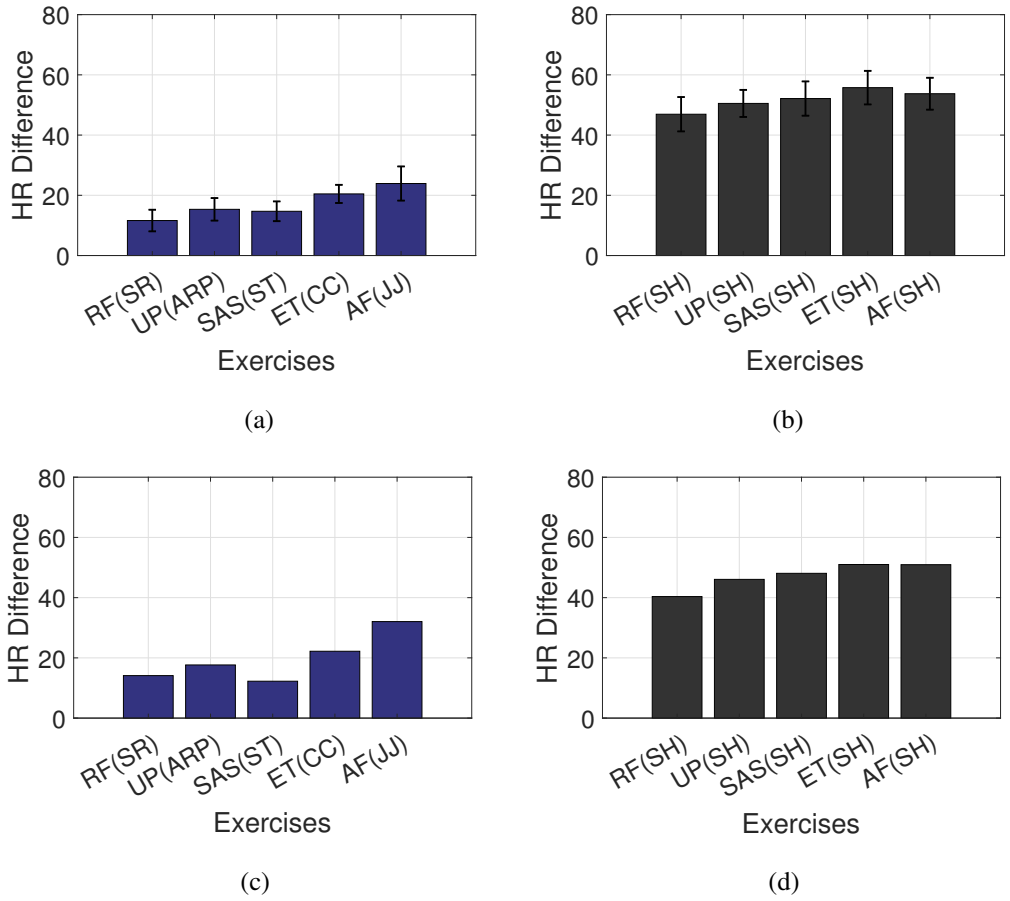

Figure 4.6: Average HR difference results for combinations of 5 upper-body exercises with the SH lower-body exercise across different participants. (a) Average intensity of upper-body exercises with no lower body movements. (b) The average intensity of upper-body exercises combined with SH for the lower body. (c) and (d) each is an identical plot to (a) and (d) but of a single subject.

4.2.3 Importance of Maintaining Motion Accuracy

The results highlighted in Figure 4.6(c) revealed an anomaly in the HR level of a specific participant during the isolated SAS exercise, showing significantly lower values compared to other participants. Upon further investigation, it was discovered that this participant performed the SAS movement with their arms positioned closer to their body than other participants, deviating from the intended motion.

To validate the impact of this deviation, additional experiments were conducted where participants were instructed to perform the SAS exercise both in a “Close” variation, with arms closer to the torso, and a “Far” variation, with arms extended farther away from the body. The results, illustrated in Figure 4.8, showed that the “Far” varia-

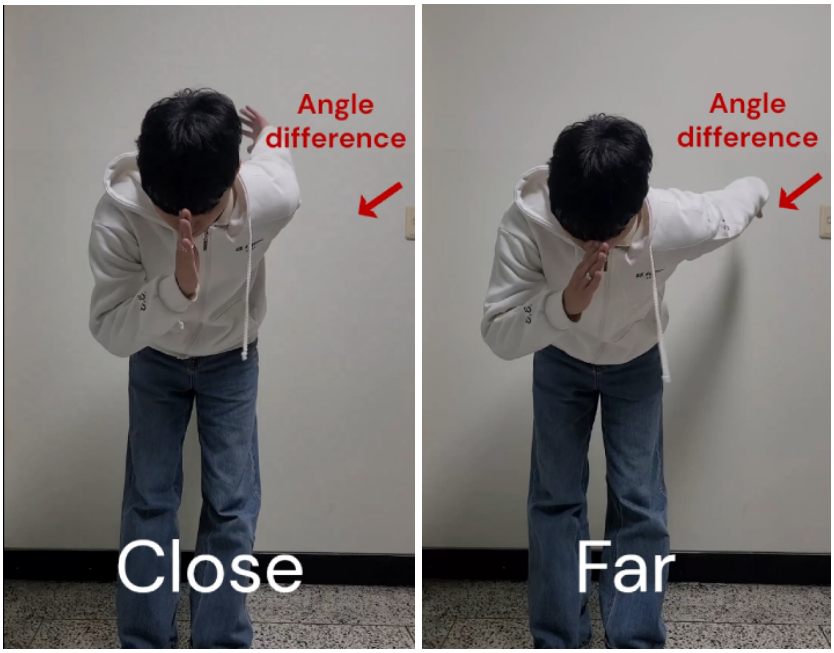

(a) (b)

Figure 4.7: Image comparison between “Close” and “Far” upper body exercise. (a) Exercise motion with “Close” variation (b) Exercise motion with “Far” variation.

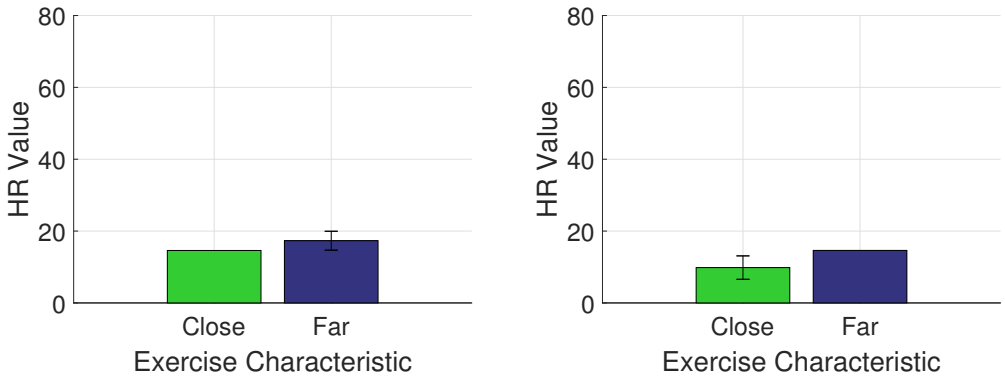

(a) (b)

Figure 4.8: HR comparison between “Close” and “Far” variations of the SAS exercise. (a) Average across all participants, with error bars for “Far”. (b) Results of the participants from Figure 6(c) and 6(d).

tion not only elicited a higher HR response but also aligned more closely with the HR levels intended for the SAS movement. This finding underscores the influence of even subtle deviations in exercise form on physiological responses.

These results emphasize the critical importance of maintaining motion accuracy in

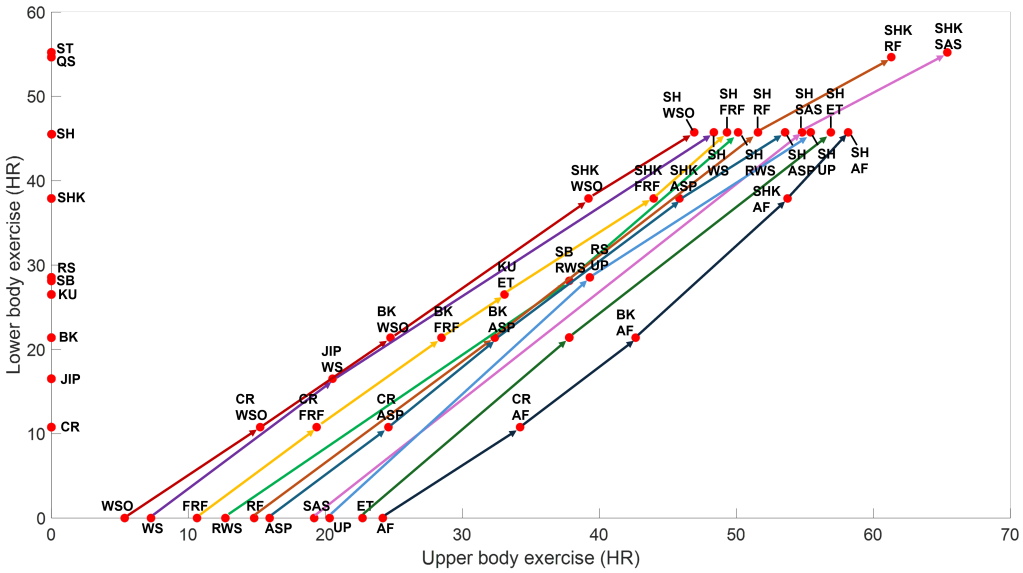

Figure 4.9: Visualization of HR differences using the vector-based method for all exercise combinations listed in Figure 4.3. Each point represents the HR level of an individual upper or lower body exercise. Exercises with the same upper body movement but paired with different lower body movements are connected by lines of the same color.

exercise studies. Small variations in movement execution, often perceived as insignificant, can lead to measurable differences in HR due to the biomechanical and muscular demands they impose. Ensuring participants adhere to consistent and standardized motion patterns is therefore vital for reliable data collection and accurate interpretation of activity load.

4.2.4 Hierarchy and Differentiation in Activity Load Levels

The interplay between upper and lower body exercises is inherently complex, particularly in the context of differentiating activity load. Figures 4.9 (based on equations 4.3 to 4.6), and 4.10 collectively highlight how HR data can uncover subtle yet meaningful distinctions in exercise difficulty, providing a deeper understanding of movement combinations and their cardiovascular impact.

Figure 4.9 illustrates the intricate relationship between upper and lower body contributions by visualizing HR levels for all exercise combinations. Each line connects exercises that share the same upper body movement, linking them to various lower body movements. The consistent downward trend across these lines reaffirms the dominant role of lower body exercises in driving the overall HR response. However, this visualization also highlights the influence of upper body exercises on the HR gradient,

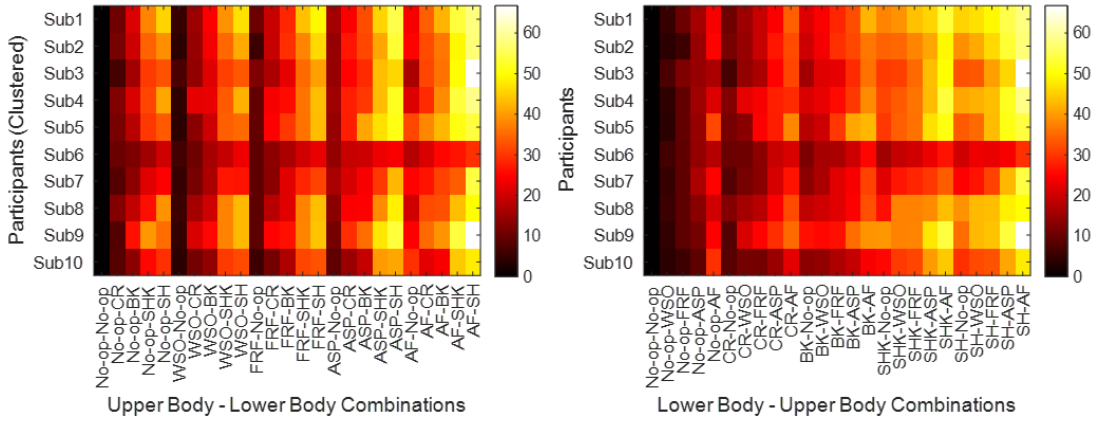

(a) (b)

Figure 4.10: Heatmaps of HR responses across exercise combinations for all participants. (a) Upper body exercises clustered with varying lower body combinations, showing stronger lower body exercises leading to higher HR levels. (b) Lower body exercises clustered with different upper body combinations, highlighting a greater impact of lower body variability on HR levels. In (a) No-op represents the exclusion of lower body movement and in (b) No-op represents the exclusion of upper body movement.

particularly when combined with moderate-intensity lower body movements.

Additionally, while the lines do not perfectly separate each exercise, they exhibit a discernible pattern of differentiation. The exercises collectively follow a downward-right trajectory, showing a structured increase in intensity as new combinations are formed. This indicates that newly combined exercises align with the linear progression of intensity seen in isolated upper and lower body movements. This structured pattern underscores the dynamic yet predictable interaction between upper and lower body exercises in determining overall HR levels.

Moving into Figure 4.10, the clustering heatmaps provide additional insights by focusing on participant-specific responses. In Figure 4.10(a), the clustering of upper body movements across participants shows that while lower body variations significantly shift the HR level within the same upper body cluster, upper body movements still maintain distinguishable clusters. This suggests that upper body exercises, despite contributing less overall to HR differences, retain their influence within specific combinations. Conversely, Figure 4.10(b) demonstrates the linear impact of lower body movements. The HR levels increase predictably as lower body intensity grows, even when combined with various upper body exercises. This pattern underlines the foundational role of lower body movements in dictating overall exercise difficulty, though

it also shows that subtle variations in HR due to upper body changes are consistent across participants.

These findings collectively emphasize the nuanced relationship between upper and lower body contributions to activity load. While lower body movements generally dominate HR responses, upper body movements provide critical refinements, particularly in combinations where lower body intensity is moderate or consistent. This reinforces the potential of HR-based analysis to quantify and rank activity load, even when subtle differences exist.

4.2.5 Comparison of Activity Load Evaluation Methods

To evaluate the reliability of the proposed method for assessing activity load, which relies on the difference between heart rate at the end of exercise and resting heart rate ($HR_{\text{exercise}} - HR_{\text{rest}}$), and to explore whether alternative metrics could also classify activity load, a validation was conducted using HRV metrics derived from (Seiler et al., 2007). By comparing exercise intensities classified through $HR_{\text{exercise}} - HR_{\text{rest}}$ with those derived from HRV-based metrics, the aim was twofold: to establish the robustness of the proposed method and to determine if movement difficulty, as reflected in HR changes, aligns with broader physiological indicators.

Figure 4.11 (based on equations 4.7 to 4.9) illustrates the comparison of upper-body and lower-body exercises across multiple metrics. The proposed $HR_{\text{exercise}} - HR_{\text{rest}}$ method (Figure 4.11a) provides a straightforward yet effective representation of activity load. Meanwhile, HRV-derived metrics—mean RR intervals (Figure 4.11b), rMSSD (Figure 4.11c), and pNN50 (Figure 4.11d)—offer additional insights into the physiological responses associated with different movements. Importantly, these metrics reveal the ability to differentiate movement intensities not just through HR but through broader autonomic nervous system dynamics.

Figure 4.12 (based on equation 4.10) quantitatively highlights the correlation between the proposed method and HRV metrics. Unsurprisingly, mean RR intervals exhibit the strongest correlation ($r = 0.87$), as HR and RR intervals are inversely related and closely tied. The high correlation supports the idea that $HR_{\text{exercise}} - HR_{\text{rest}}$ effectively captures the same physiological patterns reflected in mean RR intervals. Similarly, rMSSD shows a moderate correlation ($r = 0.64$), suggesting that HR-based movement classification aligns well with parasympathetic activity changes, reinforcing the reliability of HR as an indicator of activity load.

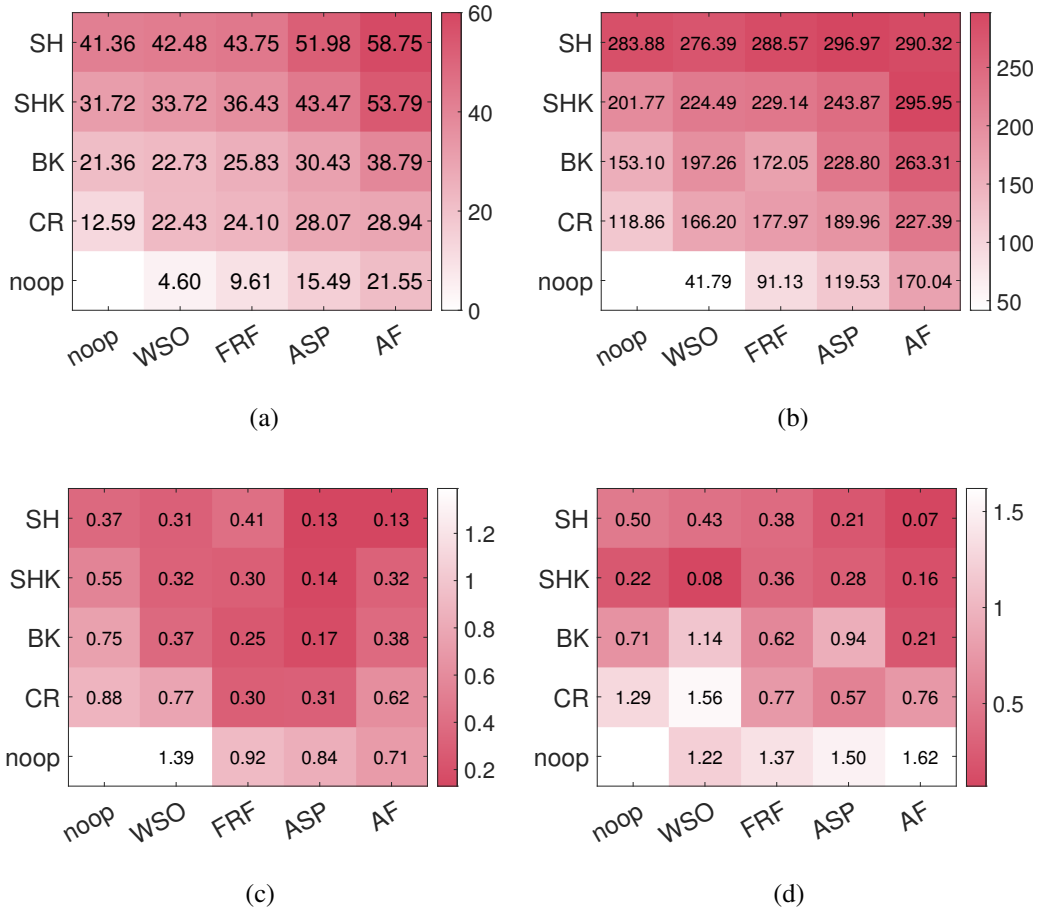

Figure 4.11: Heatmaps illustrating the intensity comparison between five upper-body (rows) and five lower-body (columns) exercises. (a) Activity load is calculated as the difference between post-exercise heart rate and resting heart rate. (b) Mean RR intervals(ms) difference between resting and exercise phases. (c) Ratio of rMSSD values in resting and exercise phases. (d) Ratio of pNN50 values in resting and exercise phases. The No-op on the x-axis represents the exclusion of upper body movement, while the No-op on the y-axis represents the exclusion of lower body movement.

Interestingly, pNN50 displays a much weaker correlation ($r = 0.38$) with the proposed method, raising questions about its utility as a universal indicator of activity load. However, upon closer examination of Figure 4.11d, pNN50 appears to capture meaningful trends within lower-body exercises, which are typically more demanding and influential in determining overall intensity. This aligns with observations in earlier sections, where lower-body movements were found to play a dominant role in driving physiological responses. Within upper-body exercises, however, pNN50 shows less differentiation, potentially due to the smaller physiological impact of these movements

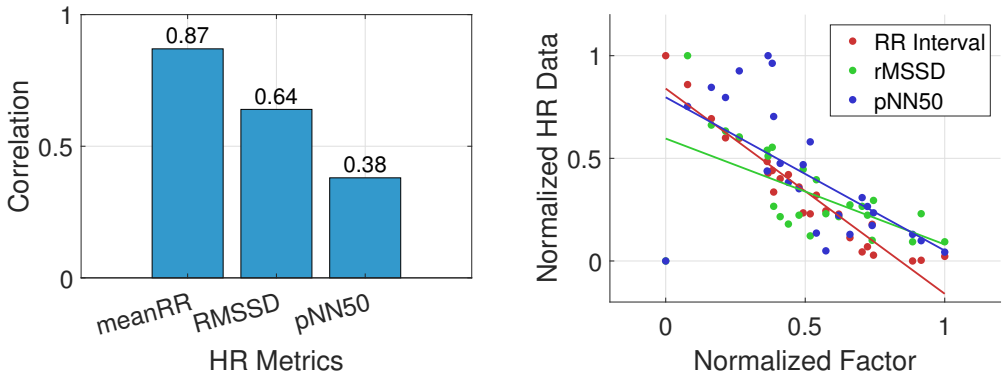

(a) (b)

Figure 4.12: Correlation analysis between the HR-based intensity metric from the proposed method (Figure 4.12a) and various HRV metrics: mean RR interval (meanRR), rMSSD, and pNN50 (Figure 4.12b–d). (a) bar plot showing the correlation of different HRV metrics, (b) linear regression fit and correlation for each factor. The results highlight a strong correlation with meanRR (0.87), moderate correlation with rMSSD (0.64), and weaker correlation with pNN50 (0.38).

on autonomic nervous system balance.

The results suggest that while $HR_{\text{exercise}} - HR_{\text{rest}}$ provides a reliable and practical measure of activity load, HRV metrics like mean RR intervals and rMSSD can further validate this approach, offering complementary perspectives on movement difficulty. Moreover, the nuanced behavior of pNN50 underscores the importance of considering movement-specific characteristics when interpreting HRV metrics, particularly for lower-body exercises, where pNN50 seems more reflective of intensity changes.

In conclusion, the strong alignment between HR-based classifications and HRV metrics reinforces the reliability of the proposed method. Additionally, the ability of HRV metrics to capture intensity differences, especially in lower-body movements, highlights the physiological basis of exercise difficulty classification, extending the applicability of this approach beyond simple HR measurements. This multidimensional validation not only strengthens the credibility of $HR_{\text{exercise}} - HR_{\text{rest}}$ as an intensity metric but also underscores its potential for broader applications in movement analysis and classification.

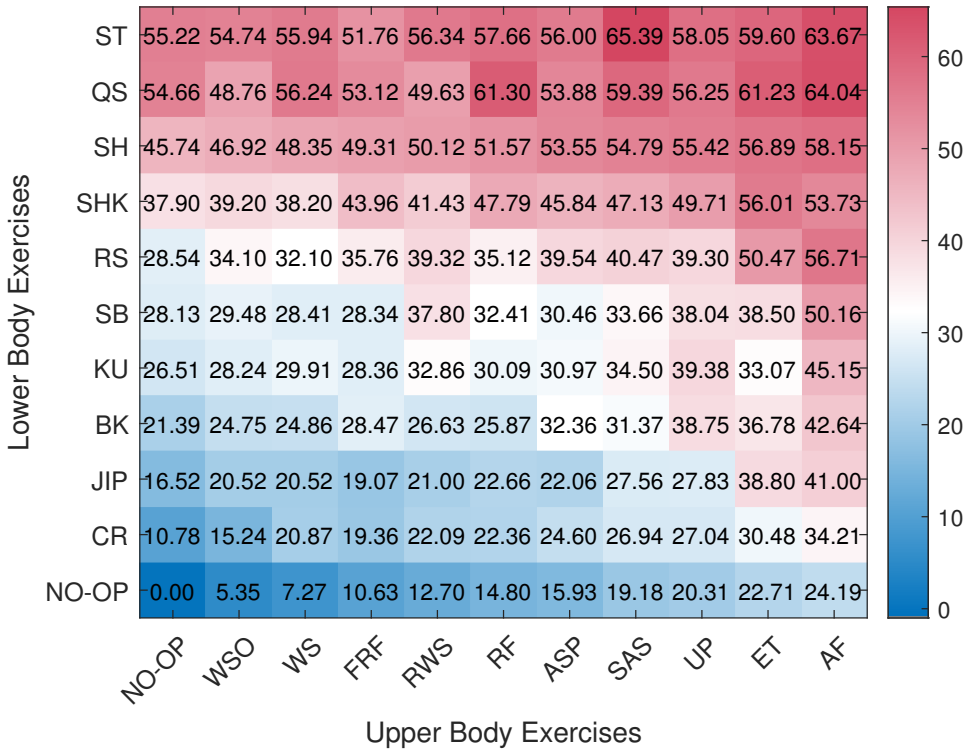

Figure 4.13: An example heart rate heatmap representing 120 exercises, showcasing all exercise combinations analyzed in Section 4.3. The heatmap illustrates the difference between maximum HR and resting HR across various combinations. The x-axis represents different upper body exercises, and the y-axis shows different lower body exercises. Color intensity indicates the magnitude of the HR difference, with warmer colors representing greater increases relative to resting levels. Each heatmap corresponds to a different subject. The No-op on the x-axis represents the exclusion of upper body movement, while the No-op on the y-axis represents the exclusion of lower body movement.

Table 4.4: Average Deviation of All Participants

Participant	Sub1	Sub2	Sub3	Sub4	Sub5	Sub6	Sub7	Sub8	Sub9	Sub10
Avg Deviation	0.34	1.36	-.102	0.98	3.74	-0.66	0.76	2.42	1.04	1.27

4.3 Activity Load Prediction From the Representative Exercise to the Whole Exercise Combinations

Predicting the difficulty levels of exercise combinations derived from ten selected movements builds upon the findings of Chapter 3. The earlier discovery that partial

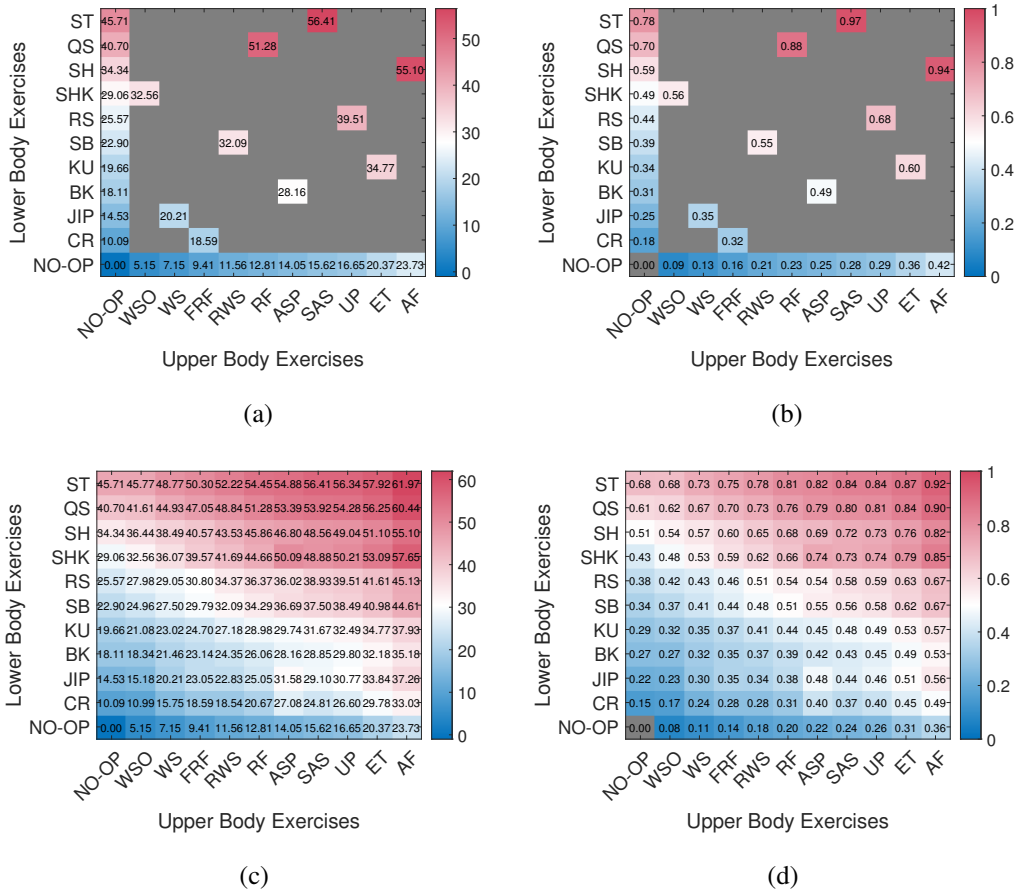

Figure 4.14: Heatmap comparison of actual and predicted data across 30 exercises for all participants. (a) Averaged actual data of 30 exercises across all participants. (b) Normalized average of the actual data for all participants. (c) Predicted data generated using the actual data in (a). (d) Normalized average of the predicted data for all participants. The No-op on the x-axis represents the exclusion of upper body movement, while the No-op on the y-axis represents the exclusion of lower body movement.

order relationships are preserved even when exercises are separated into upper and lower body movements serves as the foundation for this analysis. By isolating these movements into "Noop" (exclusion of upper or lower body movements) combination exercises, a total of 30 individual exercises were conducted, providing the baseline data necessary for further predictions.

Figure 4.14 (a) and (b) present the averaged and normalized average data across participants for these foundational exercises. Using these results, predictions were extended to the remaining 90 exercise combinations. The methodology involved calculating heart rate (HR) intensity differences between the Noop combination exercises

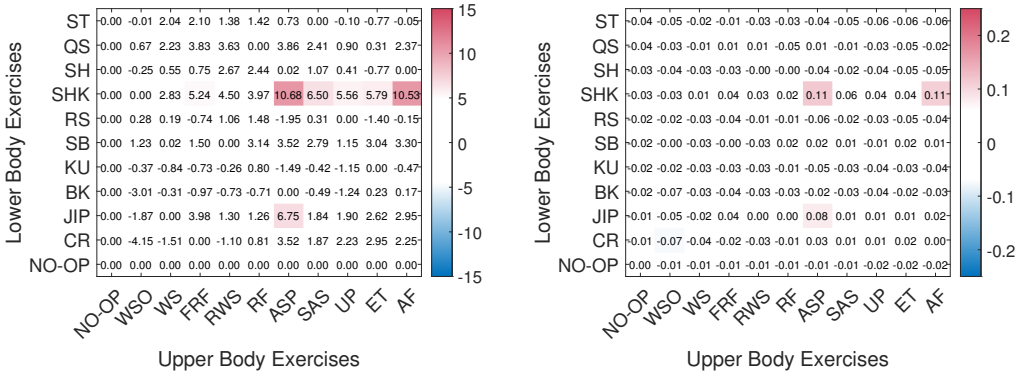

(a) (b)

Figure 4.15: Heatmap showing the differences between predicted data and actual exercise results. (a) The average difference between predicted and actual data across all participants (accuracy: 95%). (b) The normalized average difference between predicted and actual data across all participants (accuracy: 97%). Red represents over estimated value and blue represents under estimated value. The No-op on the x-axis represents the exclusion of upper body movement, while the No-op on the y-axis represents the exclusion of lower body movement.

(exclusion of upper or lower body exercise) and existing movements for each row and column of the heatmap. These differences were scaled proportionally based on the distances between exercises, enabling the estimation of HR intensities for the remaining combinations. The final predicted intensity values were computed by averaging the row- and column-based predictions. Figure 4.14 (c) and (d) display the averaged predictions and normalized averages for these estimates.

To validate these predictions, the ground truth data for all 90 additional combinations were collected through participant trials. The accuracy of the predictions was evaluated by comparing the differences in averages between predicted and actual exercise intensities. Table 4.4 summarizes the average deviations across all participants, indicating minimal overall deviations. Figure 4.15 (a) and (b) further illustrate these comparisons, showing that for most combinations, HR differences remained within an acceptable range of approximately 5, with only a few outliers exceeding this range (accuracy of 95%).

An essential aspect of this analysis involved assessing the preservation of partial order across participants. Figure 4.16 focuses on the partial order of upper body movements while maintaining a fixed lower body posture, revealing that the overall flow

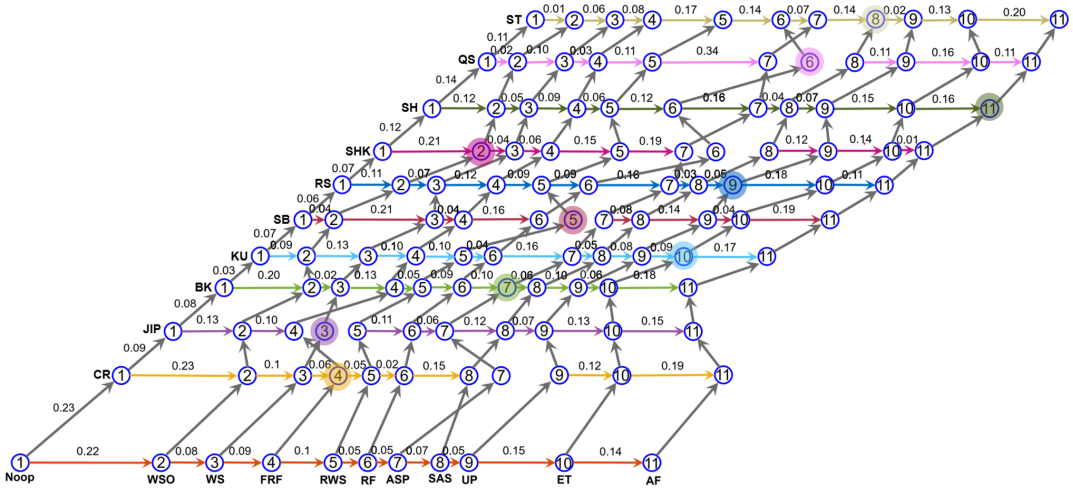

Figure 4.16: Average partial order representation of all exercises across participants, focusing on the quality aspect. This figure illustrates the partial order of upper body movements by maintaining a fixed lower body posture, enabling the analysis of variations in upper body actions. The diagram illustrates the relative relationships and transition probabilities between different exercise combinations, with edge weights representing the normalized average values of HR difference. For the broken partial orders, adjacent exercise arrows were not drawn. 10 original exercises are highlighted. The Noop on the x-axis represents the exclusion of upper body movement, while the Noop on the y-axis represents the exclusion of lower body movement.

of the partial order was largely preserved despite occasional minor disruptions. These disruptions, represented by unconnected arrows, were infrequent and did not compromise the general structure of the order. In contrast, Figure 4.17 examines the partial order for lower body movements while fixing upper body postures. Remarkably, the lower body exercises exhibited complete preservation of the partial order, suggesting a greater consistency in distinguishing lower body exercise intensities compared to upper body movements. This contrast underscores the robustness of lower body movements in maintaining partial order and highlights their relative clarity in intensity differentiation.

A deeper analysis was conducted to investigate exercises with significant deviations in Figure 4.15 (five combinations identified) and cases where partial order was disrupted in Figure 4.18 (where fewer than 50% of participants adhered to the order). Comparing the individual data of all participants revealed that only the combination of "ASP" and "SHK" failed to satisfy both quantitative (number of participants maintaining partial order) and qualitative (high HR deviation) criteria. Among six participants

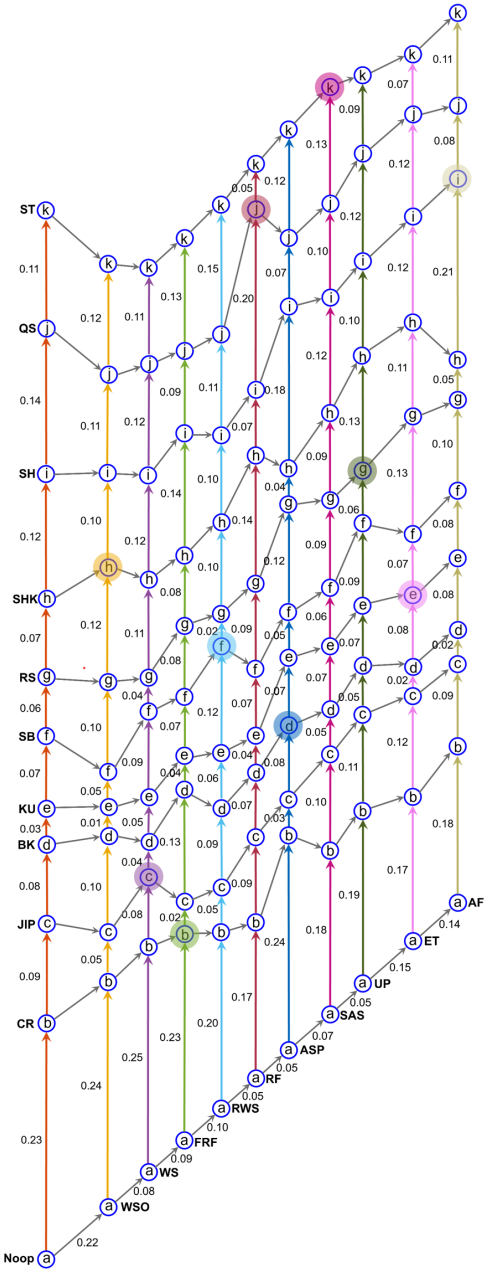

Figure 4.17: Average partial order representation of all exercises across participants, focusing on the quality aspect. This figure illustrates the partial order of lower body movements by maintaining a fixed upper body posture, enabling the analysis of variations in lower body actions. The diagram illustrates the relative relationships and transition probabilities between different exercise combinations, with edge weights representing the normalized average values of HR difference. 10 original exercises are highlighted. The No-op on the x-axis represents the exclusion of upper body movement, while the Noop on the y-axis represents the exclusion of lower body movement.

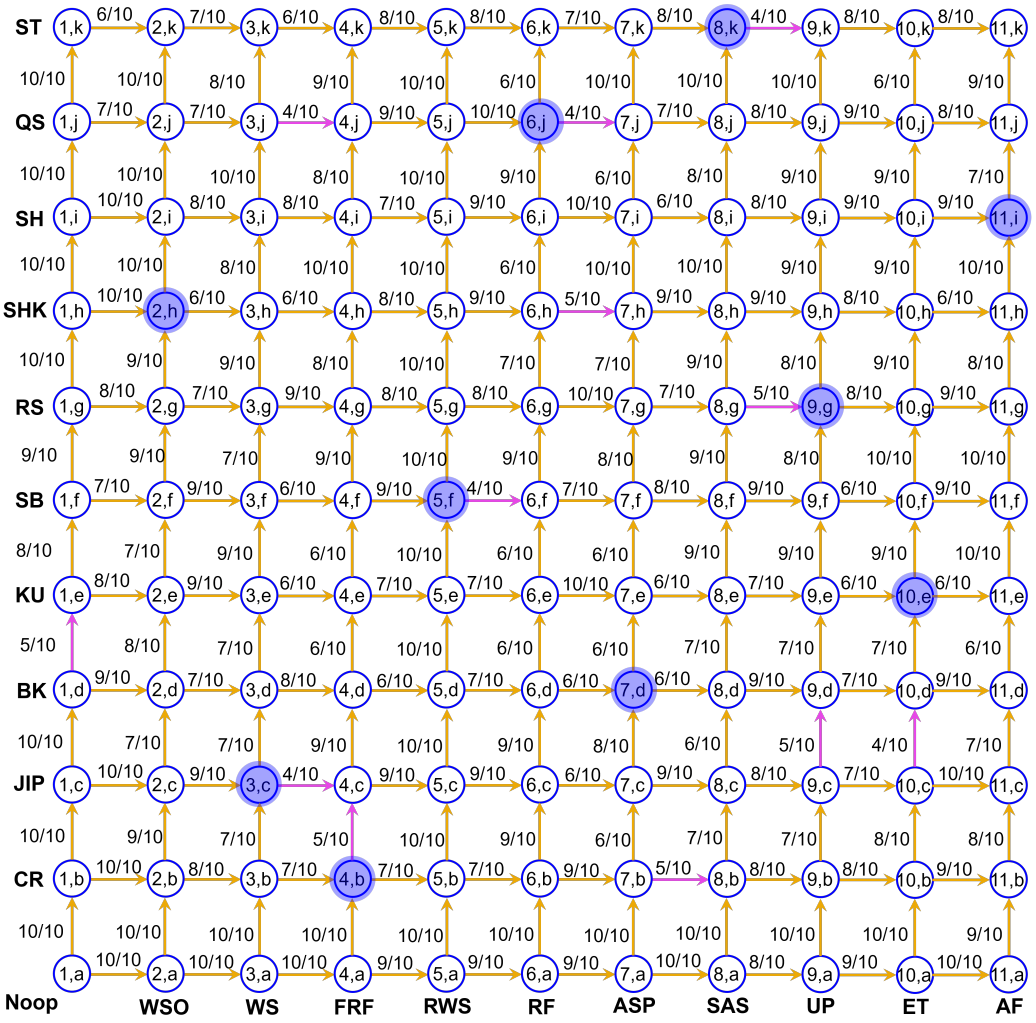

Figure 4.18: Quantitative representation of the average partial order across all exercises for participants. Based on the partial orders in Figure 4.16 (numerical exercise labels) and Figure 4.17 (alphabetical exercise labels), this figure indicates the number of participants who followed the partial order for each exercise combination. Yellow arrows indicate if the partial order was followed over 50% of the participants, if not the arrows were colored pink. 10 original exercises are highlighted. The Noop on the x-axis represents the exclusion of upper body movement, while the Noop on the y-axis represents the exclusion of lower body movement.

who did not maintain partial order for this combination, the normalized HR difference (Figure 4.16) was -0.21 (overall average: 0.09). After removing the two most significant outliers, this value improved to -0.075, a negligible difference. A closer inspection of these outliers' performance highlighted motion-related issues during the exercise, emphasizing the importance of accurate execution for maintaining order.

For the remaining four exercises, although partial order was disrupted, the deviations were minor, reflecting natural variations in activity load rather than significant inconsistencies. This suggests that these exercises shared similar activity loads, leading to slight overlaps in HR intensities without undermining their order-based rankings.

A deeper analysis was conducted to investigate the distances where partial order was disrupted, as indicated by unconnected arrows in Figure 4.16. The average distance between all nodes in Figure 4.16 (measured as the vector length of the arrows) was 0.1 ± 0.7, while the average distance for disrupted partial orders (e.g., where exercise 3 was mistakenly ranked below exercise 4) was -0.06 ± 0.02. If the partial order were intact, the average distance would shift to approximately 0.16, suggesting that these disruptions occurred within the range of adjacent exercises. This finding aligns with the interpretation that such errors reflect natural variations in activity load rather than significant inconsistencies, as the errors remain within a narrow HR difference range.

Further analysis of HR values for disrupted partial orders revealed whether the lower-difficulty exercise (e.g., exercise 3) was performed more strenuously than expected, or the higher-difficulty exercise (e.g., exercise 4) was performed less strenuously. Comparisons with exercises preceding and following the disrupted segment showed that participants tended to overexert on the lower-difficulty exercise in 65% of cases, underexert on the higher-difficulty exercise in 28% of cases, and perform inconsistently on both exercises in 7% of cases. These results underscore the importance of accurate motion execution to maintain partial order consistency.

Analysis of HR data in cases where partial order was disrupted revealed that the actual HR differences in most cases were minimal, with an average of -3.15 ± 3.33. This supports the notion that disruptions typically occur between exercises of adjacent difficulty levels, reflecting natural variations. However, specific combinations, such as the lower-body movement "JIP" paired with upper-body movements "WS" and "FRF" (-3.37 ± 3.94), and the lower-body movement "SB" paired with upper-body movements "RWS" and "RF" (-3.81 ± 3.58), showed outlier-like tendencies for one participant. For these combinations, HR differences of -10 and -10.58, respectively, were observed, indicating that the participant exerted more effort on an easier exercise and less effort on a harder one. This participant was identified as having little prior exercise experience and was unaccustomed to maintaining proper guided movements, likely contributing to these outlier values.

From Figure 4.15's heatmap, overestimated values (red regions) predominantly contributed to deviations, indicating participants performed these exercises more eas-

ily than predicted. For example, the combination of “AF” and “SHK” had a prediction error of 10.53, which reduced to 5.91 after removing a significant outlier, highlighting the impact of individual participant variability. This pattern suggests that inaccuracies in estimating difficulty arise when baseline data are limited to proximal exercises with substantial variability. As such, future studies should aim to diversify the foundational exercise set to improve estimation accuracy.

Interestingly, exercises disrupting partial order in Figure 4.18 also exhibited high error rates in Figure 4.15, further linking motion consistency with partial order preservation. For instance, when participants deviated from predicted partial orders, their HR data revealed irregularities stemming from motion inconsistencies or execution errors. These findings emphasize the feasibility of using partial order frameworks to identify and address discrepancies in activity load estimation, enabling more robust predictions.

The preservation of partial order across exercises implies that while absolute intensity values may pose challenges, relative rankings based on partial order provide a reliable framework for estimating exercise difficulty. Figure 4.18 quantitatively evaluates partial order maintenance across all exercise combinations, showing the proportion of participants who adhered to the partial order for each combination. The majority of combinations demonstrated consistent partial order adherence, with only a few deviations observed. These deviations often corresponded to the exercises identified in Figure 4.15 as having higher HR differences, further emphasizing the connection between motion consistency and partial order preservation.

By leveraging the concept of partial order preservation, this approach offers a robust mechanism for predicting exercise difficulty through relative rankings rather than absolute intensity values. While refinements may be necessary for specific exercises to improve consistency, the findings demonstrate the feasibility and effectiveness of using partial order as a guiding principle for understanding and predicting activity load across diverse combinations. Additionally, the analysis suggests that partial order disruptions are more likely to occur in exercises with closely matched difficulty levels, reflecting natural variations in activity load. The insights gained from these disruptions can guide refinements in methodology and ensure more robust predictions for future studies.

4.4 Discussion

This chapter extends the understanding of exercise difficulty prediction by exploring how the interplay between upper and lower body movements defines HR responses during exercise. The findings emphasize that the difficulty of combined movements cannot be reduced to a simple additive sum of their components (e.g., upper + lower = sum of HR effects). Instead, the results demonstrate that relative intensities and interactions between the upper and lower body modulate the overall difficulty.

Building upon the insights from Chapter 3, the concept of partial order preservation was pivotal in this analysis. Figures 4.14 (c) and (d) illustrate the predicted HR intensity levels for exercise combinations derived using proportional differences between Noop exercises and existing movements. These predictions, validated against ground truth data for 90 additional combinations, showed high accuracy with minimal deviations, as reflected in Table 4.4 and Figure 4.15. This accuracy highlights the feasibility of using relative rankings to systematically predict activity load.

The preservation of partial order, as demonstrated in Figures 4.16 and 4.17, underscores its robustness as a framework for understanding exercise difficulty. While minor disruptions in partial order were observed for upper body movements, lower body exercises maintained complete order consistency. These findings reveal the distinctiveness of lower body movement intensities and their ability to sustain clear differentiation. Moreover, Figure 4.18 quantitatively reinforces the reliability of partial order preservation across participants, showcasing its potential as a foundation for predicting exercise difficulty.

Figures 4.9 and 4.10 from earlier analysis further support this conclusion by highlighting the hierarchical nature of HR responses and the nuanced contributions of both upper and lower body movements. Lower body exercises consistently dominated overall intensity levels, while upper body exercises introduced subtle variations that refined the combined response. The clustering analysis in Figure 4.10 demonstrated how systematic relationships between movements enable the prediction of activity load.

Interestingly, the exercises that disrupted partial order correlated strongly with those showing higher HR deviations in Figure 4.15. These deviations are linked to inconsistencies in motion execution among participants, as discussed in the “Importance of Maintaining Motion Accuracy” section. Such findings suggest that exercises with less consistent execution require stricter motion control protocols to enhance predictability and reliability.

By leveraging the proportional HR relationships and partial order framework, exercise programs can be tailored to diverse needs. This approach ensures inclusivity, safety, and effectiveness across varying fitness levels and goals.

4.5 Conclusion

This chapter establishes a scientific foundation for understanding and designing combined exercises based on proportional HR contributions and partial order preservation. The findings challenge the simplistic assumption that combined movement difficulty is merely the sum of its components. Instead, the proportional relationships revealed in this analysis demonstrate that relative intensities and systematic interactions between upper and lower body movements modulate overall exercise difficulty.

By isolating upper and lower body movements into Noop combinations, this study developed a robust framework for predicting the difficulty of diverse exercise pairings. The validation of predictions against actual data revealed strong alignment, with minimal deviations, as highlighted in Table 4.4 and Figure 4.15. The preservation of partial order across participants, as demonstrated in Figures 4.16 and 4.17, underscores the reliability of this approach. Lower body movements, in particular, exhibited complete order consistency, reinforcing their distinctiveness and predictability compared to upper body exercises.

The practical implications of these findings are significant. By understanding the proportional contributions of upper and lower body movements, exercise programs can be systematically designed to meet diverse needs. For instance, low-impact protocols can be developed for individuals with physical limitations, age-appropriate routines can be designed for children or older adults, and HIIT workouts can be optimized to balance cardiovascular demands. This framework ensures both accessibility and effectiveness, paving the way for more inclusive and tailored fitness programming.

In conclusion, this chapter provides a comprehensive analysis of the interplay between upper and lower body movements, offering a scientifically grounded approach to predicting exercise difficulty. Focusing on relative rankings and partial order preservation, it establishes a foundation for designing personalized exercise protocols that are both effective and accessible to diverse populations.

4.6 Summary of Chapter 4

Chapter 4 explored the prediction of exercise difficulty through the lens of proportional relationships and partial order preservation. By isolating upper and lower body movements into Noop combinations, the analysis provided a baseline for predicting the HR intensities of diverse exercise pairings. Figures 4.14 (a) and (b) detailed the averaged and normalized foundational data, while Figures 4.14 (c) and (d) showcased the predicted intensities for the remaining combinations, derived using a proportional difference methodology.

Validation of these predictions against actual exercise data revealed strong alignment, with minimal deviations, as highlighted in Table 4.4 and Figure 4.15. These results demonstrate the reliability of this predictive approach, particularly when supported by the concept of partial order preservation. Figures 4.16 and 4.17 illustrated how partial order was maintained across most combinations, with lower body movements displaying complete consistency. This finding emphasizes the distinctiveness and predictability of lower body exercises compared to upper body movements.

Figure 4.18 quantitatively examined the adherence to partial order across participants, revealing a strong trend of consistency despite minor individual variations. Exercises that deviated from partial order were identified as those with less motion consistency, reinforcing the need for refined motion control in certain cases. By leveraging these insights, this chapter provides a scientifically grounded framework for predicting exercise difficulty through relative rankings and partial order preservation.

These findings have significant practical implications. By understanding the proportional contributions of upper and lower body movements, exercise programs can be systematically designed to meet diverse needs. The framework enables the development of tailored protocols for injury recovery, age-appropriate routines, and optimized HIIT workouts, ensuring both accessibility and effectiveness. Chapter 4 thus offers a comprehensive approach to predicting and designing exercises, advancing the understanding of HR responses and exercise difficulty.

Chapter 5

Predicting Heart Rate and Blood Glucose Trends from Daily Activities

The intricate relationship between heart rate (HR) and blood glucose (BG) is critical in understanding physiological regulation, health monitoring, and disease management. With the increasing prevalence of conditions like diabetes and cardiovascular diseases, exploring the dynamic interplay between HR and BG during daily activities and dietary intake has become essential for maintaining physiological stability.

Motivated by prior research (Yoon and Kim, 2025b; Yoon and Kim, 2025a) that highlighted the significant influence of meal status on resting HR, this study expands the focus to BG fluctuations and their predictive capability for HR stability. Additionally, it explores the potential for using HR patterns to approximate BG levels, demonstrating a novel bidirectional predictive framework. These insights not only enhance our understanding of metabolic and cardiovascular interactions but also pave the way for more controlled HR experiments that account for BG-induced variability, ensuring greater accuracy and consistency in experimental outcomes.

This study leverages technologies, including the Polar Verity Sense and FreeStyle Libre systems, to collect continuous, real-time data on HR and BG during participants' typical daily routines. By integrating dietary and activity logs, the data captures natural lifestyle patterns, reflecting realistic physiological responses. Statistical techniques such as cross-correlation analysis and similarity functions were used to analyze temporal alignments and variability between HR and BG, revealing patterns of synchronization influenced by dietary and activity-related changes.

The findings highlight the predictive potential of BG for resting HR stability and HR for approximating BG levels, emphasizing the necessity of incorporating BG vari-

ability into HR-focused research. By bridging the gap between metabolic regulation and cardiovascular responses, this study provides a comprehensive framework for designing more robust and interpretable methodologies. This paper's contents are being prepared for submission to a journal (Yoon and Kim, 2025c).

5.1 Methods

5.1.1 Subjects

We recruited five adult male participants for this study. Each individual was thoroughly informed about the purpose of the study and provided their consent by signing a consent form prior to engaging in any experimental activities. Furthermore, all researchers involved in this project completed online research ethics training before the experiments began. The study protocol received approval from the Institutional Review Board (IRB) of Yonsei University, the institution overseeing this research (Registration number: 7001988-202410-HR-2376-04).

Participants were selected based on specific inclusion and exclusion criteria. The inclusion criteria were: 1) The ability to wear a sensor on both upper arms; 2) No mobility impairments or reliance on assistive walking devices, and the capability to attend the research facility; 3) An age range of 20 to 35 years; 4) A voluntary willingness to participate.

Exclusion criteria were: 1) Individuals with significant communication difficulties, such as those due to cognitive impairments or aphasia; 2) Those with severe cardiovascular, cardiopulmonary, or other major internal medical conditions; 3) Individuals with a history of surgeries or conditions related to musculoskeletal or neurological issues; 4) Participants deemed unsuitable for the study by the researcher.

The participants' demographic and physical characteristics, including sex, age, height, weight, and BMI, are presented in Table 5.1 below.

5.1.2 Experiment

5.1.2.1 Experimentation Platform

In the study, HR data was collected using the Polar Verity Sense, an Optical Heart Rate Sensor. This HR experimental tool consists of six channel LEDs with 1 SPS(samples per second). It was worn on participants' non-dominant forearms to minimize inter-

Table 5.1: Characteristics of the subjects. (SD, standard Deviation)

Characteristic	***Values***
Sex (male/female)	4/1
Age (mean± SD)	25.4 ± 1.14 [years]
Height (mean± SD)	175.46 ± 8.01 [cm]
Weight (mean± SD)	71.6 ± 16.28 [kg]
BMI (mean± SD)	23.12 ± 4.15 [kg/m^2]

Note: BMI denotes body mass index.

ference, with calibration and setup conducted as per manufacturer guidelines. HR data was continuously recorded via the Polar Flow app, ensuring real-time monitoring and post-session data export for analysis. Data cleaning, segmentation, and statistical methods were applied to examine heart rate variability and other metrics. Validation was achieved by comparing readings with a standard HR monitor, confirming the sensor's reliability for continuous heart rate monitoring in a research setting.

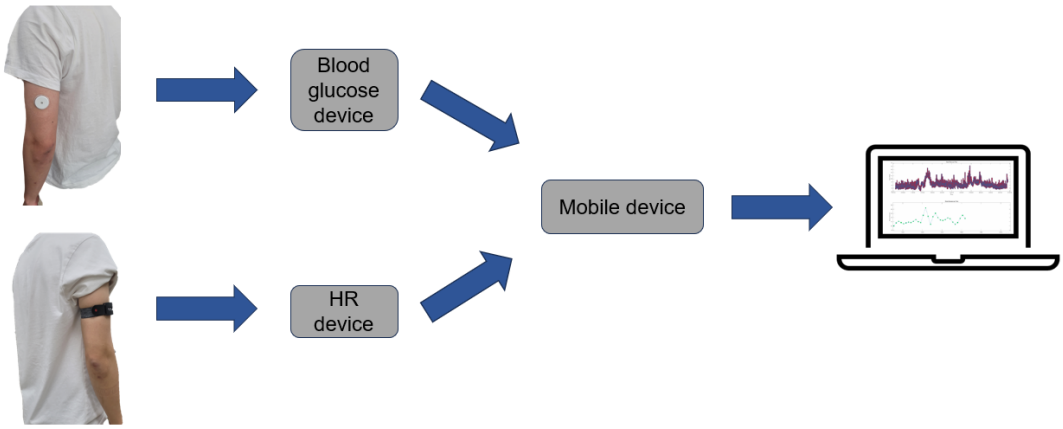

Figure 5.1: Blood glucose and heart rate monitoring system. Monitoring and analysis system of blood glucose and heart rate sensor used in this research.

For the blood glucose data, FreeStyle Libre Flash Glucose Monitoring System was used. Participants wore the sensor on the back of their upper arms, following the manufacturer's application guidelines to ensure proper adhesion and accurate readings. The system provided real-time glucose data, which was continuously monitored and logged via the FreeStyle LibreLink app. Post-session, the data was exported for analysis, involving data cleaning, segmentation, and statistical methods to assess glucose variability and trends. To validate accuracy, glucose readings from the FreeStyle Li-

bre were compared with traditional blood glucose meter measurements, confirming the system's reliability for continuous glucose monitoring in a research setting. MATLAB2021b was used for data analysis, allowing for a comprehensive investigation of the recorded bioelectric signals (Khan et al., 2012; Ravariu, 2011).

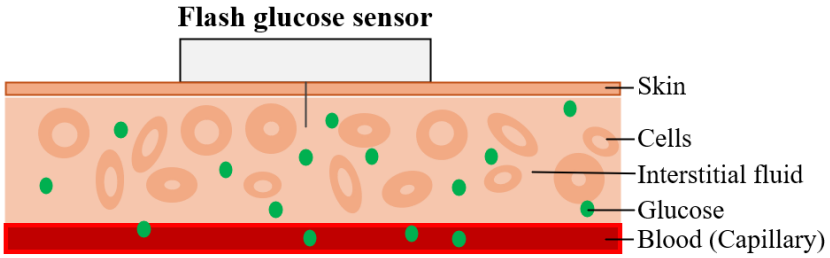

Figure 5.2: Blood glucose monitoring sensor. The sensor filament is 0.4 millimeters thick and inserted 5 millimeters under the skin surface. Using the filament blood glucose levels are continuously measured through interstitial fluid in subcutaneous fat.

The utilization of these advanced tools and technologies ensured accurate and reliable data collection, enhancing the credibility and applicability of the study's findings (Salman et al., 2012). The integration of state-of-the-art equipment and software reflects the commitment to producing high-quality research with practical implications for personalized rehabilitation and exercise interventions (Gupta and Saxena, 2012).

5.1.2.2 Experimental Protocol

This study aimed to investigate the relationship between HR and BG levels, observing how these parameters change in response to various daily activities and dietary intake. Three participants were monitored over a period of three days during their working hours, using the Polar Verity Sense for HR monitoring and the FreeStyle Libre Flash Glucose Monitoring System for BG tracking.

Participants were instructed to carry out their usual daily routines without any specific restrictions, ensuring the data reflected typical lifestyle patterns. However, they were asked to log any notable changes in activity or dietary intake, such as transitioning from sitting to walking or consuming food or beverages. This logging was crucial for correlating specific activities and intake with fluctuations in HR and BG levels.

The monitoring involved continuous real-time data collection, which was subsequently analyzed to understand the interrelationship between HR and BG, their variability, and the impact of different activities and dietary intake. Furthermore, the study aimed to identify any time-phase differences between changes in BG and HR.

(a)

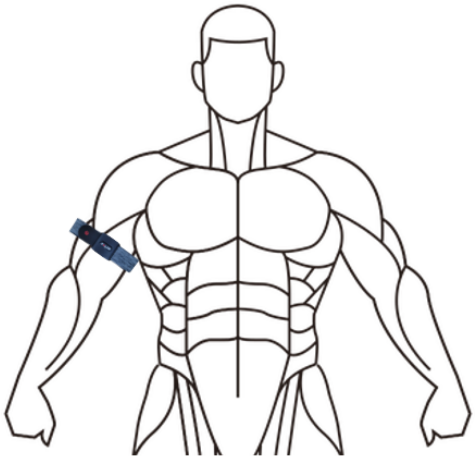

(b)

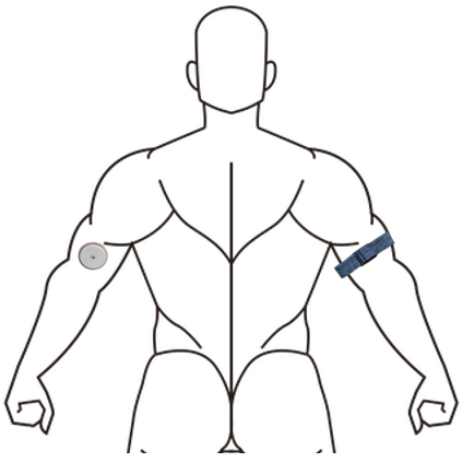

(c)

Figure 5.3: Sensor attachment drawing (a) Anterior view. (b) Posterior view. In order to minimize behavioral restrictions, a BG sensor was attached to the left upper arm muscle of the right hand grip standard, and a Polar HR sensor, which is relatively easy to attach, was worn on the right hand side of the right hand grip standard.

5.1.2.3 Methodology

Three healthy adults participated in the study, providing informed consent and being briefed on the objectives and procedures. The selection criteria included the absence of chronic health conditions and an active lifestyle. Continuous HR monitoring was performed using the Polar Verity Sense, worn on the non-dominant forearm, with data logged in real-time via the Polar Flow app. BG levels were monitored using the FreeStyle Libre Flash Glucose Monitoring System, applied to the back of the upper arm, with data logged in real-time using the FreeStyle LibreLink app. The participants were equipped with the devices and an initial baseline measurement for HR and BG levels was taken. Over three working days, continuous monitoring was conducted dur-

ing working hours, with participants maintaining their usual activities and logging any notable changes such as physical activity or food intake.

Data from both sensors were synchronized with their respective apps and later exported for analysis. Raw data were cleaned to remove artifacts, segmented based on logged activities and dietary intake, and analyzed using statistical methods to examine variability, trends, and correlations between HR and BG levels. Pearson correlation coefficients determined the strength and direction of relationships, while cross-correlation analysis identified any lag or lead times between changes in HR and BG levels. This experimental design facilitated a comprehensive analysis of the dynamic relationship between HR and BG levels in a real-world setting, providing valuable insights into how daily activities and dietary intake influence these physiological parameters.

5.1.2.4 Analysis of Categorized Behaviors

Based on the experiment results, behaviors were categorized into distinct groups reflecting various activities, dietary intake, and physiological states. Physical activities were classified into exercise, resting (including sleep or napping), and walking, each eliciting specific responses in HR and BG levels. Exercise led to significant increases in HR, while BG levels may fluctuate depending on exercise intensity. Resting states were associated with lower HR and relatively stable BG levels. Transitional movements, such as walking to the bathroom or lunch, induced minor elevations in HR compared to resting, with variable effects on BG levels. Dietary intake was categorized into different consumption (e.g., beverage or meal), with potential HR elevations due to sugar content and variable impacts on BG levels. Additionally, postprandial states, following meal consumption, resulted in BG increases as the body metabolized carbohydrates, potentially influencing HR responses. This comprehensive categorization enables a nuanced understanding of the complex relationships between behaviors and physiological parameters, facilitating targeted interventions for health optimization.

5.1.3 Data Analysis

5.1.3.1 Analysis in HR and Blood Glucose data

In electrocardiography (ECG), the R-peak represents the apex of the QRS complex(Manikandan and Dandapat, 2012; Shaik and Ramakrishna, 2015), signifying the ventricular depolarization of the heart(Kligfield and Lauer, 2006). The RR interval, the temporal

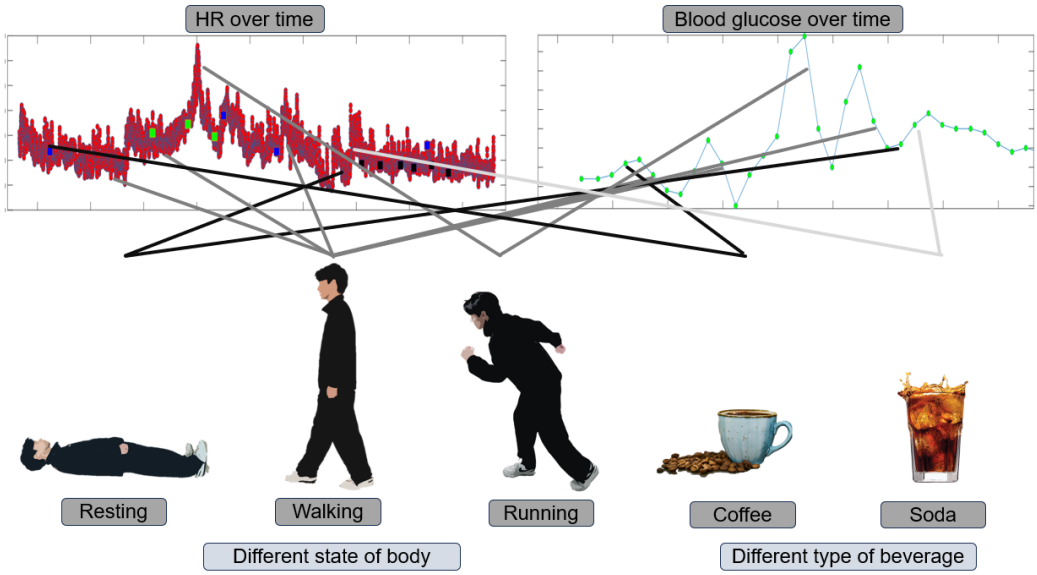

Figure 5.4: Categorized behaviors. Analysis of categorized behavior(different state of body, different types of intakes) with HR over time and Blood glucose over time.

span between two consecutive R-peaks, serves as a pivotal parameter for HR calculation(Park and Lee, 2017). After preprocessing, R-peak points were identified, and the HR(Achten and Jeukendrup, 2003; Shaik and Ramakrishna, 2015) was computed using the formula:

$$\mathrm{HR}_{subject} = \frac{60}{\mathrm{RR}_{interval}}\mathrm{sec} \tag{5.1}$$

This HR data, when contextualized with resting and maximum heart rates, facilitated the calculation of exercise intensity for each subject. Normalizing the exercise intensity using the subject's individual resting and maximum HR provided a relative measure, crucial for classifying the subject's status during each exercise(Goldberg et al., 1988).

To compare and analyze the signals of blood sugar and HR, the similarity of the two normalized signals is obtained through the formula below using MSE (mean squared error), an extended concept of correlation coefficient, and Euclidean distance.

$$\text{Cross correlation} = (f*g)[n] \stackrel{\text{def}}{=} \sum_{m=-\infty}^{\infty} f*[m]g[m+n] \tag{5.2}$$

$$\text{similarity} = \alpha \times \text{normalizedCorrelation} + \beta \times \text{normalizedMse} \tag{5.3}$$

α is the weight assigned to the correlation coefficient. β is the weight assigned to the MSE. Normalized correlation is the correlation coefficient normalized to the range [0, 1]. normalizedMse is the mean squared error normalized to the range [0, 1].

5.2 Results

5.2.1 Estimating trends of Heart rate and Blood glucose of interaction between events

The dynamic responses of HR and blood glucose BG across different daily activities in both fasting and postprandial states reveal important insights into how the body manages physical exertion and metabolic demands. Figure 5.5 illustrates the HR changes, while Figure 5.6 presents the BG fluctuations, capturing transitions such as eating, walking, resting, and engaging in cognitively demanding activities like meetings. These figures provide a detailed view of the body's cardiovascular and metabolic responses under varying conditions, helping us to understand the coupled nature of HR and BG during daily activities.

5.2.1.1 Fasting State: A Controlled Energy Management System

In the fasting state (Figures 5.5a and 5.6a), both HR and BG exhibit relatively stable changes, reflecting the body's effort to conserve energy and maintain glucose homeostasis in the absence of food intake. For HR, transitions from more active states, like long-term walking, to resting (-5.6±1.8 bpm) showed a clear decrease, suggesting that the cardiovascular system downregulates rapidly to conserve energy. Conversely, the transition from rest to long-term walking (+6.7±7.7 bpm) resulted in an increase in HR, indicative of the body's readiness to meet physical demands even when fasting.

Similarly, BG levels in the fasting state remained largely unchanged across various transitions. For example, the minimal BG change observed between eating and long-term walking (+0.3±4.4 mg/dL) suggests that, without recent food intake, the body is more reliant on non-glucose energy reserves, such as fat. The tight control over BG, especially during transitions to resting states, like moving from long-term walking to rest (+0.33±2.46 mg/dL), underscores the body's prioritization of glucose homeostasis during fasting.

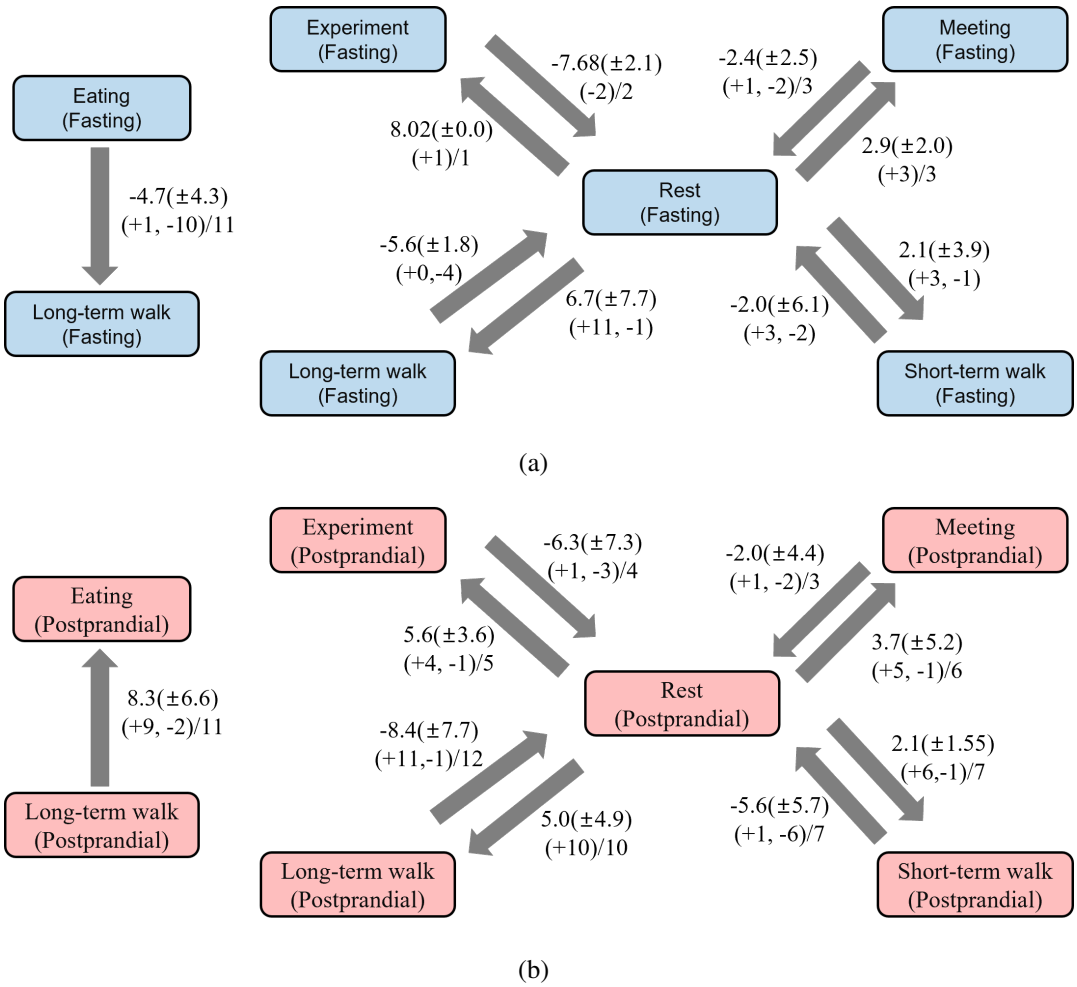

Figure 5.5: Changes in HR during transitions between different activities. (a) HR variations during fasting state transitions, showing the impact of different events such as eating, walking (short-term and long-term), and meetings on HR. (b) HR variations during postprandial (after eating) state transitions, illustrating how HR changes as a result of the same events as in the fasting state. Each arrow represents the change in the average HR leverage between the respective activities, with the values below indicating the number of data points supporting the change and the direction of the data (+ for increase, - for decrease).

The relatively stable nature of both HR and BG in the fasting state reflects a synchronized regulatory response, where the cardiovascular and metabolic systems work together to conserve energy and maintain physiological balance. Even during transitions between cognitively demanding tasks, such as meetings or experiments, HR and BG showed only slight changes, further supporting the notion of a well-controlled physiological state during fasting.

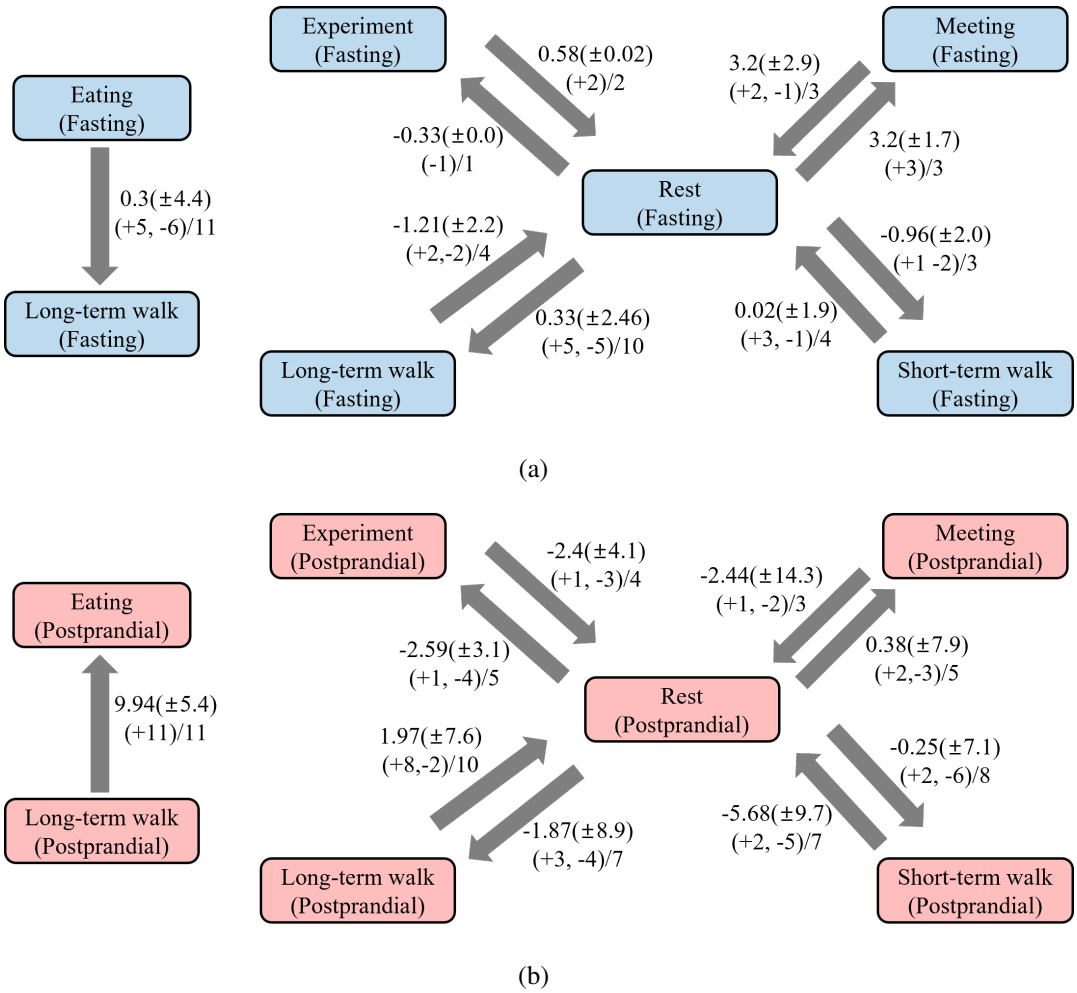

Figure 5.6: Changes in BG during transitions between different activities. (a) HR variations during fasting state transitions, showing the impact of different events such as eating, walking (short-term and long-term), and meetings on HR. (b) HR variations during postprandial (after eating) state transitions, illustrating how HR changes as a result of the same events as in the fasting state. Each arrow represents the change in the average HR leverage between the respective activities, with the values below indicating the number of data points supporting the change and the direction of the data (+ for increase, - for decrease).

5.2.1.2 Postprandial State: Elevated Physiological Activity

In contrast, the postprandial state (Figures 5.5b and 5.6b) presents a much more dynamic response in both HR and BG, driven by the dual demands of digestion and physical activity. For instance, transitioning from eating to long-term walking produced a sharp increase in both HR (+8.3±6.6 bpm) and BG (+9.94±5.4 mg/dL), reflecting the

body's need to supply glucose for digestion and physical exertion simultaneously.

Following periods of activity, such as moving from long-term walking to rest, both HR (-5.0±4.9 bpm) and BG (-5.68±9.7 mg/dL) exhibited significant decreases, indicating that the body is rapidly utilizing or storing glucose as part of the recovery process. This coordinated downregulation in both cardiovascular and metabolic activity demonstrates the body's integrated response to managing energy during postprandial recovery phases.

In the postprandial state, even low-intensity activities like short-term walking or engaging in meetings led to moderate changes in both HR and BG. The ongoing metabolic activity related to digestion creates an environment where even minor exertion can cause noticeable fluctuations in these physiological parameters. The larger range of variation in both HR and BG compared to the fasting state highlights the body's increased metabolic flexibility after eating.

5.2.1.3 Integrated Analysis: Cardiovascular-Metabolic Coupling

When analyzed together, the HR and BG data from fasting and postprandial states reveal key insights into how the cardiovascular and metabolic systems operate in tandem under varying conditions. In the fasting state, the body maintains a tightly controlled environment, with minimal fluctuations in both HR and BG. This suggests that during fasting, energy conservation and homeostasis are the primary goals, with the body limiting unnecessary energy expenditure.

In contrast, the postprandial state is characterized by more pronounced changes in both HR and BG, reflecting the body's need to balance digestion with physical exertion. The simultaneous rise in HR and BG following eating and activity suggests that the body actively mobilizes energy to meet these demands, while the sharp decreases during rest indicate a coordinated recovery process. The alignment of these physiological responses underscores the intricate connection between cardiovascular function and metabolic regulation, particularly in how they jointly respond to daily activities under different nutritional states.

These findings demonstrate the importance of considering both metabolic context and physical activity when analyzing HR and BG variability, as the body's responses are not isolated but rather part of a broader, integrated physiological system.

5.2.2 Estimating trends of Blood glucose in diverse conditions

BG regulation is a complex process influenced by numerous factors, including metabolic state, physical activity, and food or beverage intake. Understanding how these factors shape BG trends is essential for interpreting physiological responses in real-world settings. In this section, we utilize decision tree analysis, supported by Table 5.2, to explore BG fluctuations under various conditions.

5.2.2.1 Candle Chart Analysis and Underlying Data Patterns

Figure 5.7 presents candle charts showing BG and HR fluctuations throughout the day at 5-minute intervals. Red sections signify rising BG or HR, while blue sections indicate decreasing values. Maximum and minimum lines further enhance each candle's visual depiction. These charts capture key BG fluctuations, especially during meal and beverage consumption periods.

The postprandial period exhibits the sharpest BG fluctuations, with a marked increase followed by a gradual decline. This is reflected in the odd-numbered T intervals (T1, T3) of the candle charts, which denote rising BG levels after food intake, while the even-numbered T intervals (T2, T4) show BG falling as digestion proceeds. Similarly, beverage intake patterns align with B intervals, with B1 and B3 representing BG increases and B2 and B4 signifying declines. These visual trends were used to construct both Table 5.2 and the decision tree, making these fluctuations the basis for classification.

5.2.2.2 Decision Tree Overview and Key Factors

The decision tree, illustrated in Figure 5.8, provides a structured framework to classify and predict BG trends based on a set of physiological conditions. The tree sequentially considers important metrics such as the fasting state, the current BG status, and whether an event like food or beverage consumption has occurred. This stepwise structure mirrors how the body's physiological systems respond to varying conditions.

The fasting state emerges as the most critical factor in predicting BG fluctuations. The tree begins by distinguishing between fasting (F1, F2 intervals) and non-fasting periods. This reflects the biological significance of fasting, where the absence of recent nutrient intake leads to relatively stable or lower BG levels. In contrast, non-fasting periods exhibit larger fluctuations due to the body's active processing of glucose from food or drink. The prominent placement of the fasting state at the top of the decision

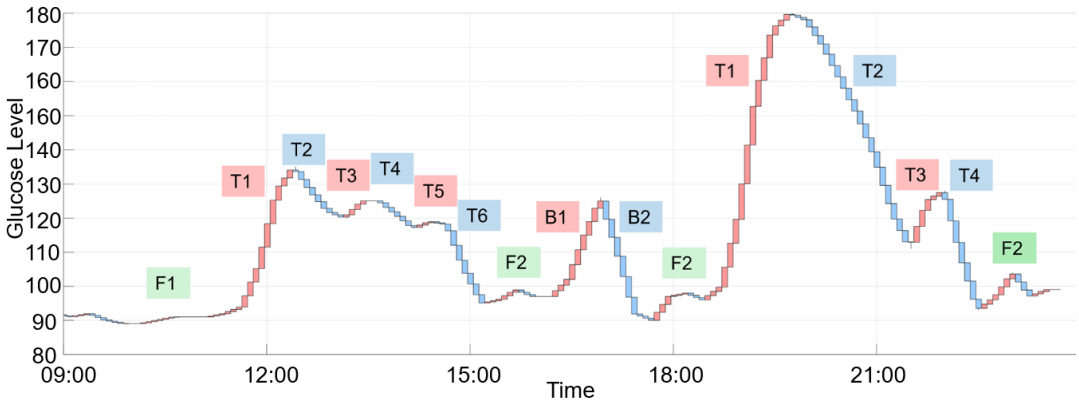

Figure 5.7: BG level trends with different time intervals. This figure illustrates the fluctuations in blood glucose levels over the course of a day, represented by step-like changes along the timeline. The x-axis shows the time of day, while the y-axis indicates the BG level. The labels represent different intervals or periods throughout the day, where 'F' denotes fasting periods, 'T' represents postprandial (after eating) intervals, and 'B' refers to beverage consumption intervals. The red color indicates periods of increasing BG, while the blue indicates decreasing BG levels. Green-colored labels mark fasting intervals.

tree emphasizes its importance as a primary determinant of BG behavior.

Another fascinating observation from the decision tree is that, just as the body strives to regulate heart rate toward a stable resting HR, it similarly aims to stabilize BG levels. This is evident from the decision tree's second key factor: current BG status. When the current BG level is lower than the stable baseline, the tree predicts an increase in BG, while higher-than-normal levels lead to decreases. This natural balancing mechanism aligns with the body's effort to maintain homeostasis, illustrating a fundamental principle of BG regulation.

Following these primary factors, the decision tree branches further into more specific conditions related to food and beverage intake. The third layer of classification considers events, particularly food and beverage consumption, and the corresponding post-consumption intervals. For example, the tree predicts that immediately after consuming a meal, there will be a strong or weak increase in BG, depending on the type of event and interval. This reflects the metabolic surge as the body processes nutrients, with intervals like T1 and B1 showing the strongest increases.

Interestingly, despite physical activity being commonly associated with BG regulation, the decision tree does not emphasize activity-related events (such as walking or exercise) as primary predictors. While exercise is known to aid in stabilizing BG levels,

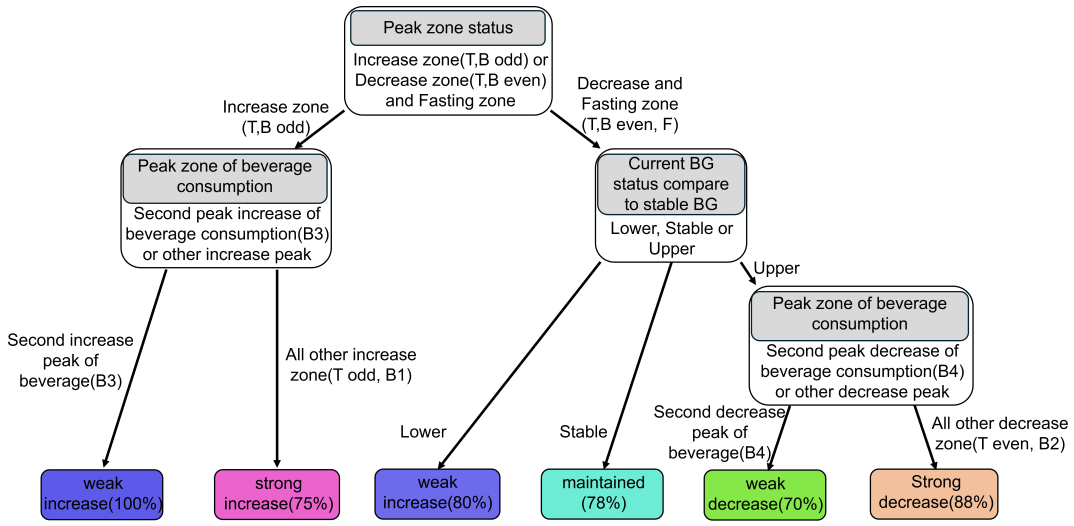

Figure 5.8: Decision tree illustrating the classification of BG trends based on various conditions, including current BG status, time intervals, and event type. The tree shows how these factors influence BG fluctuations, with each node leading to a specific outcome such as a weak or strong increase or decrease in BG. The percentages at each outcome represent the accuracy of the classification in the dataset.

its effect appears less significant in the overall picture compared to post-meal insulin responses and other physiological processes that dominate the body's glucose regulation mechanisms after eating. This suggests that the body's internal processes related to nutrient metabolism and hormonal responses (e.g., insulin release, and glucagon regulation) play a much more pivotal role in BG fluctuations than exercise itself. This aligns with the established understanding that the body prioritizes managing the postprandial glucose surge through insulin-mediated pathways rather than relying on physical activity as the primary modulator.

5.2.2.3 Decision Tree Results and Interpretation

The decision tree provides valuable insights into how BG levels respond under different physiological states, influenced by beverage consumption patterns, fasting status, and current BG levels. When the interval corresponds to an increase zone (T, B odd) and a second increase peak of beverage consumption (B3), the tree predicts a weak increase in BG with a certainty of 100%. This suggests that during these conditions, the body's glucose levels rise in a controlled manner, likely due to the timing of beverage absorption and its impact on glucose metabolism.

In other increase zones (T odd, B1), the tree predicts a strong increase in BG (75%),

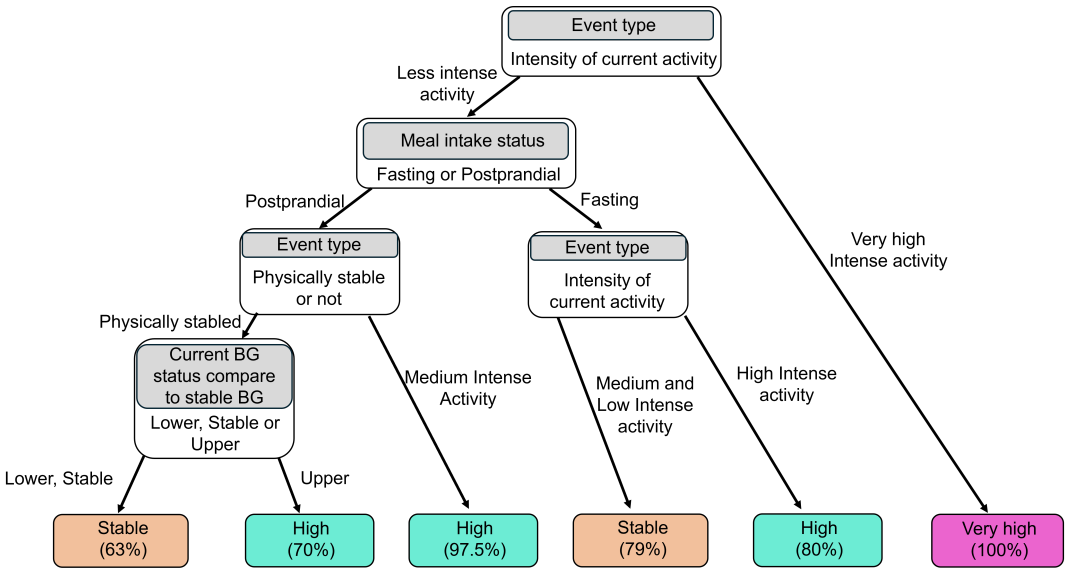

Figure 5.9: Decision tree for determining current HR levels based on factors such as BG status, time intervals, and event type. The tree highlights how meal intake status, activity intensity, and physical stability influence HR levels, with each outcome categorized as stable, high, or very high. Percentages represent the classification accuracy.

indicating that in most post-consumption scenarios, the body experiences a significant glucose rise as it absorbs nutrients from recent intake. This highlights how the timing of consumption influences the rate at which glucose enters the bloodstream, particularly in response to food and beverages.

When the fasting zone is in effect (T, B even, F) and the current BG status is compared to stable BG levels, various outcomes emerge based on the body's glucose status. If the BG status is lower, the tree predicts a weak increase (80%), suggesting that during fasting periods, the body attempts to stabilize glucose levels, likely through gluconeogenesis or other compensatory mechanisms to avoid hypoglycemia. If the BG status is stable, the prediction shows that glucose levels are maintained (78%), reflecting the body's effective glucose regulation during fasting. However, if the BG status is upper, the prediction depends on the type of consumption peak. For the second decrease peak of beverage consumption (B4), the tree forecasts a weak decrease (70%), indicating that even in the presence of prior glucose elevation, the body can lower BG levels moderately. In contrast, for all other decrease zones (T even, B2), the tree predicts a strong decrease (88%), reflecting the body's capacity to bring down glucose levels effectively after meals, likely driven by insulin response and metabolic regulation.

Table 5.2: Explanation of key metrics used in the decision tree analysis for classifying blood glucose (BG) trends.

Metrics	Explanations & Remarks
Current BG Status	Current blood glucose level compare to fasting stable blood glucose level. Classified into three types: Lower, stable, and upper.
Interval	F refers to the fasting state, with F1 representing fasting blood glucose in the morning and F2 representing the fasting state after digestion has occurred, typically in the afternoon or evening. T indicates the postprandial blood glucose fluctuation periods, where odd-numbered T intervals (T1, T3, etc.) represent rising blood glucose levels, and even-numbered T intervals (T2, T4, etc.) represent falling blood glucose levels. B denotes the blood glucose fluctuation periods following beverage intake, with odd-numbered B intervals (B1, B3, etc.) signifying rising glucose levels and even-numbered B intervals (B2, B4, etc.) indicating falling glucose levels.
Event	Represents various physiological and activity states. Events during the experiment are divided into those that cause a rise in heart rate (Walk, Aerobic exercise) and those that do not significantly affect heart rate (Rest, Eating, Beverage, Meeting).

In non-fasting conditions (T, B odd), if the BG status is upper and the event involves a second increase peak of beverage consumption (B3), the tree predicts a strong increase in BG (100%), highlighting that beverages, especially those rich in sugars or carbohydrates, cause a rapid and significant rise in glucose levels. This rapid rise can be attributed to the quick absorption of liquid calories compared to solid foods. Conversely, for other decrease zones (T even, B2), the tree predicts a strong decrease in BG (88%), underscoring the body's natural ability to lower BG after food consumption, aligning with postprandial insulin activity.

Additionally, it is commonly assumed that HR is determined solely by the current event. However, further decision tree analysis of the same dataset used in Figure 5.8,

incorporating HR data, Figure 5.9 reveals that HR levels can also vary depending on meal status and the stability of current blood glucose levels, in addition to the influence of the ongoing event.

Overall, the decision tree emphasizes how both fasting and post-consumption periods play crucial roles in glucose regulation. The results demonstrate that beverage consumption, particularly during non-fasting intervals, leads to more pronounced glucose increases, whereas fasting intervals, along with the body's insulin responses, are effective in moderating or reducing glucose levels.

5.2.2.4 Importance of the Decision Tree

The decision tree serves as the core analytical tool in this study, providing a clear, step-by-step model to interpret BG behavior under various conditions. The factors at the top of the tree, such as fasting state and current BG levels, are the most influential in determining BG outcomes. The tree's sequential nature reflects the body's physiological processes, where the largest impact on BG comes from metabolic factors rather than external stimuli like physical activity.

Each decision point in the tree is grounded in physiological principles, starting with the most crucial factor—whether the subject is in a fasting state. The subsequent differentiation by current BG status further reinforces the body's tendency to seek balance, as lower BG levels naturally trend upwards, and higher BG levels trend downward. By the time the tree evaluates food and beverage events, much of the BG trajectory has already been determined by these initial physiological conditions.

In conclusion, this decision tree not only summarizes data but also reflects the hierarchical importance of physiological processes in BG regulation. It demonstrates that while physical activity does play a role, the body's immediate priority after meals is glucose management via insulin and other metabolic processes. These findings highlight the importance of context when evaluating BG variability and reinforce the decision tree as an essential tool for understanding how various conditions shape BG responses.

5.2.3 The Effect of Meal Status on the resting heart rate

The relationship between meal status and resting HR is crucial for understanding how metabolic demands affect cardiovascular behavior. Resting HR, a marker of cardiovascular efficiency, is influenced by multiple factors, including food intake, as the body's

physiological systems respond to the absorption and digestion of nutrients. This section explores how meal status, reflected by BG fluctuations, correlates with resting HR and how these interactions manifest in both controlled and everyday settings.

5.2.3.1 Controlled Resting HR Experiments

In our initial controlled experiments, participants' HR was carefully stabilized at regular intervals throughout the day to isolate the relationship between resting HR and BG. Figure 5.10 presents the results of these controlled sessions, where HR was measured after 5-10 minutes of rest, approximately every 15 minutes. By examining both raw HR data and the midpoints(HR estimation points) between moving average and envelope lines, we sought to identify consistent resting HR points that could reliably correlate with BG levels.

The correlation between BG and these stabilized HR points is depicted in Figure 5.10. The analysis reveals moderate to strong correlations across all days, with correlation coefficients ranging from 0.7228 to 0.79668 for actual resting HR points and slightly lower but comparable values for midpoints (0.61895 to 0.72892). These findings suggest a direct relationship between resting HR and BG during controlled periods of rest, where meal status directly influences BG levels, and in turn, resting HR. This confirms that the body's effort to metabolize glucose after meals leads to measurable variations in resting HR, aligning with existing literature that indicates postprandial metabolic activity increases cardiovascular workload.

Interestingly, during fasting intervals (F1 and F2), the stabilization of both BG and HR was more apparent. The correlation during these intervals was notably stronger, implying that without the immediate metabolic demand from food intake, the body maintains more efficient HR regulation. The data reflect that after meals, the metabolic demand alters the homeostasis of resting HR as the body responds to glucose absorption and insulin action.

5.2.3.2 HR and BG Correlation in Everyday Activities

To further validate these findings in a more naturalistic setting, we applied the same methodology to everyday activity data without the controlled stabilization sessions, as illustrated in Figure 5.11. Unlike the controlled experiment, where the relationship between HR and BG could be precisely measured, these data capture typical daily fluctuations in HR and BG, marked by different types of events. Rest events, represented

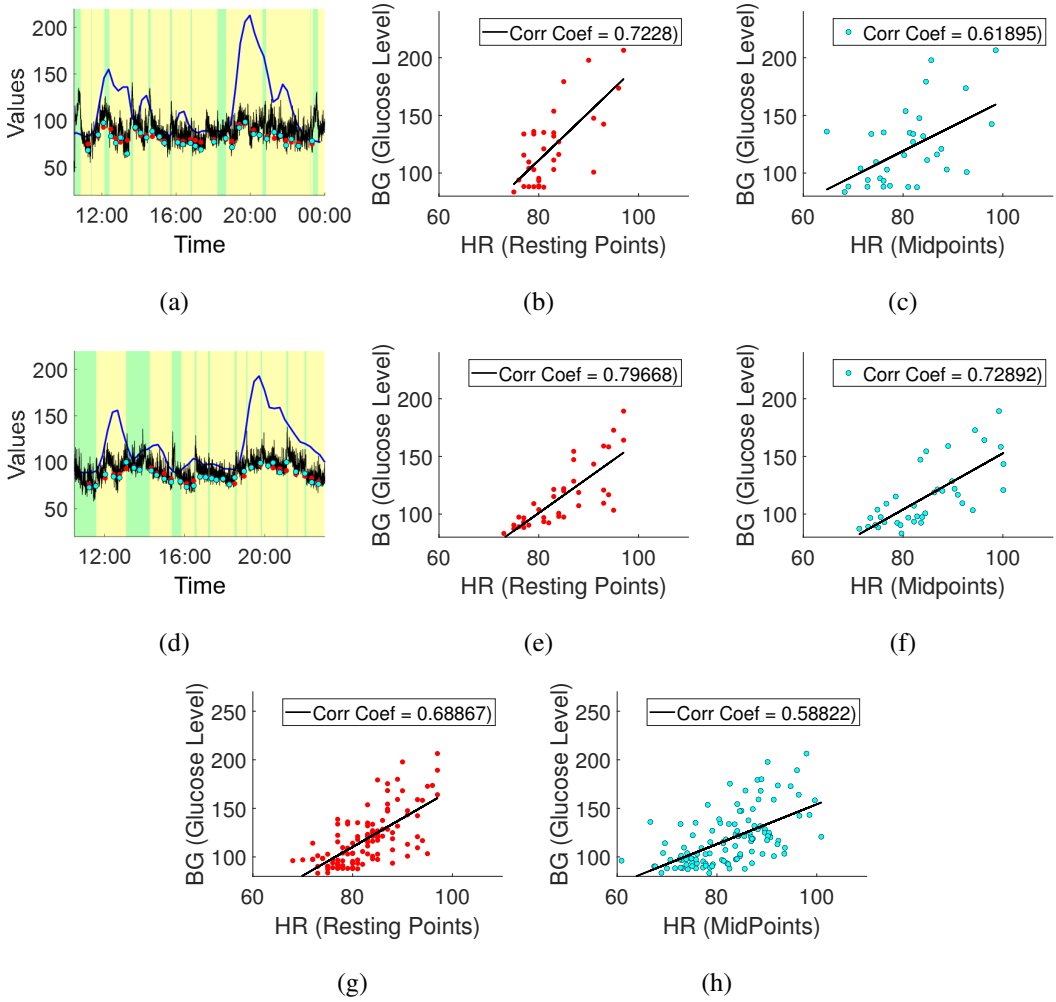

Figure 5.10: Resting HR and BG correlation analysis (data acquisition). (a) to (f) depict the raw HR and BG data collected throughout the day during an experiment focused on stabilizing HR at intervals to evaluate the relationship between resting HR and BG. The blue line represents the raw BG data, the black line represents the raw HR data, and the yellow line connects the midpoints between the moving average and the envelope of the HR data. The yellow background patches indicate rest events (non-HR increasing), while the green background patches represent non-rest events (HR-increasing). The red dots represent actual HR points measured after 5-10 minutes of stabilization at approximately 15-minute intervals. The cyan dots are the corresponding points from the yellow prediction line at the same times as the red dots. Subplots (b) and (e) show the correlation between red dots and their corresponding BG values. Subplots (c) and (f) show the correlation between cyan dots and their corresponding BG values. Subplots (g) and (h) show a correlation of all the red or cyan dots from the data.

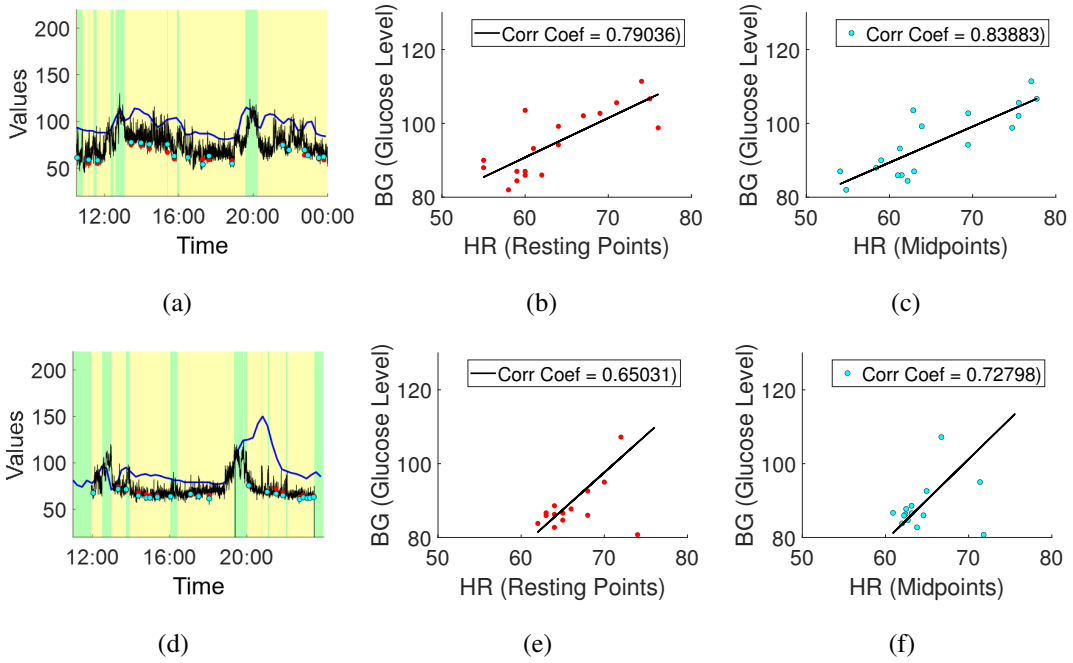

Figure 5.11: Resting HR and BG correlation analysis (data acquisition) of different subjects. (a) to (f) depict the raw HR and BG data collected throughout the day during an experiment focused on stabilizing HR at intervals to evaluate the relationship between resting HR and BG. Subplots (b) and (e) show the correlation between red dots and their corresponding BG values. Subplots (c) and (f) show the correlation between cyan dots and their corresponding BG values.

by the yellow background patches, indicate periods where participants were engaged in activities that did not significantly increase HR, while green patches mark periods of higher physical exertion.

The data presented in Figures 5.12(a)-(i) show that even in less controlled environments, a meaningful relationship between HR and BG persists, particularly during rest events. The yellow line, representing the midpoint between moving average and envelope, and the red dots (representing minimum HR points during rest events) align well with periods of stable BG levels. This suggests that even without strict stabilization, the body continues to regulate HR in a manner closely tied to metabolic activity, particularly during post-meal periods.

Correlation analysis from these natural settings, as shown in Figures 5.12(d)-(l), supports this connection, with coefficients ranging from 0.69554 to 0.72679. The stronger correlations observed during rest periods, especially following meals, reinforce the idea that the body prioritizes cardiovascular stability in response to food intake. The

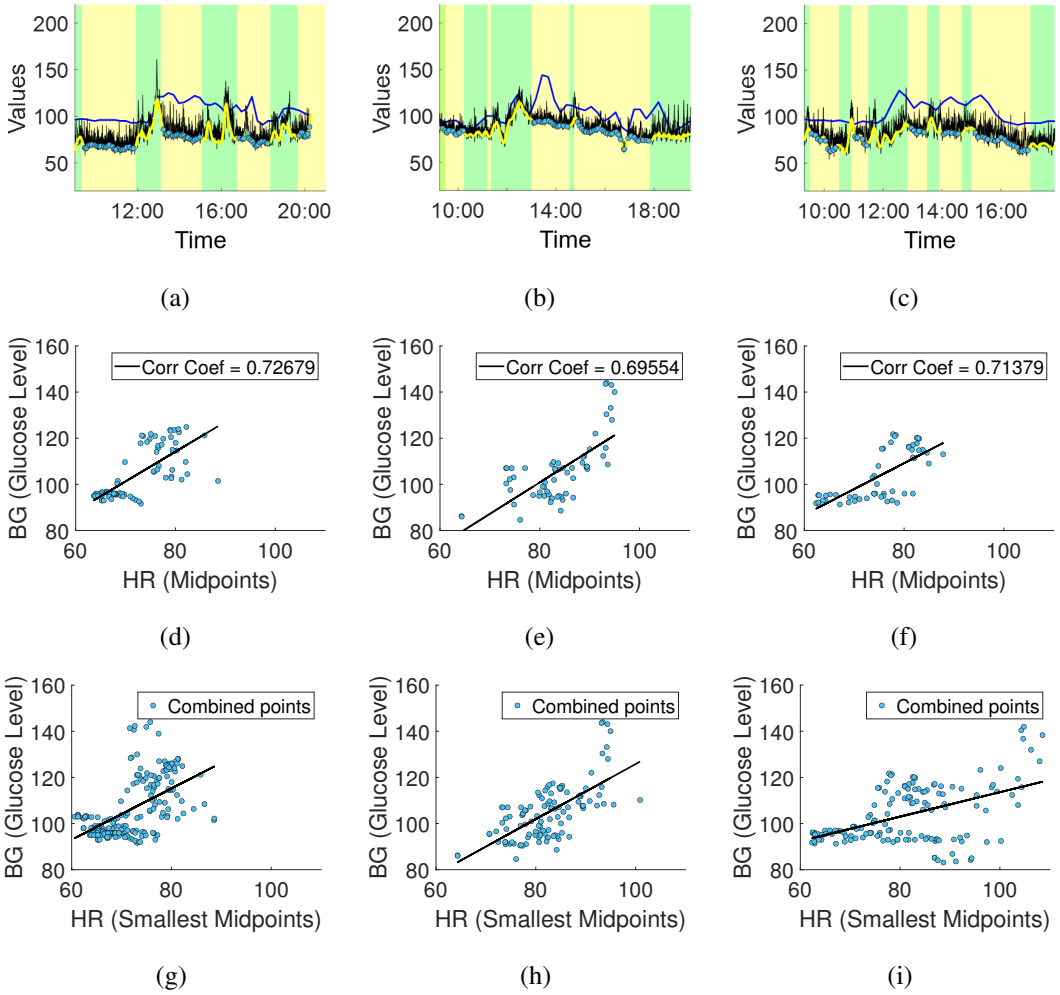

Figure 5.12: Correlation analysis of resting HR and BG during everyday activities.(a), (b), (c) Daily HR and BG measurements without controlled stabilization experiments. The blue line represents BG data, the black line shows raw HR data, and the yellow line represents the midpoint between the moving average and the envelope of the HR data. The yellow background patches indicate rest events (non-HR increasing), while the green background patches represent non-rest events (HR-increasing). (d), (e), (f) Correlation between the HR midpoints and corresponding BG values for the same time points as marked by the red dots. (g), (h), (i) Correlation of all predicted midpoints.

consistent correlations found between midpoints and BG levels, despite the absence of controlled resting periods, emphasize the robustness of the relationship between meal status and resting HR.

5.2.3.3 Interpretation and Broader Implications

The results from both controlled and everyday settings underline the significant impact of meal status on resting HR. Postprandial increases in BG, as the body absorbs and processes nutrients, create an observable rise in resting HR, which is most pronounced in the hours following food intake. This suggests that metabolic demands exert a measurable load on the cardiovascular system, even during periods of relative physical inactivity.

Conversely, during fasting or periods without significant food intake, resting HR remains more stable, and closely aligned with the body's baseline metabolic requirements. This more stable state is likely a reflection of reduced insulin activity and a lesser demand for glucose regulation, allowing the cardiovascular system to operate more efficiently.

Moreover, the correlation coefficients found in both controlled and uncontrolled settings provide key insights into the underlying physiological processes. The moderate-to-strong correlations indicate that the body's regulatory mechanisms between metabolic demand (as measured by BG) and cardiovascular output (as reflected by HR) are tightly coupled. The body's natural oscillation between energy absorption and metabolic balance is directly mirrored in HR fluctuations, highlighting how interconnected these systems are.

5.2.3.4 Blood Glucose Estimation based on Heart Rates

The relationship between HR and BG presents an intriguing opportunity for estimating BG trends using HR data. By employing the decision tree model illustrated in Figure 5.13, this study explored how HR data, contextualized by activity levels and physiological states, could estimate BG levels. This method provides a practical solution for long-term BG monitoring, especially in scenarios where continuous glucose monitoring is unavailable.

The decision tree classified BG levels based on HR states (stable or high) and activity involvement. For high HR levels without activity, the tree identified an 88% probability of elevated BG levels, reflecting a physiological stress response rather than activity-induced HR elevation. Conversely, during high HR with activity, the probability of elevated BG decreased to 66%, indicating the reduced likelihood of BG elevation due to the exertion-driven HR increase. In contrast, when HR levels were stable, BG levels were likely to remain stable at a 69% probability in non-active states but showed

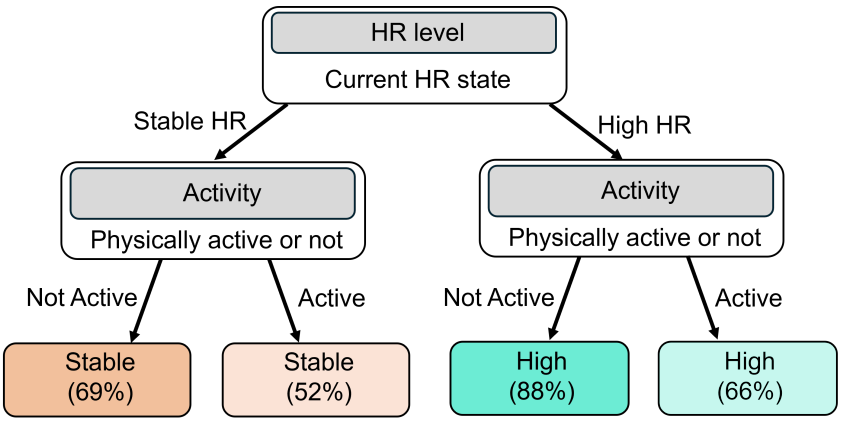

Figure 5.13: Decision tree illustrating the estimation of BG status based on HR levels. The tree integrates concepts from Figure 5.8 (BG dynamics), Figure 5.9 (HR level decision-making), and Figures 5.10, 5.11, and 5.12 (correlation analysis of resting HR and BG).

reduced stability (52%) during activity, suggesting even mild exertion could destabilize BG regulation.

The HR-based BG estimation results showed varying degrees of alignment with raw BG data. In Figure 5.14(b), the estimated BG curve for Participant 1 captured the long-term rising and falling trends but exhibited misalignment in specific peak timings and magnitudes. Such discrepancies highlight the complexity of BG regulation, where individual metabolic responses and external factors influence short-term BG dynamics. On the other hand, for Participant 2 (Figure 5.14(d)), the estimated curve closely matched the raw BG data in both magnitude and timing, demonstrating the model's ability to effectively capture BG fluctuations when physiological patterns are more predictable.

The findings underscore the potential of HR-based BG estimation in providing non-invasive insights into BG trends. However, certain limitations were evident. The method showed reduced precision in capturing peak alignment for Participant 1, suggesting that factors like dietary variations, stress, and individual metabolic differences play a role in BG dynamics and may need to be integrated into future models. Additionally, while spline interpolation ensured a smooth estimation curve, it may have introduced artifacts that obscured finer details in the raw data.

Despite these challenges, the overall trends—such as BG decreases during rest periods or increases during stress responses—were captured effectively. For example, the alignment of long-term trends in Figure 5.14(b) and the close fit in Figure 5.14(d)

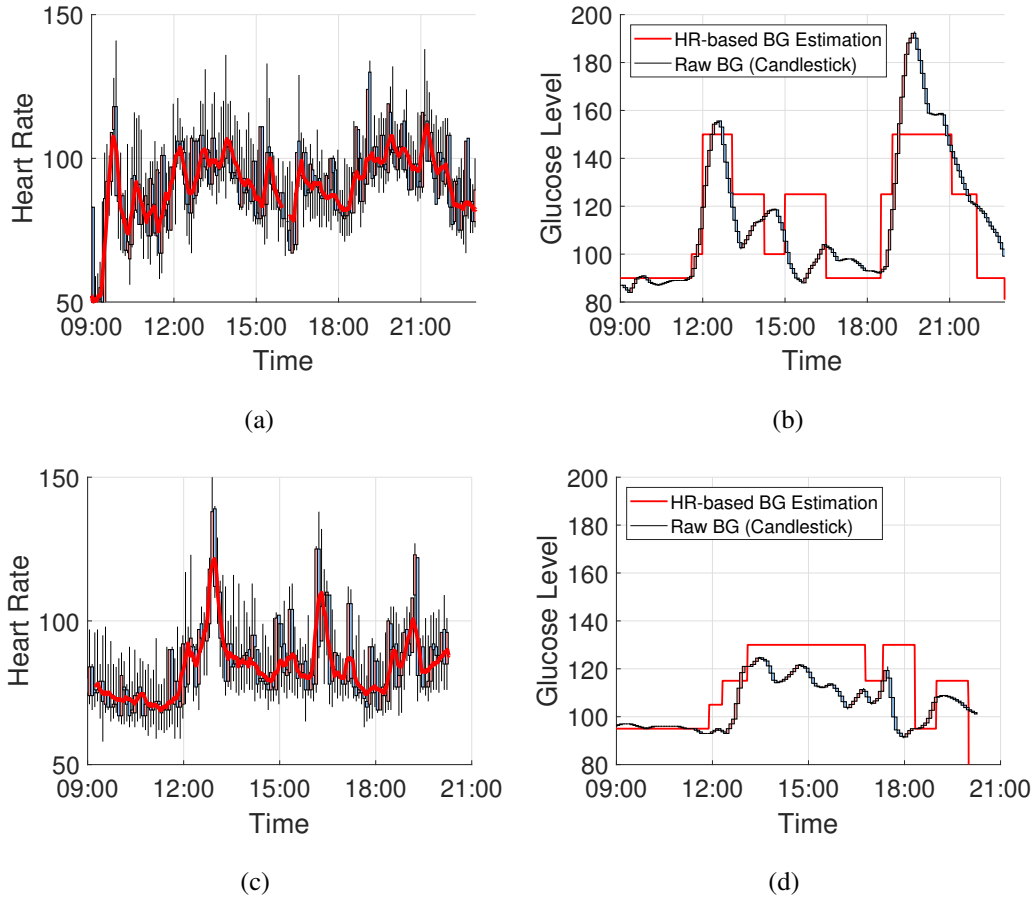

Figure 5.14: HR based BG estimation Graph. (a) and (c) Raw HR data with the red line representing the smoothed HR data. (b) and (d) Corresponding raw BG data (candlestick format) alongside the interpolated BG estimation (red line) derived using the decision tree in Figure 5.13. (a) and (b), (c), and (d) each corresponds to the same participant.

suggest that the method could reliably inform users about broader BG patterns.

This study's findings emphasize the broader role of HR variability and activity context in BG estimation. While HR alone cannot capture every nuance of BG dynamics, its integration with decision tree-based modeling provides a robust framework for estimating BG trends. The decision tree's emphasis on activity status and HR levels highlights the complex interplay between cardiovascular and metabolic responses. For example, the model's differentiation between high HR with and without activity reflects its ability to adapt to physiological and behavioral contexts, making it particularly relevant for personalized health monitoring.

In summary, HR-based BG estimation demonstrates promise as a tool for non-

invasive monitoring of BG levels, particularly for long-term trend analysis. While the model shows variability in its precision across individuals, it effectively captures the general patterns of BG dynamics. Future iterations of this approach could benefit from incorporating additional contextual factors such as dietary intake, stress levels, and environmental conditions to improve accuracy and expand its applicability across diverse populations.

5.2.3.5 Further Considerations for Exercise Experiments

These findings also have implications for future studies, particularly those involving physical activity or exercise testing. As we have shown, meal status and fasting play critical roles in determining resting HR stability. Therefore, in exercise experiments, it is essential to carefully control for fasting conditions. If the participant's meal status is not accounted for, the results could reflect postprandial HR fluctuations rather than those caused by the exercise itself. Fasting may help achieve a baseline HR more representative of true cardiovascular response, thus avoiding confounding variables introduced by metabolic demands related to food intake.

In conclusion, the effect of meal status on resting HR is evident across both controlled and everyday scenarios. Postprandial increases in metabolic demand lead to elevated resting HR, a reflection of the cardiovascular system's role in managing glucose metabolism. These findings underscore the importance of considering meal timing and nutritional intake when evaluating resting HR patterns, especially in metabolic or cardiovascular studies. Additionally, the robustness of the HR-BG relationship, even in everyday conditions, offers valuable insights into how the body maintains homeostasis in response to routine activities.

5.2.4 Influence of Exercise Timing on Postprandial Blood Glucose Dynamics

Managing postprandial BG levels is critical for maintaining metabolic health, particularly in individuals at risk for insulin resistance or type 2 diabetes. While the general recommendation to exercise for reducing BG is well-established, the precise timing of exercise relative to meal consumption and BG fluctuations can play a pivotal role in determining the effectiveness of the intervention. In this study, we explored how exercise performed at different phases of the first BG peak after a meal influences postprandial glucose dynamics, as summarized in Figure 5.17 and Tables 5.3 and 5.4.

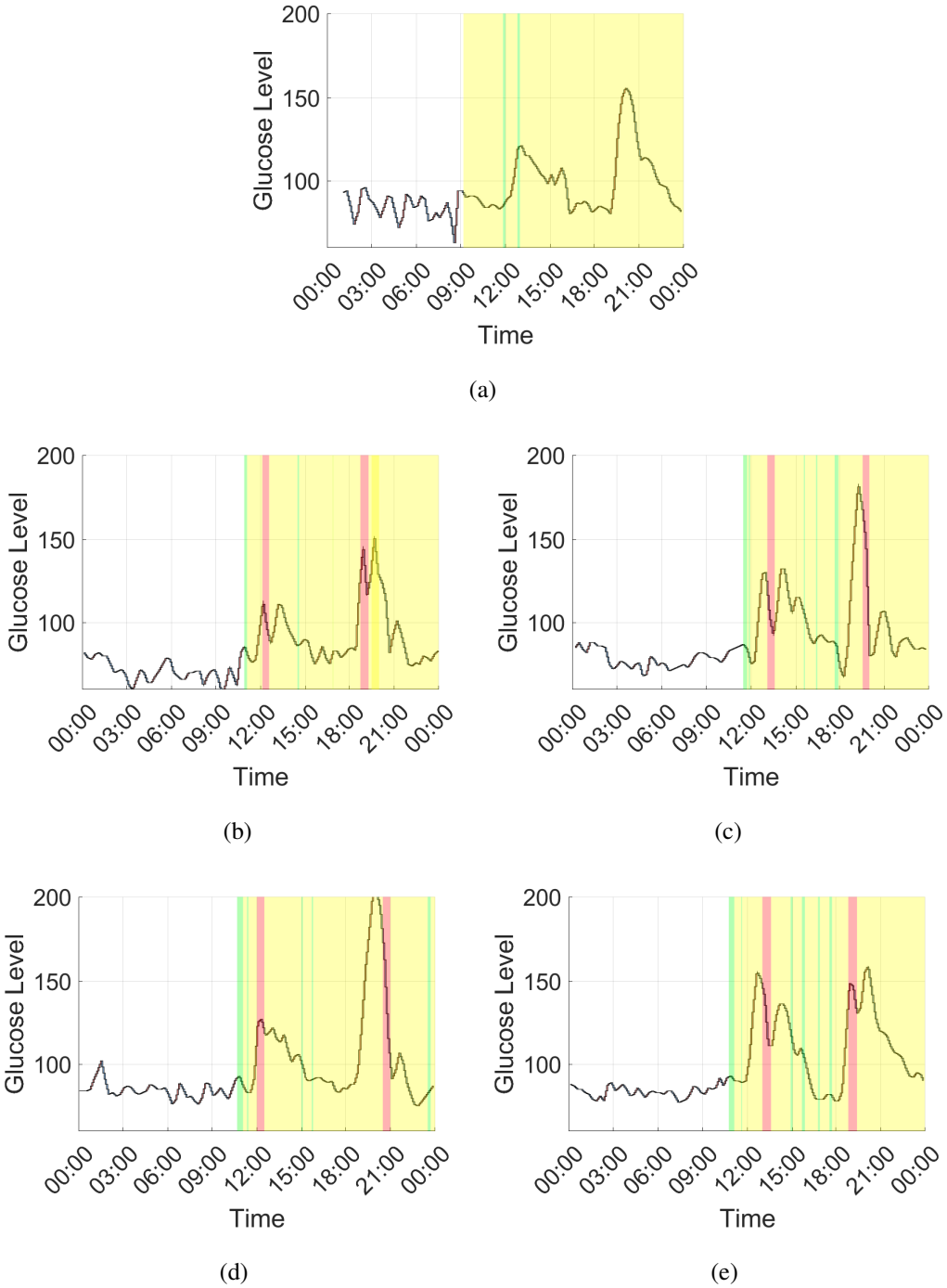

Figure 5.15: BG response to exercise at different points of the first postprandial peak. (a) No exercise was conducted. (b) Exercise during the rising phase after lunch and dinner. (c) Exercise during the falling phase after lunch and dinner. (d) Exercise during the rising phase after lunch and the falling phase after dinner. (e) Exercise during the falling phase after lunch and the rising phase after dinner. The green and yellow regions represent rest and postprandial periods, respectively, with the red lines indicating the exercise time. After lunch, walking and aerobic exercise after dinner were performed. The red area represents the time of the exercise.

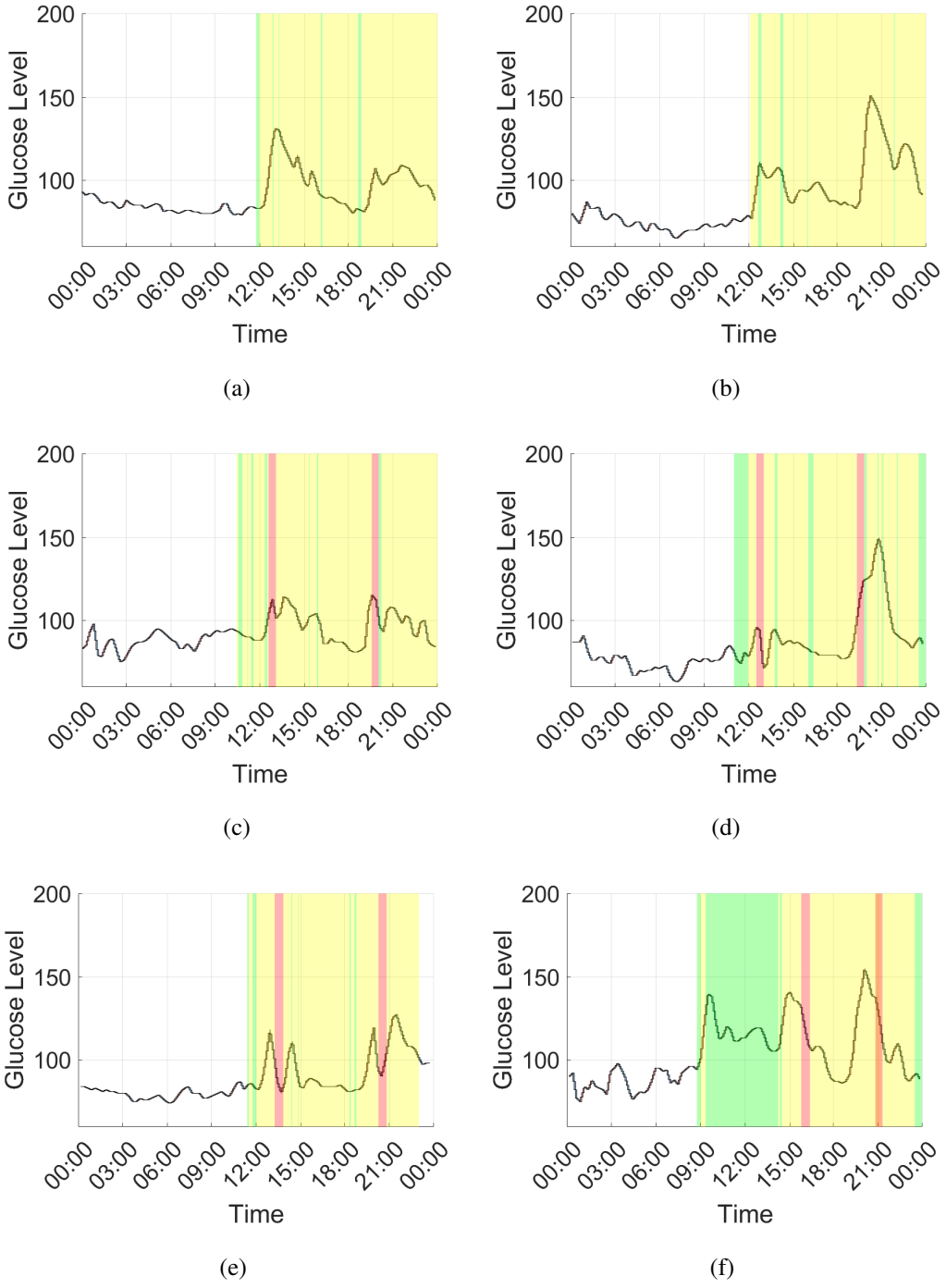

Figure 5.16: BG Response of different subjects to exercise at different exercise points of the first postprandial peak. (a),(b) No exercise conducted. (c),(d) Exercise during the rising phase after lunch and dinner. (e),(f) Exercise during the falling phase after lunch and dinner. Subplots in each vertical line are from the same subject. Walking exercises were performed after meals. The red area represents the time of the exercise.

Table 5.3: Integral Blood Glucose Values after Exercise.

	Integral Value (lunch) (mg/dL)		Integral Value (dinner) (mg/dL)	
Exercise point(1st peak)	Increase	Decrease	Increase	Decrease
No exercise	3313		5022	
Increase, Increase	2564		3095	
Decrease, Decrease		5077		6341
Increase, Decrease	3832			6412
Decrease, Increase		4819	7537	

Table 5.4: Maximum Blood Glucose Values after Exercise.

	Max Value (lunch) (mg/dL)		Max Value (dinner) (mg/dL)	
Exercise point(1st peak)	Increase	Decrease	Increase	Decrease
No exercise	121		156	
Increase, Increase	113		152	
Decrease, Decrease		132		183
Increase, Decrease	127			203
Decrease, Increase		156	159	

To ensure consistency, participants consumed identical meals on each day, and any non-exercise activities were minimized during periods where BG was elevated due to food intake. Despite efforts to control these variables, it is important to note that daily BG fluctuations may still vary due to natural physiological differences. Nevertheless, the patterns observed when comparing exercise timing offer valuable insights.

The first clear observation from Figure 5.15 is that exercise exerts a noticeable influence on BG levels, with exercise during both the rising and falling phases of the first postprandial peak leading to distinct effects. In the rising phase, exercise dampened the peak BG levels, with the magnitude of the first peak noticeably reduced compared to when no exercise was performed (Figure 5.15(a)). In fact, in some cases, BG began to decline during exercise, even though it would have typically continued rising if left uninterrupted. On the other hand, when exercise was performed during the decreasing phase of the BG curve, we observed an amplified decline in BG, with the rate of decrease being much more pronounced than during a non-exercise scenario. This

Table 5.5: Integral Blood Glucose Values of Different Subjects after Exercise.

	Integral Value (lunch) (mg/dL · min)		Integral Value (dinner) (mg/dL · min)	
Exercise point(1st peak)	Increase	Decrease	Increase	Decrease
No exercise	3255		3011	
Increase, Increase	2208		2875	
Decrease, Decrease		1538		4081
No exercise	3707		5612	
Increase, Increase	670		4659	
Decrease, Decrease		1711		4863

Table 5.6: Maximum Blood Glucose of different subjects Values after Exercise.

	Max Value (lunch) (mg/dL · min)		Max Value (dinner) (mg/dL · min)	
Exercise point(1st peak)	Increase	Decrease	Increase	Decrease
No exercise	130		108	
Increase, Increase	113		115	
Decrease, Decrease		115		127
No exercise	111		151	
Increase, Increase	96		150	
Decrease, Decrease		142		155

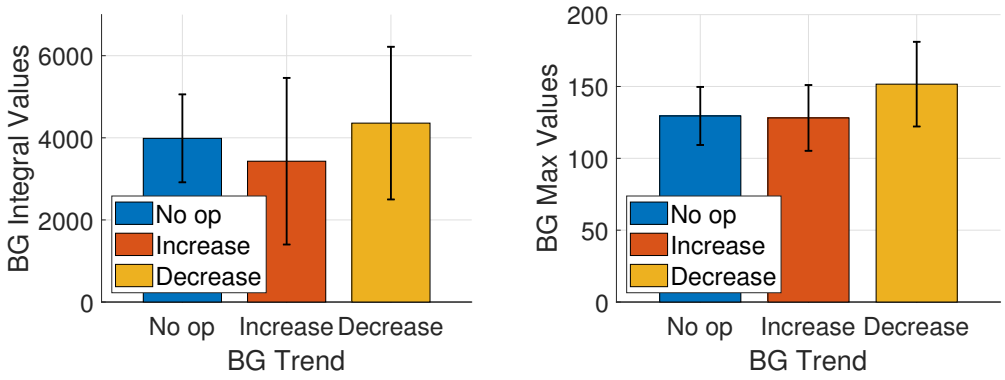

(a) (b)

Figure 5.17: Bar graphs showing the blood glucose (BG) metrics under different BG trend conditions: No exercise, Increase, and Decrease. (a) Displays the integral BG values during exercise periods after BG stabilization. (b) Represents the maximum BG peaks observed after meals. Error bars indicate standard deviations.

confirms the widely accepted understanding that exercise contributes to BG reduction, but it also reveals that the timing of exercise can have different outcomes on post-meal glucose management.

One important aspect of evaluating exercise effectiveness lies in how we measure these changes. For exercise during the rising phase, the integral values, which represent the total BG exposure over time, serve as a reliable metric. As seen in Table 5.3, exercising during the rising phase consistently results in lower integral values, suggesting that this timing minimizes overall BG load. This provides a clear, quantitative method for assessing the impact of exercise on BG during this phase.

However, for exercise performed during the decreasing phase, integral values alone may not fully capture the extent of the BG reduction. In these cases, it is more useful to evaluate the shape of the BG curve itself. For instance, if we observe Figure 5.15(c) and (d), where exercise was conducted during the falling phase after dinner, the BG patterns reveal more subtle yet important changes. Both show a rapid return to baseline after the first major peak, with subsequent smaller peaks being significantly blunted or even absent. In contrast, without exercise, the BG curve typically shows a slower decline and may exhibit additional minor peaks as the body continues to process the meal. The quicker return to baseline in the exercise scenarios, accompanied by the absence of secondary peaks, indicates that the exercise not only accelerated BG reduction but also stabilized levels more effectively.

This distinction between rising and falling phases highlights that while integral values are an effective metric for quantifying total BG load during rising phases, the shape of the BG curve offers a more nuanced evaluation of the exercise's effectiveness during decreasing phases. In these cases, the reduction in the magnitude of subsequent peaks and the speed of return to baseline can be key indicators of success.

Delving deeper into the data, we can quantify these effects using the integral values (total BG load) shown in Table 5.5. Interestingly, the integral values are consistently lower when exercise is performed during the rising phase compared to other phases, indicating that engaging in exercise during the initial postprandial increase may be the most effective in minimizing overall BG exposure. The act of exercising during this phase seems to preemptively blunt the BG spike, reducing the total glycemic load over time. In contrast, exercising during the decreasing phase still contributes to BG reduction but does not appear to reduce the overall glycemic load as significantly. This suggests that targeting the rising BG phase may be a more strategic intervention point for individuals aiming to minimize postprandial BG spikes.

Moreover, Table 5.6, which focuses on maximum BG values, further supports this finding. The highest BG spikes were consistently lower when exercise was performed during the rising phase, particularly when comparing more intense activities like running to walking. Running appears to have a stronger effect on attenuating the peak BG levels, offering an even greater reduction in the magnitude of BG spikes compared to walking. However, while running may be more effective at lowering the peak, it is important to note that the overall reduction in BG (as reflected by the integral values in Table 5.5) does not vary as drastically between running and walking. This suggests that while running may offer an added benefit in terms of reducing peak BG, walking remains an effective and more accessible form of exercise for lowering total postprandial BG levels, especially in the context of the rising phase.

From a practical perspective, this analysis highlights that exercising during the rising phase of postprandial BG offers the most benefits, particularly in reducing overall BG load and preventing sharp spikes. However, it is also clear that the intensity of the exercise—whether running or walking—plays a role in modulating these effects. Running during the rising phase may be ideal for those who are physically able and aiming to aggressively manage BG spikes. However, for individuals who may be constrained by physical limitations or concerns about digestion during more intense exercise, walking during the same phase appears to be a highly effective alternative.

5.2.5 Estimating trends of Heart rate and Blood glucose by history of events

Understanding how past events influence present physiological metrics like HR and BG is crucial for developing accurate models of human metabolism and cardiovascular function. In this section, we propose a methodology for evaluating the lingering effects of past events on current HR and BG levels using a time-history-based visualization approach.

Figure 5.18 (for HR) and Figure 5.19 (for BG) display daily event histories and their cumulative effects over time. Both figures share a common structure, with the x-axis representing time and the bottom box at each time point denoting the current event. The y-axis tracks how long the effects of past events continue to influence the present, and the color intensity indicates the strength of the impact (red for increases, blue for decreases). This methodology provides a clear, visual way to assess how different types of events affect HR and BG, both immediately and over time.

5.2.5.1 Key Observations: Heart Rate Trends

As shown in Figure 5.18, HR changes exhibit more localized and transient effects. The impact of an event, such as exercise (cardio or walking), tends to dissipate relatively quickly once the event concludes. Resting events (R) typically result in a rapid stabilization of HR, demonstrating how the cardiovascular system seeks equilibrium shortly after a stimulus ceases. This suggests that HR, driven by the autonomic nervous system, responds promptly to physical activity and returns to baseline within a shorter time frame.

Furthermore, the influence of past events on current HR levels diminishes significantly within a short period. Even strenuous events such as long-term walking (L.W) or cardio (C) show a steep decline in their impact as time progresses. This indicates that while HR responds strongly to physical activity, its residual effects do not persist for long after the activity ends. The body seems to focus on real-time cardiovascular demands rather than maintaining a prolonged response to earlier events.

5.2.5.2 Key Observations: Blood Glucose Trends

In contrast, Figure 5.19 reveals that BG levels are influenced by events over a much longer time scale. The most striking feature is the prolonged impact of ingestion events (I). When food is consumed, BG levels spike sharply, as expected, but unlike HR, this

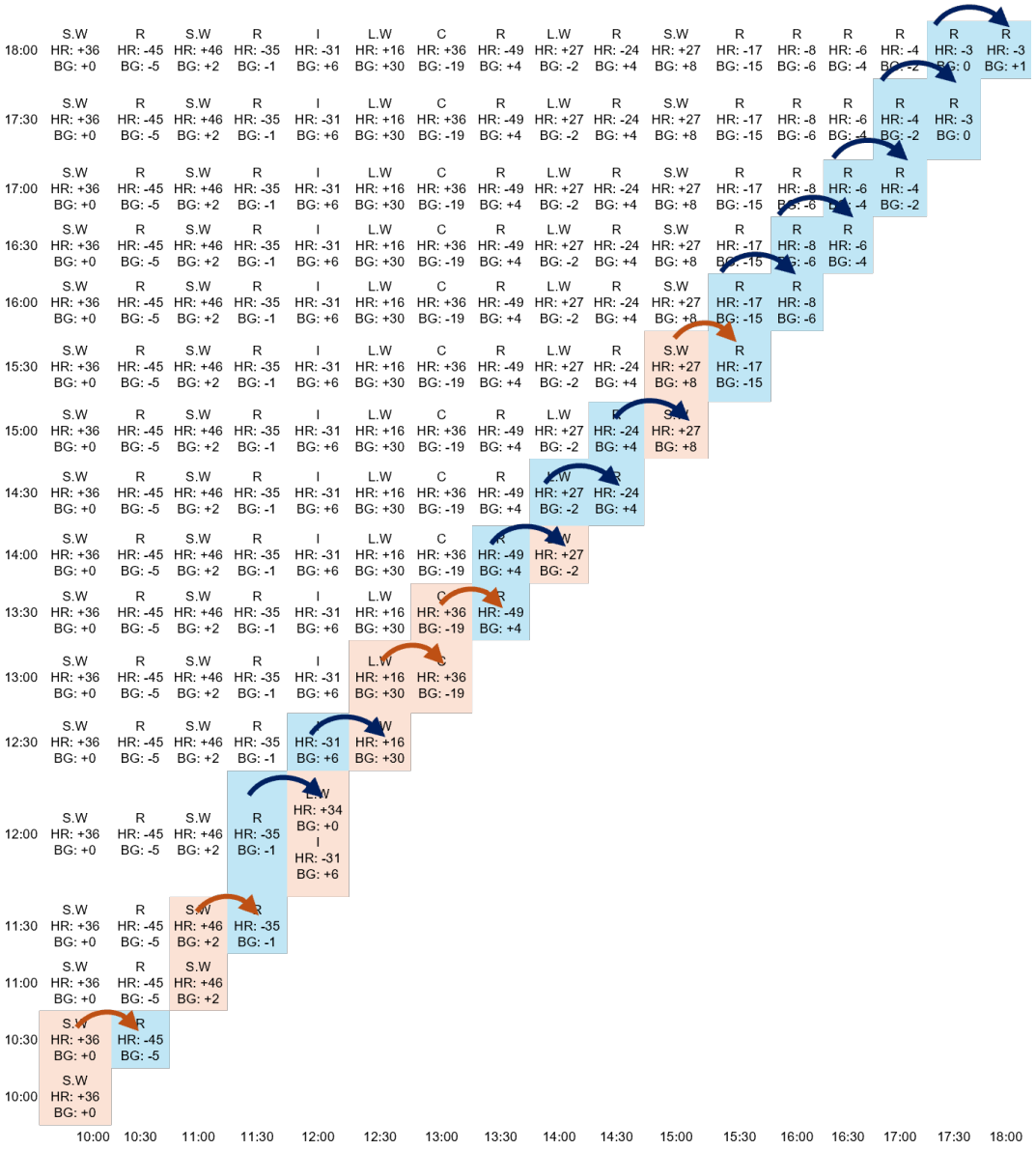

Figure 5.18: Illustration of daily events and their cumulative effect on HR over time. The x-axis represents the timeline, with the bottom box at each point indicating the current event. The y-axis represents how long the influence of past events lingers. Events are labeled as follows: S.W (short-term walk), R (rest), I (ingestion), L.W (long-term walk), and C (cardio). The color intensity corresponds to the strength of the event's impact, with darker colors indicating stronger effects. Red tones indicate an increase in HR, while blue tones indicate a decrease. Arrows trace how previous events continue to influence HR over time, showing the cumulative effect of both past and current events on HR fluctuations at each point in the day.

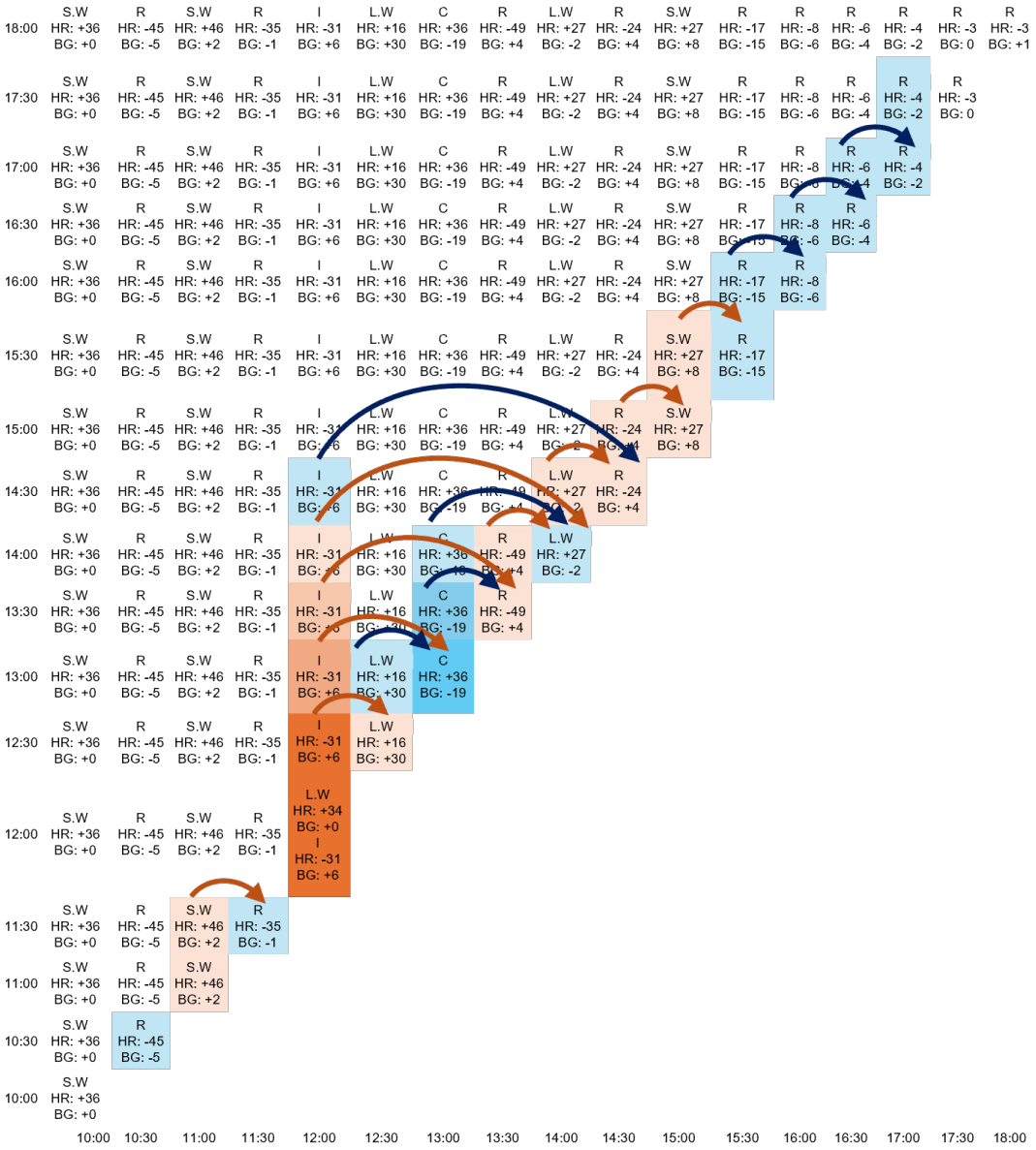

Figure 5.19: Illustration of daily events and their cumulative influence on BGmover time. The structure mirrors the HR diagram: the x-axis is the timeline with the bottom box representing the current event, while the y-axis reflects the lingering influence of previous events. Events are labeled similarly: S.W (short-term walk), R (rest), I (ingestion), L.W (long-term walk), and C (cardio). The color scheme follows the same pattern, with red representing an increase in BG and blue indicating a decrease. Arrows illustrate how past events continue to impact current BG levels, demonstrating the combined influence of both past and present events on BG changes throughout the day.

effect does not dissipate quickly. Instead, the effect of food ingestion lingers, gradually tapering off over a longer period. Even hours after the ingestion, BG levels remain elevated or continue to adjust, often blending into the effects of subsequent events.

This prolonged influence of ingestion on BG is particularly important. It reflects the slower and more complex metabolic processes involved in glucose absorption, insulin response, and overall metabolic regulation. Unlike HR, which can stabilize quickly after an event, BG levels often require extended periods to normalize, especially after meals. The data also suggest that BG regulation depends on the cumulative impact of past and present events. For instance, an exercise event that follows a meal (C or L.W after I) does not immediately return BG to baseline; instead, it results in a gradual blending of the two effects, with exercise moderating the elevated BG levels over time.

5.2.5.3 Implications for HR and BG Modelling

The contrasting behaviors of HR and BG, as observed in these history-based visualizations, have important implications for how these physiological parameters should be modeled. The transient nature of HR's response to events suggests that HR data is best analyzed in short, localized time windows, where immediate reactions to stimuli can be captured. In contrast, BG trends require a more integrative approach that accounts for the prolonged influence of past events, particularly after food intake.

This methodology offers a clear framework for evaluating HR and BG dynamics in various contexts. For HR, real-time monitoring can provide meaningful insights, as the body's response to exercise, rest, or other activities is almost immediate and short-lived. However, for BG, the analysis must take a broader time horizon into account, factoring in both current and historical events. This is particularly relevant for ingestion-related activities, which have long-lasting effects on BG levels that persist well after the initial spike, affecting future events and their metabolic outcomes.

5.2.5.4 Further Methodological Considerations

One of the major strengths of this approach is that it visually and analytically distinguishes the temporal effects of events on HR and BG. The methodology highlights how HR's real-time response is largely driven by present conditions, while BG exhibits a slower, more drawn-out response. This suggests that HR-based models should focus on short-term responses, while BG models must incorporate historical data and anticipate delayed responses, especially in post-meal periods.

The visualization technique also simplifies the process of identifying cumulative effects. In practice, this allows researchers to better estimate the real-time physiological state by understanding how long prior events, such as exercise or meals, continue to affect a subject. For example, if a research study is evaluating the impact of physical activity on metabolic health, it is important to account for the fact that HR quickly stabilizes, while BG requires longer to adjust, particularly after food consumption.

5.2.5.5 Broader Implications

These findings carry important implications for both experimental design and real-world applications. In exercise studies, it may be critical to monitor fasting states or control for meal timing, as past meals may continue to influence BG levels long after HR has stabilized. If this is not considered, the lingering metabolic effects of a meal could confound the interpretation of exercise-induced changes in BG. By considering the differential responses of HR and BG to past events, researchers can create more accurate models that account for both immediate and delayed physiological reactions.

Additionally, this methodology can be extended to various health monitoring applications, where the history of activities needs to be taken into account. For instance, in continuous glucose monitoring (CGM) or exercise tracking, users could benefit from tools that factor in not just current activity but also the residual impact of earlier events. This approach could help personalize health interventions, providing more accurate insights into an individual's real-time metabolic and cardiovascular states.

5.3 Discussion

This chapter explores the intricate relationships between HR and BG, delving into event-driven interactions, meal status, and historical effects to provide a comprehensive understanding of their dynamic interplay. The findings not only underscore the integrated nature of cardiovascular and metabolic systems but also highlight key distinctions in their responses to various physiological conditions and events.

When examining the relationship between HR and BG during event-driven interactions, a clear dichotomy emerges. HR reacts rapidly to physical activities such as walking or exercise, reflecting the cardiovascular system's role in meeting immediate metabolic demands. In contrast, BG levels, particularly following food intake, exhibit a more gradual and sustained response due to the slower processes of digestion, insulin

release, and glucose uptake. This highlights the body's dual mechanisms for energy management: one fast-acting and the other prolonged.

The analysis of BG trends under varying conditions revealed the enduring impact of food ingestion on BG fluctuations. Postprandial BG spikes not only persisted long after the initial increase but also blended into subsequent events, emphasizing the importance of considering both immediate and historical events in BG analysis. The prolonged fluctuations in BG highlight the metabolic complexity of glucose regulation, offering critical insights for studies focused on diabetes management and metabolic health.

Meal status was also shown to significantly influence resting HR. Postprandial periods were characterized by elevated HR levels, reflecting the cardiovascular workload associated with metabolic demands of digestion and nutrient absorption. In contrast, fasting periods exhibited more stable HR patterns. These findings emphasize the need to account for meal status when studying resting HR, especially in exercise physiology research where postprandial HR variability could mask the effects of physical activity.

The addition of history-based event analysis provided a deeper understanding of the lingering effects of past events on both HR and BG. HR trends were primarily driven by real-time stimuli with minimal influence from past events, whereas BG displayed a longer temporal lag. Ingestion events, in particular, continued to shape BG levels long after their occurrence, demonstrating the need to incorporate both immediate and historical data when modeling BG trends. Conversely, HR analysis can largely focus on real-time responses.

Building on these findings, the section on Blood Glucose Estimation Based on Heart Rate introduced an innovative method for estimating BG levels using HR data. By leveraging the decision tree from Figure 4.13, BG levels were inferred based on HR states and activity levels, offering a contextual understanding of how HR variations reflect metabolic conditions. For example, high HR levels in the absence of physical activity were associated with elevated BG, likely due to metabolic factors driving the HR increase. Conversely, when high HR levels occurred during physical activity, BG estimation reflected the reduced likelihood of elevated BG, as the HR changes were more likely attributed to exertion. Similarly, stable HR states showed differing BG patterns depending on the presence or absence of activity, illustrating the nuanced relationship between HR, activity, and BG.

The results of this HR-based BG estimation were visualized in Figure 4.14, where interpolated BG estimation curves captured the overall trends in raw BG data, partic-

ularly in long-term patterns. Although some discrepancies were noted, such as in (b), where timing and magnitude occasionally diverged, the general alignment between the estimated and raw BG data demonstrates the potential of this approach for capturing broader BG fluctuations in daily life. This method highlights the feasibility of using HR as a non-invasive proxy for BG estimation, especially for long-term monitoring and trend analysis.

Overall, this chapter reveals a fundamental distinction: HR is highly sensitive to immediate stimuli, stabilizing quickly after events, while BG regulation is a slower, more sustained process shaped significantly by historical and postprandial factors. Integrating these findings, the use of HR as a proxy for BG estimation offers promising applications in health monitoring, particularly for scenarios where continuous BG measurement is not feasible. By bridging the gap between cardiovascular and metabolic research, these insights pave the way for more holistic approaches to studying energy management and physiological responses.

5.4 Conclusion

This chapter explored the multifaceted relationship between HR and BG across varying conditions, focusing on event-driven interactions, meal status, and historical event influences. A key insight was the importance of maintaining a stable baseline during exercise experiments, particularly those involving HR analysis. Through Chapters 3 and 4, it became evident that meal status significantly affects resting HR, underscoring the need for controlled conditions when designing HR-related studies. This realization prompted a deeper investigation into BG variability, as understanding when and how BG levels fluctuate provides critical context for ensuring consistent experimental conditions.

The findings also introduced the novel concept of estimating BG using HR data. By leveraging the relationship between HR states and activity levels, this chapter demonstrated the potential for HR-based BG estimation, offering a non-invasive approach to understanding metabolic dynamics. This innovation holds promise for developing systems capable of approximating BG levels without the need for direct invasive measurements, broadening accessibility to metabolic monitoring in everyday life.

Additionally, the contrasting temporal dynamics of HR and BG were highlighted. HR responds rapidly to immediate stimuli and stabilizes quickly, whereas BG trends are slower, with lasting effects influenced by past events, particularly food intake. This

distinction emphasizes the importance of integrating both real-time and historical data when analyzing BG trends or conducting physiological studies.

By combining these insights, this chapter lays the groundwork for a more holistic approach to physiological monitoring. Beyond improving the accuracy of HR-related exercise studies, the integration of BG variability and HR-based BG estimation opens possibilities for personalized exercise program design. This approach can provide individuals with tailored insights into their metabolic and cardiovascular responses, enhancing both health outcomes and the effectiveness of fitness regimens.

5.5 Summary of Chapter 5

Chapter 5 examined the interplay between HR and BG from multiple perspectives, including event-driven changes, the impact of meal status, and historical event effects. A significant finding was that meal status plays a critical role in influencing resting HR, with postprandial periods marked by elevated HR levels due to metabolic demands. In contrast, fasting periods showed more stable HR patterns, highlighting the need to control meal timing in studies involving resting HR or exercise physiology.

The analysis also revealed that while HR primarily reflects real-time events, BG regulation is slower and influenced by both immediate and past events. Postprandial BG levels exhibit prolonged fluctuations, blending into subsequent events and demonstrating the importance of historical data in understanding BG trends. Ingestion events, in particular, were shown to have lasting effects on BG levels long after their occurrence, contrasting with HR's more immediate and transient responses.

This chapter introduced the innovative concept of HR-based BG estimation, leveraging decision tree analysis to infer BG levels from HR data. This approach represents a step toward non-invasive BG monitoring systems, offering a practical solution for approximating BG levels in real-world settings without direct invasive measurements. The interpolated BG estimation curves demonstrated strong potential for capturing long-term trends, though minor discrepancies highlighted the need for further refinement.

Integrating these findings, the chapter underscores the broader implications of HR and BG dynamics for personalized health monitoring. By providing insights into when and how BG levels fluctuate, as well as demonstrating the feasibility of HR-based BG estimation, this chapter offers a foundation for tailoring exercise programs to individual metabolic and cardiovascular responses. Together, these contributions pave the way for

a more precise and holistic approach to physiological research and health management.

Chapter 6

Conclusions

This study has provided valuable insights into the interaction between HR and BG levels during various activities, and the distinct contributions of upper and lower body exercises in driving HR variations during combined movements. By employing a novel vector-based HR analysis and detailed examination of HR-BG trends, this research offers important findings relevant to HIIT, aerobic exercises, and metabolic health management.

6.1 Visualizing Exercise Intensity and the 40-Second Rule

Chapter 3 introduced a novel vector-based approach for analyzing HR data, allowing for a multidimensional representation of exercise intensity that surpasses traditional metrics such as maximum HR. This method revealed that different combinations of upper and lower body exercises generate distinct HR trajectories, captured effectively through vectorization. The identification of the 40-second rule, which shows that HR trends stabilize around 40 seconds of exercise, stands out as a critical discovery. This finding was consistent across multiple participants and exercise types, making it an optimal interval for assessing exercise intensity.

The practical implications of the 40-second rule extend to exercise protocol design, particularly for HIIT and aerobic programs, where short, intense intervals are common. The vector-based method, in turn, provides a robust framework for differentiating between exercise intensities, helping trainers and athletes fine-tune workouts to meet cardiovascular and metabolic goals more efficiently.

6.2 Exercise Intensity and the Role of Upper and Lower Body Movements

Chapter 4 explored the integration of upper and lower body exercises to evaluate their combined impact on HR responses, particularly in the context of HIIT and aerobic exercise routines. The analysis revealed that while the HR levels of upper and lower body exercises are not purely additive (e.g., $1+1 \neq 2$), they are proportionally related to the intensity of each component, allowing for predictable patterns in HR outcomes.

Lower body exercises consistently emerged as dominant drivers of HR responses due to their engagement of larger muscle groups and higher cardiovascular demands. However, upper body movements also contributed to HR variation, particularly when paired with lower-intensity lower body exercises. This highlights the interplay between upper and lower body contributions, where each component can influence overall exercise intensity depending on the combination and context.

These findings underline the potential for constructing exercise routines that target specific HR levels by strategically combining upper and lower body movements. By understanding the proportional contributions of each movement, trainers and practitioners can design tailored programs to achieve desired intensities, accommodate individual needs, and optimize exercise efficacy. This approach opens avenues for creating adaptive, personalized workout protocols for various populations, including those requiring rehabilitative or low-impact exercise plans.

6.3 Interactions Between Heart Rate and Blood Glucose

Chapter 5 examined the intricate relationship between HR and BG under various physiological conditions, particularly focusing on fasting and postprandial states. The findings revealed that in the fasting state, HR and BG were relatively stable, reflecting balanced metabolic demand. In contrast, the postprandial state was marked by significant fluctuations in both HR and BG, driven by the dual demands of digestion and physical activity. These observations underscore the critical influence of meal timing and nutritional context on physiological responses, as the body operates under distinctly different mechanisms depending on fasting or post-meal conditions.

One of the key insights from this chapter was the realization of the critical role meal status plays in maintaining stable baseline conditions, especially for exercise experiments involving HR. During the studies in Chapters 3 and 4, it became evident that

meal status significantly impacts resting HR, which is essential for consistent experimental outcomes. This recognition led to a deeper exploration of BG variability, aiming to identify patterns of BG fluctuations to better control and standardize experimental conditions for HR-focused exercise studies.

Furthermore, the chapter introduced the novel concept of estimating BG using HR data. By leveraging decision tree models and correlating HR dynamics with BG fluctuations, the study presented a potential framework for non-invasive BG estimation. This approach proposes a pathway to approximate BG levels without the need for direct invasive measurements, opening possibilities for practical and accessible metabolic monitoring systems.

Integrating these findings, this chapter highlights the potential to not only enhance the accuracy of HR-related experiments but also to provide actionable insights for personalized exercise program design. By understanding the timing of BG fluctuations and developing HR-based BG estimation methods, this chapter offers a foundation for creating individualized health and fitness strategies that align with both metabolic and cardiovascular needs.

6.4 Future works

While this study has provided valuable insights into the interaction between heart rate and blood glucose during exercise and daily activities, several areas remain open for further exploration. Future research could focus on expanding the findings to different populations, such as individuals with metabolic conditions or cardiovascular disorders, to determine whether the observed trends hold universally or require adjustments. Additionally, incorporating more advanced monitoring technologies that track other physiological metrics like respiratory rate or muscle oxygenation could further enhance our understanding of the body's response to physical activity. Long-term studies would also be beneficial to observe how heart rate and blood glucose trends evolve over extended periods, shedding light on adaptive responses to consistent training or lifestyle changes. Investigating the effects of various exercise modalities, beyond just high-intensity interval training and aerobic exercises, would also broaden the applicability of these findings. Furthermore, exploring how different meal compositions affect postprandial exercise outcomes could provide more targeted recommendations for managing blood glucose levels. Finally, the development of real-time feedback systems, which integrate heart rate and blood glucose data, could enable personalized exercise

regimens that optimize cardiovascular and metabolic health outcomes.

6.5 Final Remarks

This study has provided a comprehensive framework for understanding the interplay between HR responses and exercise dynamics, particularly the roles of upper and lower body movements in shaping overall exercise intensity. By leveraging the vector-based HR analysis, HR changes with upper and lower body combinations, and insights into HR-BG interactions, this research highlights the potential to develop more accurate methods for assessing exercise difficulty and tailoring fitness programs to individual needs. The findings emphasize that HR responses are not only influenced by the intensity of the movements but also by the specific combination of upper and lower body exercises.

The practical implications of this research extend to designing personalized exercise protocols, optimizing cardiovascular and metabolic outcomes, and developing health monitoring systems for diverse populations. As future studies delve deeper into these interactions, incorporating diverse demographics, advanced wearable technologies, and longitudinal assessments will be crucial. Moreover, applying these findings to real-world scenarios—such as adaptive training programs and real-time feedback systems—can pave the way for significant advancements in fitness and health management.

Bibliography

Achten, J. and Jeukendrup, A. (2003). Heart rate monitoring: applications and limitations. *Sports medicine*, 33(7):517–538.

Adams, D. and Nsugbe, E. (2021). Predictive Glucose Monitoring for People with Diabetes Using Wearable Sensors. *Engineering Proceedings*, 10(1):20.

Barbara, A. M. and Grobelna, A. (2022). Real-Time Continuous Glucose Monitoring for People Living With Type 1 Diabetes. *Canadian Journal of Health Technologies*, 2(8).

Battelino, T., Danne, T., Bergenstal, R. M., Amiel, S. A., Beck, R., Biester, T., Bosi, E., Buckingham, B. A., Cefalu, W. T., Close, K. L., et al. (2019). Clinical targets for continuous glucose monitoring data interpretation: recommendations from the international consensus on time in range. *Diabetes care*, 42(8):1593–1603.

Blum, A. (2018). Freestyle libre glucose monitoring system. *Clinical Diabetes*, 36(2):203–204.

Cheung, C. C., Krahn, A. D., and Andrade, J. G. (2018). The emerging role of wearable technologies in detection of arrhythmia. *Canadian Journal of Cardiology*, 34(8):1083–1087.

Colberg, S. R., Laan, R., Dassau, E., and Kerr, D. (2015). Physical activity and type 1 diabetes: time for a rewire? *Journal of diabetes science and technology*, 9(3):609–618.

Colberg, S. R., Sigal, R. J., Fernhall, B., Regensteiner, J. G., Blissmer, B. J., Rubin, R. R., Chasan-Taber, L., Albright, A. L., and Braun, B. (2010). Exercise and type 2 diabetes: the American College of Sports Medicine and the American Diabetes Association: joint position statement. *Diabetes care*, 33(12):e147–e167.

Cooney, M. T., Vartiainen, E., Laakitainen, T., Juolevi, A., Dudina, A., and Graham, I. M. (2010). Elevated resting heart rate is an independent risk factor for cardiovascular disease in healthy men and women. *American heart journal*, 159(4):612–619.

de Oliveira Teles, G., da Silva, C. S., Rezende, V. R., and Rebelo, A. C. S. (2022). Acute effects of high-intensity interval training on diabetes mellitus: a systematic review. *International Journal of Environmental Research and Public Health*, 19(12):7049.

DeBoer, M. D., Cherñavvsky, D. R., Topchyan, K., Kovatchev, B. P., Francis, G. L., and Breton, M. D. (2017). Heart rate informed artificial pancreas system enhances glycemic control during exercise in adolescents with T1D. *Pediatric diabetes*, 18(7):540–546.

Dehghani Zahedani, A., Shariat Torbaghan, S., Rahili, S., Karlin, K., Scilley, D., Thakkar, R., Saberi, M., Hashemi, N., Perelman, D., Aghaeepour, N., et al. (2021). Improvement in glucose regulation using a digital tracker and continuous glucose monitoring in healthy adults and those with type 2 diabetes. *Diabetes Therapy*, 12(7):1871–1886.

Ema, R., Sakaguchi, M., Akagi, R., and Kawakami, Y. (2016). Unique activation of the quadriceps femoris during single-and multi-joint exercises. *European journal of applied physiology*, 116:1031–1041.

Engeroff, T., Groneberg, D. A., and Wilke, J. (2023). After dinner rest a while, after supper walk a mile? a systematic review with meta-analysis on the acute postprandial glycemic response to exercise before and after meal ingestion in healthy subjects and patients with impaired glucose tolerance. *Sports Medicine*, 53(4):849–869.

Erickson, M. L., Jenkins, N. T., and McCully, K. K. (2017a). Exercise after you eat: hitting the postprandial glucose target. *Frontiers in endocrinology*, 8:228.

Erickson, M. L., Little, J. P., Gay, J. L., McCully, K. K., and Jenkins, N. T. (2017b). Postmeal exercise blunts postprandial glucose excursions in people on metformin monotherapy. *Journal of Applied Physiology*, 123(2):444–450.

Flandrin, P., Rilling, G., and Gonçalves, P. (2003). Applications of empirical mode decomposition and Hilbert-Huang transform. *Advances in adaptive data analysis*, 1(01):43–61.

Frampton, J., Cobbold, B., Nozdrin, M., Oo, H. T., Wilson, H., Murphy, K. G., Frost, G., and Chambers, E. S. (2021). The effect of a single bout of continuous aerobic exercise on glucose, insulin and glucagon concentrations compared to resting conditions in healthy adults: a systematic review, meta-analysis and meta-regression. *Sports Medicine*, 51(9):1949–1966.

Friedman, J. G., Cardona Matos, Z., Szmuilowicz, E. D., and Aleppo, G. (2023). Use of continuous glucose monitors to manage type 1 diabetes mellitus: progress, challenges, and recommendations. *Pharmacogenomics and Personalized Medicine*, pages 263–276.

Fujimoto, W. Y. (2000). The importance of insulin resistance in the pathogenesis of type 2 diabetes mellitus. *The American journal of medicine*, 108(6):9–14.

Goldberg, L., Elliot, D., and Kuehl, K. (1988). Assessment of exercise intensity formulas by use of ventilatory threshold. *Chest*, 94(1):95–98.

Goodyear, L. J. and Kahn, B. B. (1998). Exercise, glucose transport, and insulin sensitivity. *Annual review of medicine*, 49(1):235–261.

Gupta, M. and Saxena, P. (2012). Analysis of a capacitive pressure sensor using fem for robotic hand applications. *Sensors & Transducers*, 13:120–127.

Gupta, N. C., Tiwari, P., and Gupta, A. (2021). A critical review on energy harvesting techniques from human-powered devices. *Energy*, 230:120817.

Haghi, M., Thurow, K., and Stoll, R. (2017). Wearable devices in medical internet of things: scientific research and commercially available devices. *Healthcare informatics research*, 23(1):4–15.

Hahnen, C., Freeman, C. G., Haldar, N., Hamati, J. N., Bard, D. M., Murali, V., Merli, G. J., Joseph, J. I., and van Helmond, N. (2020). Accuracy of vital signs measurements by a smartwatch and a portable health device: validation study. *JMIR mHealth and uHealth*, 8(2):e16811.

Hawley, J. A. and Lessard, S. (2008). Exercise training-induced improvements in insulin action. *Acta physiologica*, 192(1):127–135.

Holloszy, J. O. and Booth, F. W. (1976). Biochemical adaptations to endurance exercise in muscle. *Annual review of physiology*, 38(1):273–291.

Hong, Y. J., Lee, H., Kim, J., Lee, M., Choi, H. J., Hyeon, T., and Kim, D.-H. (2018). Multifunctional wearable system that integrates sweat-based sensing and vital-sign monitoring to estimate pre-/post-exercise glucose levels. *Advanced Functional Materials*, 28(47):1805754.

Hug, F., Del Vecchio, A., Avrillon, S., Farina, D., and Tucker, K. (2021). Muscles from the same muscle group do not necessarily share common drive: evidence from the human triceps surae. *Journal of applied physiology*, 130(2):342–354.

Jiang, G. and Zhang, B. B. (2003). Glucagon and regulation of glucose metabolism. *American Journal of Physiology-Endocrinology and Metabolism*, 284(4):E671–E678.

Kassiano, W., Costa, B., Kunevaliki, G., Soares, D., Stavinski, N., Francsuel, J., Carneiro, M. A., Tricoli, I., Nunes, J. P., Ribeiro, A. S., et al. (2023). Muscle swelling of the triceps surae in response to straight-leg and bent-leg calf raise exercises in young women. *The Journal of Strength & Conditioning Research*, 37(7):e438–e443.

Khan, S., Iqbal, K., Islam, N., and Choudhry, M. (2012). Design and analysis of mems based capacitive pressure sensor for low pressure biomedical applications. *Sensors and Transducers*, 13:90–105.

Khan, Y., Ostfeld, A. E., Lochner, C. M., Pierre, A., and Arias, A. C. (2016). Monitoring of vital signs with flexible and wearable medical devices. *Advanced materials*, 28(22):4373–4395.

Kinoshita, M., Maeo, S., Kobayashi, Y., Eihara, Y., Ono, M., Sato, M., Sugiyama, T., Kanehisa, H., and Isaka, T. (2023). Triceps surae muscle hypertrophy is greater after standing versus seated calf-raise training. *Frontiers in Physiology*, 14:1272106.

Kligfield, P. and Lauer, M. S. (2006). Exercise electrocardiogram testing: beyond the ST segment. *Circulation*, 114(19):2070–2082.

Kusmakar, S., Karmakar, C. K., Yan, B., O'Brien, T. J., Muthuganapathy, R., and Palaniswami, M. (2018). Automated detection of convulsive seizures using a wearable accelerometer device. *IEEE Transactions on biomedical engineering*, 66(2):421–432.

Lee, S. M. and Lee, D. (2020). Healthcare wearable devices: an analysis of key factors for continuous use intention. *Service Business*, 14(4):503–531.

Lu, L., Zhang, J., Xie, Y., Gao, F., Xu, S., Wu, X., Ye, Z., et al. (2020). Wearable health devices in health care: narrative systematic review. *JMIR mHealth and uHealth*, 8(11):e18907.

MacInnis, M. J., McGlory, C., Gibala, M. J., and Phillips, S. M. (2017). Investigating human skeletal muscle physiology with unilateral exercise models: when one limb is more powerful than two. *Applied Physiology, Nutrition, and Metabolism*, 42(6):563–570.

Manikandan, M. S. and Dandapat, S. (2012). A novel method for detecting r-peaks in electrocardiogram (ECG) signal. *Biomedical Signal Processing and Control*, 7(2):118–128.

Moser, E., Crew, L., and Garg, S. (2010). Role of continuous glucose monitoring in diabetes management. *Avances en Diabetología*, 26(2):73–78.

Nahiduzzaman, M., Tasnim, M., Newaz, N. T., Kaiser, M. S., and Mahmud, M. (2020). Machine learning based early fall detection for elderly people with neurological disorder using multimodal data fusion. In *International Conference on Brain Informatics*, pages 204–214. Springer.

Pahra, D., Sharma, N., Ghai, S., Hajela, A., Bhansali, S., and Bhansali, A. (2017). Impact of post-meal and one-time daily exercise in patient with type 2 diabetes mellitus: a randomized crossover study. *Diabetology & Metabolic Syndrome*, 9:1–7.

Park, J. K. and Lee, D. H. (2017). R-peak detection method for ECG using k-nearest neighbors algorithm and its evaluation using AAMI standard. *Computers in biology and medicine*, 87:204–212.

Patel, S., Park, H., Bonato, P., Chan, L., and Rodgers, M. (2012). A review of wearable sensors and systems with application in rehabilitation. *Journal of neuroengineering and rehabilitation*, 9:1–17.

Ravariu, C. (2011). Contributions to specific bio-sensors achievements by improving the technology and devices. *Sensors & Transducers*, 12(12):50.

Riddell, M. and Perkins, B. A. (2009). Exercise and glucose metabolism in persons with diabetes mellitus: perspectives on the role for continuous glucose monitoring. *Journal of diabetes science and technology*, 3(4):914–923.

Riddell, M. C., Gallen, I. W., Smart, C. E., Taplin, C. E., Adolfsson, P., Lumb, A. N., Kowalski, A., Rabasa-Lhoret, R., McCrimmon, R. J., Hume, C., et al. (2017). Exercise management in type 1 diabetes: a consensus statement. *The lancet Diabetes & endocrinology*, 5(5):377–390.

Salman, M., Abo-Zahhad, M., and Ahmed, S. (2012). Optimized circuit design and simulation of low-power ADC for portable ECG devices. *Sensors & Transducers*, 16(3):163–170.

Schwartz, F. L., Marling, C. R., and Bunescu, R. C. (2018). The promise and perils of wearable physiological sensors for diabetes management. *Journal of diabetes science and technology*, 12(3):587–591.

Seiler, S., Haugen, O., and Kuffel, E. (2007). Autonomic recovery after exercise in trained athletes: intensity and duration effects. *Medicine and science in sports and exercise*, 39(8):1366.

Shaik, N. and Ramakrishna, S. (2015). Method to detect R-peak in electrocardiogram signal using window and first order derivative. *Procedia Computer Science*, 46:1611–1619.

Sharma, K., Akre, S., Chakole, S., and Wanjari, M. B. (2022). Stress-induced diabetes: a review. *Cureus*, 14(9).

Shcherbina, A., Mattsson, C. M., Waggott, D., Salisbury, H., Christle, J. W., Hastie, T., Wheeler, M. T., and Ashley, E. A. (2017). Accuracy in wrist-worn, sensor-based measurements of heart rate and energy expenditure in a diverse cohort. *Journal of personalized medicine*, 7(2):3.

She, J., Nakamura, H., Makino, K., Ohyama, Y., and Hashimoto, H. (2015). Selection of suitable maximum-heart-rate formulas for use with karvonen formula to calculate exercise intensity. *International journal of automation and computing*, 12:62–69.

Šlajpah, S., Čebašek, E., Munih, M., and Mihelj, M. (2023). Time-Based and Path-Based Analysis of Upper-Limb Movements during Activities of Daily Living. *Sensors*, 23(3):1289.

Tanaka, H., Monahan, K. D., and Seals, D. R. (2001). Age-predicted maximal heart rate revisited. *Journal of the american college of cardiology*, 37(1):153–156.

Tejedor, G., Posada-Gomez, R., Cortes-Perez, J. P., Fontalvo, J. E., and Pardo, J. S. (2019). Multiple regression models for predicting exercise-induced fatigue in football players using wearable technology. *Sensors*, 19(19):4125.

Topol, E. (2015). *The patient will see you now: the future of medicine is in your hands*. Basic Books.

Tsuji, H., Larson, M. G., Venditti, F. J., Manders, E. S., Evans, J. C., Feldman, C. L., and Levy, D. (1996). Impact of reduced heart rate variability on risk for cardiac events: the Framingham Heart Study. *Circulation*, 94(11):2850–2855.

Weston, K. S., Wisløff, U., and Coombes, J. S. (2014). High-intensity interval training in patients with lifestyle-induced cardiometabolic disease: a systematic review and meta-analysis. *British journal of sports medicine*, 48(16):1227–1234.

Yang, Y. and Gao, W. (2019). Wearable and flexible electronics for continuous molecular monitoring. *Chemical Society Reviews*, 48(6):1465–1491.

Yoon, S. and Kim, D. (2025a). Estimation and Analysis of Physical Activity Load Based on Heart Rates. *Journal of Exercise Science & Fitness*. In preparation for submssion.

Yoon, S. and Kim, D. (2025b). HR Modeling using HR Analysis of Multiple Exercise. *Journal of Exercise Science & Fitness*. In preparation for submssion.

Yoon, S. and Kim, D. (2025c). Predicting Heart Rate and Blood Glucose Trends from Daily Activities. *Frontiers in Physiology*. In preparation for submssion.

Zheng, M., Luo, Y., Lin, W., Khoja, A., He, Q., Yang, S., Zhao, X., and Hu, P. (2020). Comparing effects of continuous glucose monitoring systems (CGMs) and self-monitoring of blood glucose (SMBG) amongst adults with type 2 diabetes mellitus: a systematic review protocol. *Systematic reviews*, 9:1–6.